The role of vascular activation on monocytes in hypertension

By

Roxana Loperena Cortés

Dissertation

Submitted to the Faculty of the

Graduate School of Vanderbilt University

in partial fulfillment of the requirements

for the degree of

DOCTOR OF PHILOSOPHY

in

Molecular Physiology and Biophysics

August 10, 2018.

Nashville, Tennessee

Approved:

Alyssa H. Hasty, PhD

Michael L. Freeman, PhD

Fred S. Lamb, MD, PhD

Owen P. McGuinness, PhD

To my parents, Rosa Ana Cortes and Renan Loperena, for your infinite love, prayers and support in my life and throughout this process, I could not have completed this degree without you.

“A mis padres, Rosa Ana Cortés y Renán Loperena, por su infinito amor, las muchas oraciones y apoyo durante este proceso y en mi vida, sin ustedes no lo hubiera logrado. Gracias.”

ACKNOWLEDGEMENTS

First and foremost, I would like to acknowledge my advisor Dr. David G. Harrison for your infinite support and guidance throughout my PhD training and for giving me the opportunity to be a part of this wonderful laboratory. Thank you for not giving up on me even when I struggled the most. I would like to acknowledge the members of my committee including Drs. Alyssa H. Hasty, Michael L. Freeman, Fred S. Lamb and Owen P. McGuinness for their support and contribution to this work. Thank you for teaching me to think outside of the box and believing in me as a scientist. I would like to give special thanks to my undergraduate mentor Dr. Jose E. Garcia Arraras. Without his mentorship, I would have never decided to become a scientists and I would not be where I am today. I would like to thank Dr. Jose Gomez for his patience and constant help during the phase of developing iPSCs in my thesis. I would also like to acknowledge Drs. Linda Sealy and Roger Chalkley for their infinite support and for allowing me to be a part of the initiative for maximizing student diversity (IMSD), which opened many doors for me to receive multiple funding sources and for the development of my career.

I would like to thank my current and past fellow members from the Harrison, Madhur and Kirabo laboratories including: My undergraduate mentee Noah Engel, Dr. Fanny Laroumanie, Dr. Natalia R. Barbaro, Dr. Allison Norlander, Dr. Hana A. Itani, Dr. Annet Kirabo, Dr. Liang Xiao, Dr. Jing Wu, Kim R. Montaniel, Dr. Lucas Hofmeister, Dr. Jason Foss, Dr. Arvind Pandey, Dr. Alfiya Bikineyeva, Dr. William McMaster, Dr. Justin Van Beusecum, Bethany Dale, Dr. Mingfang Ao, Dr. David Patrick, Dr. Michael Alexander, Dr. Mohamed Saleh, Dr. Danielle Michelle, Dr. Daniel Trott, and Dr. Wei Chen for their valuable insight, help with performing experiments, data analysis and support throughout the past 5 years.

I would like to acknowledge the support and love I got from my friends and family. To my parents, Rosa and Renan, who supported me mentally and spiritually through this process and told me to “never give up”, I thank you. To my brother, Hadid, that even from the distance supported me through this process. I would like to acknowledge my friends in particular Fanny and Kerri for keeping me sane and for loving me unconditionally. To my friends and family back in Puerto Rico, I applaud you for setting an example on not giving up on something you have worked so hard and staying to fight in the new Puerto Rico. Finally, to my boyfriend Alex Orga for giving me tremendous support in these last two years. Thank you for your patience in this process, for all your love, keeping me grounded and for inspiring me to pursue my dreams. Without the support of this village of people, I would not be here and for that, I thank you.

Acknowledgement of support

This work would not have been possible without the salary support of the National Heart, Lung, and Blood Institute of the National Institutes of Health, Ruth L. Kirschstein National Research Service Award (NRSA) Individual Predoctoral Fellowship to Promote Diversity in Health-Related Research (F31HL132526), Immunobiology of blood and vascular systems training program (NIH 2 T32 HL069765-11A1) and the William Townsend Porter Pre-doctoral Fellowship from the American Physiological Society. The experiments would not have been completed without the supported by National Heart and Blood Institute of the National Institutes of Health Grants [R01HL039006-27, R01HL125865-04 and P01HL129941] and an American Heart Association Strategically Focused Research Network Grant (14SFRN20420046).

TABLE OF CONTENTS

Page

LIST OF FIGURES

Figures **Page**

Chapter I

Chapter II

Chapter IV

LIST OF TABLES

Table **Page**

LIST OF ABBREVIATIONS

Angiotensin II (Ang II)

Dendritic cells (DCs)

Nitric oxide (NO)

Reactive oxygen species (ROS)

Human aortic endothelial cells (HAECs)

Low-density lipoprotein (LDL)

Endothelial nitric oxide synthase (eNOS)

Interleukin (IL)

Lysozyme M-positive ($LyzM^+$)

Signal transducer and activator of transcription 3 (STAT3)

Isolevuglandins (IsoLG)

T helper 17 (T_H17)

Toll-like receptor 4 (TLR4)

Cluster of differentiation (CD)

Intracellular adhesion molecule (ICAM)

Vascular cell adhesion molecule-1 (VCAM-1)

DC-specific intracellular adhesion molecule grabbing nonintegrin (DC-SIGN or CD209)

Leukocyte cell-derived chemotaxin 2 (LECT2)

Lipopolysaccharide (LPS)

Cyclic adenosine monophosphate (cAMP)

Nuclear factor kappa-light-chain-enhancer of activated B cells (NFκB)

Phosphoinositide 3-kinase (PI3K)

Vascular endothelial (VE)-cadherin

Extracellular matrix (ECM)

Tripeptide of L-arginine, glycine, and –aspartic acid (RGD)

Platelet endothelial cell adhesion molecule-1 (PECAM-1 or CD31)

Coronary artery disease (CAD)

Extracellular signal-regulated kinases (ERK)

Mitogen-activated protein kinases (MAPK)

Guanine nucleotide binding proteins (G proteins)

Superoxide dismutase (SOD)

Glycosylphosphatidylinositol (GPI)-anchored glycoprotein

Poly (ethylene glycol) (PEG)

Fluorescent minus one (FMO)

Fluorescein isothiocyanate (FITC)

7-aminoactinomycin-D (7-AAD)

Epithelial growth factor-like module-containing mucin-like hormone receptor-like 1 (F4/80)

Tyrosine protein kinase Mer (MerTK)

Phosphate buffered saline (PBS)

Magnetic activated cell sorting (MACS)

Fluorescence activated cell sorting (FACS)

Electron spin resonance (ESR)

Sodium dodecyl sulfate polyacrylamide gel electrophoresis (SDS-PAGE)

Bovine serum albumin (BSA)

Blood pressure (BP)

Vasodilator stimulated phospho-protein (VASP)

Phosphorylated- (p-)

Bone marrow transplant (BMT)

Bone marrow (BM)

Body mass index (BMI)

Peripheral blood mononuclear cells (PBMCs)

4’, 6-diamidino-2-phenylidole (DAPI)

Lymphocyte function-associated antigen 1 (LFA1)

Macrophage receptor 1 (MAC1)

Phospholipase C (PLC)

Tumor necrosis factor alpha (TNFα)

Chemokine ligands- (CCL-)

Stretch activated (SA) channel

Guanosine triphosphate enzymes (GTPase)

Human umbilical vein endothelial cells (HUVECs)

c-Jun amino-terminal kinases (JNK)

Bovine arterial endothelial cells (BAECs)

Target of rapamycin (mTOR)

Fms-like tyrosine kinase 3 (FLT-3)

Tyrosine kinase with immunoglobulin-like and EGF-like domains (Tie)

Angiotensin converting enzyme (ACE)

Superoxide ($O_2^{\cdot -}$)

Hydroxyl radical ($OH^{\cdot}$)

Lipid peroxy-radicals ($LOO^{\cdot}$)

Alkoxy- radicals ($LO^{\cdot}$)

Hydrogen peroxide (H_2O_2)

Peroxynitrite anion ($ONOO^-$)

Hypochlorous acid ($HOCl^-$)

Nox-based nicotinamide adenosine dinucleotide phosphate (NADPH or NOX) oxidase

Matrix metalloproteinases (MMPs)

Pulse wave velocity (PWV)

Sodium-hydrogen 3 exchanger (NHE3)

Sodium-chloride cotransporter (NCC)

Sodium-potassium cotransporter (NKC)

Sodium potassium chloride cotransporter (NKC2C)

Epithelial sodium channel (ENAC)

Juxtaglomerular granular (JG) cells

Renin-angiotensin (RAS) system

Wildtype (WT)

Deoxycorticosterone acetate (DOCA)-salt

Nω-Nitro-L-arginine methyl ester hydrochloride (L-NAME)

Spontaneously hypertensive rat (SHR)

Glutathione peroxidase (Gpx)

Flavin adenine dinucleotide (FAD)

Vascular smooth muscle cells (VSMCs)

Angiotensin I receptor (AT1)

Cellular-Src Kinase (c-Src)

Protein kinase C (PKC)

Phospholipase D (PLD)

Phospholipase A_2 (PLA_2)

Ras-related C3 botulinum toxin substrate (Rac)

Molecular oxygen (O_2)

Tetrahydrobiopterin (H_4B)

Endothelium-derived relaxing factors (EDRFs)

Endothelium-derived contractile factors (EDCFs)

Antigen presenting cells (APCs)

Natural killer (NK) cells

Pathogens called pathogen-associated molecular patterns (PAMPs)

Pattern-recognition receptors (PRRs)

C-type lectin receptors (CLRs)

Leucine-rich repeat (LRR)-containing NOD-like receptors (NLRs)

RIG-I-like receptors (RLRs)

Interferons (IFN)

Toll/interleukin-1 receptor (TIR)

LPS Binding Protein (LBP)

Nuclear factor of activated T cells (NFAT)

Major histocompatibility complex (MHC)

Common monocyte progenitors (cMoP)

Histocompatibility leukocyte antigen (HLA)

Mitogen-activated protein kinase kinase (MEK)

Human immunodeficiency virus (HIV)

Angiotensin I (Ang I)

Transforming growth factor beta (TGFβ)

Recombination-activating gene 1 (RAG1)

T regulatory (reg) cells

B cell-activating factor receptor deficient mice (BAFF-$R^{-/-}$ mice)

Immunoglobulin (Ig)

tert-butyl hydroperoxide (t-BHP)

Subfornical organ (SFO)

Anteroventricular third ventricle (AV3v)

Placental-like growth (PlGF) production

Glucocorticoid-related kinase 1 (SGK1)

Lymphocyte adaptor protein (LNK)

Rho-associated kinase (ROCK)

Janus Kinases (JAK)

Src-homology 2 (SH2)

Retineic-acid-receptor-related orphan nuclear receptor gamma (RORγt)

Mass cytometry (CyTOF)

Tyrosine (Y)

Serine (S)

Co-immunoprecipitation (co-IP)

Radioimmunoprecipitation assay buffer (RIPA)

Bicinchoninic acid assay (BCA)

Tris buffered saline containing 0.1% tween 20 (TBS-T)

Horseradish peroxidase (HRP)

Paraformaldehyde (PFA)

Cycle threshold (CT)

Standard error of mean (SEM)

Apolipoprotein E knockout ($ApoE^{-/-}$)

Cyclooxygenase-2 (COX-2)

Induced pluripotent stem cells (iPSCs)

Ethylenediaminetetraacetic acid (EDTA)

Mean fluorescent intensity (MFI)

Phycoerythrin (PE)

Cyanine 5.5, 7 (Cy5.5, CY7)

Allophycocyanin (APC)

Peridinin-chlorophyll-protein (PerCP)

2-hydroxybenxylamine (2-HOBA)

Enzyme-Linked Immunosorbent Assay (ELISA)

Pyruvate kinase M2 (PKM2)

Institutional Animal Care and Use Committee (IACUC)

Acetylcholine (Ach)

Sodium nitroprusside (SNP)

Knockout (KO)

Macrophages (MΦ)

Carboxyfluorescein succinimidyl ester (CFSE)

Vascular endothelial growth factor (VEGF)

Glycogen synthase kinase 3 (GSK3)

Bone morphogenic protein 4 (BMP4)

Krueppel-like factor 4 (Klf4)

Endothelial cells (ECs)

Guanosine monophosphate (cGMP)

cGMP-dependent protein kinase (PKG)

Octamer-binding transcription factor 4 (Oct4)

Sex determining region Y-box 2 (Sox2)

Skp1-Cdc53-F-box protein (SCF)

Epidermal growth factor receptor (EGFR)

Monocyte chemoattractant peptide 1 (MCP-1)

High Mobility Group Box-1 (HMGB-1)

DETA-NONOate (DETA NONO)

Chapter I

Introduction

Hypertension

Hypertension is clinically defined as a condition in which blood pressure (BP) is persistently elevated above 130/90 mmHg (systolic/diastolic) [1]. Hypertension is a major healthcare problem and is a risk factor for myocardial infarction, stroke, renal and heart failure. Despite decades of studying this disease, the cause of most cases of adult hypertension remains unknown [2]. Perturbations of the kidney, vasculature, heart and central nervous system have been implicated in this disease. According to the new guidelines, 46% of the population in United States is hypertensive, and the occurrence of this disease increases with age. In 2010 and 2016, hypertension was ranked as the leading risk factor for global burden of disease in both developed and under-developed countries [1, 3]. Current treatments for hypertension include ACE inhibitors, β-blocking drugs, calcium-blocking drugs, and thiazide diuretics. In spite of our understanding of the renin/angiotensin system and the drugs available in the market, some people still have hypertension refractory to treatment. This indicates that the etiology of hypertension is still unknown, emphasizing the need to determine other mechanisms by which hypertension develops. Further, 90% of cases of hypertension do not have an identifiable etiology and are defined as “essential”. Essential hypertension in many cases co-exists with obesity, diabetes, other metabolic disorders and aging [4].

In the past several years, emerging evidence indicates that hypertension is an inflammatory process in which innate and adaptive immune cells infiltrate into the kidney, vasculature and the

brain. These cells secrete powerful mediators such as cytokines, chemokines and reactive oxygen species (ROS) that alter function of these organs, cause tissue damage and elevate BP. However, the precise mechanism in which this process occurs remains poorly understood. Blood pressure is the product of systemic vascular resistance and cardiac output and, thus, one of these must be elevated in chronic hypertension. Cardiac output is elevated early in hypertension and results in vascular adaptations including vasoconstriction, vascular remodeling and vascular rarefaction. These increase systemic vascular resistance and concomitantly normalize cardiac output. Guyton defined the concept of the “pressure-natriuresis” curve that determines a relationship between BP with sodium and water excretion [5]. There is a rightward shift in the relationship of BP with sodium and water retention that results in sustained hypertension. A change in the ability of the kidney to excrete water and sodium will result in an increase in mean arterial pressure. Enhanced reabsorption of sodium and water along the nephron is regulated through the activities of various proximal and distal sodium transporters. These include the sodium-hydrogen 3 exchanger (NHE3), the sodium-chloride cotransporter (NCC), the sodium-potassium cotransporter (NKC), sodium-potassium chloride cotransporter (NKC2C) and the epithelial sodium channel (ENAC). Hypertension is associated with renal fibrosis, renal oxidative stress, glomerular injury and chronic kidney disease. Various hypertensive stimuli like angiotensin (Ang II), catecholamines, loss of nitric oxide and endothelin can increase sodium reuptake in the nephron, which is mediated by increased expression and activity of these transporters.

In cases of sustained hypertension, vascular rarefaction within the kidney and fibrotic replacement of renal parenchymal tissue can occur, which results in defects of renal function. Vascular rarefaction is defined as loss of capillaries and resistance vessels [6]. Diuretic

treatment in hypertensive humans helps to normalize the pressure natriuresis curve. Guyton also proposed that an increase in cardiac output leads to systemic vasoconstriction, which further increases the BP. This vasoconstriction returns blood volume to near normal levels and promotes the pressure natriuresis. However, these sustained elevations of pressure lead to end-organ damage commonly observed in hypertensive patients.

Folkow et al. described a phenomenon in hypertension in which the vascular lumen is narrowed as the media thickens [6]. This remodeling process can reduce the cross-sectional area of resistance arterioles and thus increases systemic vascular resistance. Another phenomenon is aortic stiffening. The thoracic aorta serves a buffering function in which it accommodates a portion of the blood ejected from the heart during systole. During diastole, the aorta recoils and ejects blood into the periphery to the downstream circulation. This capacitance function of the aorta, also referred to as the “Windkessel” function, blunts systolic BP and maintains diastolic pressure and perfusion. In several diseases and aging, the aorta stiffens and the Windkessel function of the aorta is lost. The rapidity of the forward wave plus the increase in reflected waves raises systolic BP. Clinically, aortic stiffness can be estimated by measuring pulse wave velocity (PWV). Increased PWV is associated with diseases such as stroke, chronic kidney disease, heart failure and peripheral vascular disease [7, 8].

The central nervous system also plays a crucial role in hypertension. Regions of the forebrain, the hypothalamus and the brain stem controlling the sympathetic and parasympathetic outflow and modulate vasoconstriction, vascular remodeling, vascular smooth muscle proliferation and increases cardiac output [9]. Sympathetic nerves innervate renal tubules, the juxtaglomerular granular (JG) cells of the kidney and renal vessels. Increased renal sympathetic nerve activity promotes an increase in sodium and water reabsorption in the nephron. Constriction of the renal

vasculature also stimulates renin release from JG cells in a feed-forward fashion that activates the renin-angiotensin (RAS) system [10]. Recent data indicate that renal sympathetic nerves can modulate activation and infiltration of innate and adaptive immune cells [11].

Models of Hypertension

Several rodent models are used to study hypertension. A common model involves Ang II infusion in mice or rats via osmotic mini pumps. These pumps are placed subcutaneously and release Ang II over the course of 7 to 28 days [12, 13]. Another commonly employed model of hypertension is the deoxycorticosterone acetate (DOCA)-salt model [14]. This results in a salt-sensitive form of hypertension in which Ang II levels are markedly suppressed [15]. In the DOCA-salt model, one kidney is removed, a pellet of DOCA is inserted subcutaneously and the animals are given excess sodium in their drinking water. DOCA is an aldosterone-like agent that increases sodium and water reabsorption in the kidney. Another model of hypertension involves administration of the nitric oxide synthase antagonist Nω-Nitro-L-arginine methyl ester hydrochloride (L-NAME). This raises systolic BP to about 140 mmHg [16]. A variant of this model, involves stopping L-NAME after a two to three week infusion. These animals then exhibit salt-sensitivity in which adding salt to their diet increases their BP [17]. There are also genetic models of hypertension including the Dahl salt-sensitive (DSS) rats that were bred by Lewis K. Dahl [18]. These animals develop severe hypertension and renal damage when fed salt. There is another salt-resistant strain that is used as a control Dalh salt-resistant (DSR). Extensive research has employed inner crosses between these two strains to identify chromosomes that convey hypertension [19]. Of late, researchers have begun to manipulate the DSS rat using zinc-finger DNAse gene targeting [20]. Another model of hypertension is the spontaneously hypertensive rat (SHR). These rats were made by outbreeding Wistar Kyoto rats and selecting for animals

with higher blood pressures. A variant of these is called the SHR stroke-prone has severe hypertension and is predisposed to stroke [21]. Loft et al. created a double transgenic rat expressing the human angiotensinogen and renin genes. These rats develop hypertension and die of end-organ damage by 7 weeks of age [22]. Another model is the Schlager mouse, which have an increase in sympathetic nerve activity in hypertension [23]. There are advantages and disadvantages to these and other models of hypertension, but they exhibit similar phenotypes to humans with this disease. These models demonstrate left ventricular hypertrophy, renal damage, vascular dysfunction, and can develop stroke. The drugs used to treat human hypertension lower blood pressure in these various models. Advantages of rat models are that the animals are larger. The advantages of mice are that they are more easily genetically modified, and the murine immune system is much better characterized. Reagents needed to study the immune system are readily available for mice and not for rats.

Oxidative stress in hypertensive disease

It has become increasingly evident that ROS contribute to the development of hypertension. In addition, our laboratory and others have shown a role of ROS and immune activation during hypertension disease. ROS can be divided into two major groups: free radicals and non-radical derivatives. Free radicals possess an unpaired electron in their outer orbital making them highly reactive. Among these are superoxide ($O_2^{\cdot -}$), the hydroxyl radical ($OH^{\cdot}$), lipid peroxy-radicals ($LOO^{\cdot}$) and alkoxy- radicals ($LO^{\cdot}$) [24]. Nitric oxide (NO) is also a free radical, and often referred to as a reactive nitrogen species. Non-radical ROS include hydrogen peroxide (H_2O_2), the Peroxynitrite anion ($ONOO^-$), hypochlorous acid ($HOCl^-$) and reactive carbonyls. These latter are more stable because they do not possess unpaired electrons and have a longer half-life, but maintain strong oxidant properties.

Although originally considered toxic by-products of cellular metabolism, ROS are now recognized to have signaling roles that are critical for normal cell function including proliferation, differentiation, aging, host-defense and repair processes [25]. Recent studies show that ROS, including H_2O_2, may drive pro-survival signaling and protection from the aging process [26]. As a part of innate immunity, phagocytes exhibit a respiratory burst in which they release large amounts of ROS to kill bacteria and other pathogens. This is accomplished by activation of the Nox-based nicotinamide adenosine dinucleotide phosphate (NADPH) oxidase discussed below. ROS also participate in tissue repair and remodeling by inducing expression of matrix metalloproteinases (MMPs) [27]. These vital responses for normal cell function and are exacerbated in disease states and promote pathological processes. The term oxidative stress refers to an imbalance between the production of ROS and antioxidant defenses [28]. Superoxide, produced by 1-electron reduction of molecular oxygen, can act both as an oxidant and as a reductant in biological systems, depending on the redox potential of the molecule with which it is reacting [29]. Superoxide is important because it serves as a progenitor for many other biologically relevant ROS, including H_2O_2, $HO^{\cdot}$ and $OONO^{-}$. The last of these forms upon reaction of $O_2^{\cdot -}$ with NO [30]. Hydrogen peroxide is formed by dismutation of $O_2^{\cdot -}$, which can occur either spontaneously or can be catalyzed by the superoxide dismutases (SODs). In contrast to superoxide, H_2O_2 is relatively stable under physiological conditions. Because it is uncharged and lipophilic, H_2O_2 can readily diffuse across membranes and thus can react with targets in organelles and cells apart from where it is formed [24]. In this regard, H_2O_2 has been implicated as a signaling molecule that can, among other actions, promote vasodilatation, activate gene transcription, modify phosphatase activity and activate other sources of ROS [31]. As part of the antioxidant defense mechanisms, catalase and glutathione peroxidase (Gpx) can

reduce H_2O_2 to H_2O. As mentioned above, $OONO^-$ is the product of the spontaneous reaction between $O_2^{\cdot -}$ and NO. This reaction is essentially diffusion limited, and its rate has been estimated to be 9 X 10^9 mols X sec-1, which is faster than that of the reaction of $O_2^{\cdot -}$ with the superoxide dismutases [32]. At physiological pH, $OONO^-$ exists in the protonated form, HOONO or peroxynitrous acid, which is uncharged and can diffuse across cell membranes. Peroxynitrite often reacts and modify proteins and other cellular structures causing oxidative damage to these molecules. In particular, $OONO^-$ modifies protein tyrosine residues to form 3-nitrotyrosine, a biomarker for $OONO^-$ in tissues and blood.

The NADPH oxidases are major sources of ROS in mammalian cells, which play a role in host defense. The catalytic subunits of these enzyme complexes are the NOX proteins. Seven NOX proteins have been identified with differential tissue distribution, diverse function and regulation mechanisms. NOX1 is known to exist in colon, muscle, prostate, uterus and blood vessels and plays important roles in host defense and blood pressure regulation [33]. NOX2 is found in phagocytes, where it is responsible for the oxidative burst. It is also present in endothelial cells and the tubular cells of the kidney [34]. NOX3 is present in fetal tissue and inner ear and is essential for vestibular function. NOX4, expressed in kidneys, vessels and bone, is involved in vasoregulation and erythropoietin synthesis. NOX5, not present in rodents, is a $Ca2^+$-dependent homolog that produces $O_2^{\cdot -}$ in response to intracellular $Ca2^+$ mobilization in lymph nodes, testes and blood vessels. NOX5 is also expressed in atherosclerotic lesions and seems to be higher in more complex lesions [35].

The phagocytic NADPH oxidase is composed of membrane-bound and cytoplasmic components. The membrane components include the large glycosylated protein, $gp91^{phox}$ (NOX2), and a smaller adaptor protein $p22^{phox}$ which together compose the cytochrome b_{558} [36].

NOX2 has two heme groups and binds to the redox cofactor flavin adenine dinucleotide (FAD) that is essential for the electron transfer. During NOX2 activation, the proline rich area in the C-terminal region of $p22^{phox}$ functions as a docking unit for activated $p47^{phox}$ and can also bind $p40^{phox}$ [37, 38]. In addition to $p47^{phox}$, other subunits located in the cytoplasm are required for NOX2 activation including $p67^{phox}$ and the small GTPase Rac2. Upon activation, these subunits translocate to the membrane components initiating electron transfer. The electron transfer occurs from NADPH to FAD and then to the heme groups; ultimately reducing molecular oxygen (O_2) to produce superoxide [39].

A major development in the past two decades has been the realization that NADPH oxidases exist in non-phagocytic cells. As mentioned above, NOX subunits are present in various vascular cells and can be activated by pathophysiological stimuli. As an example, Ang II activates the NADPH oxidases via the AT1 receptor and stimulation of a signaling pathway involving c-Src, protein kinase C (PKC), phospholipase D (PLD) and phospholipase A_2 (PLA_2) and activating Rac1 [40]. In addition Ang II increases vascular $p22^{phox}$ expression *in vivo* and deletion of this subunit in vascular smooth muscle cells (VSMCs) prevents ROS formation [41, 42]. The NADPH oxidases are also activated by a variety of physiological and pathophysiological stimuli, including inflammatory cytokines, growth factors, mechanical forces and various G protein coupled receptor agonists. Overexpression of VSMCs $p22^{phox}$ enhances hypertension and hypertrophy in response to Ang II [43]. In addition, we found that overexpression of $p22^{phox}$ in VSMCs of mice increases collagen deposition, aortic stiffness, renal dysfunction and hypertension with age [44]. Patients with chronic granulomatous disease lack subunits of the NADPH oxide and suffer from recurrent and life-threatening infections [45].

The nitric oxide synthase (NOS) enzymes are the endogenous sources of NO in mammalian cells. By producing NO, these enzymes have myriad effects on cardiovascular function, including modulation of vascular tone, blood pressure, sympathetic outflow, renal renin release and renal sodium excretion [46]. In the absence of their critical cofactor tetrahydrobiopterin (H_4B), or their substrate L-arginine, the NOS enzymes become uncoupled, such that they produce $O_2^{\cdot -}$ rather than NO. NOS uncoupling has been documented as a source of ROS in diseases such as hypertension, atherosclerosis, diabetes and following ischemia and reperfusion injury [47]. Importantly, oral H_4B blunts the elevation of BP in Ang II- and salt-induced hypertension in animals and has been shown to lower BP in humans with hypertension [47-49]. A major cause of NOS uncoupling is oxidation of H_4B by oxidants such as peroxynitrite [50]. Interestingly, ROS produced by the NADPH oxidase play a role in this process, and mice lacking the NADPH oxidase are protected against H_4B oxidation in the setting of hypertension [51].

A large body of literature has shown that excessive production of ROS contributes to hypertension and that scavenging of ROS decreases BP. In an initial study, Nakazono and colleagues showed that bolus administration of a modified form of SOD acutely lowered BP in hypertensive rats [52]. Our laboratory was among the first to show that membrane-targeted forms of SOD and SOD mimetics such as tempol lower blood pressure and decrease renovascular resistance in hypertensive animal models [53-55]. There is ample evidence suggesting that ROS not only contribute to hypertension but that the NADPH oxidase is their major source. Components of this enzyme system are up-regulated by hypertensive stimuli, and NADPH oxidase enzyme activity is increased by these same stimuli. Moreover, both Ang II-induced hypertension and DOCA-salt hypertension are blunted in mice lacking components of the NADPH oxidase [56]. Hypertension is associated with increased ROS production by multiple

organs, including the brain, the vasculature, and the kidney, all of which are likely important. It is likely that all of these organs are important in the genesis of hypertension and that there is important interplay between these that causes this disease. Elevated vascular ROS promotes the development of hypertension in various animal models, including Ang II-induced, DOCA-salt hypertension [56-58], Dahl salt-sensitive hypertension and SHR rats [59-61].

Humans with hypertension have alterations of vascular reactivity. The endothelium regulates vascular tone via release of endothelium-derived relaxing factors (EDRFs) and endothelium-derived contractile factors (EDCFs). Oxidative stress causes imbalanced production and bioavailability of these molecules leading to endothelial dysfunction. NO is one of the most important mediators of endothelium-dependent relaxation in BP regulation. The major mechanism for alteration of NO bioavailability when superoxide is increased is that this radical reacts with NO at an extremely rapid rate, as discussed above. Uncoupling of endothelial NOS (eNOS), due to deprivation of the cofactor H_4B,results in reduced NO release, increased superoxide production, impaired endothelium-dependent relaxation and elevated arterial pressure [47, 48, 62]. Similarly, lack of eNOS substrate L-arginine also reduces NO bioavailability and impairs NO-induced dilation. L-arginine is the substrate for both eNOS and arginase, and increased arginase activity reduces the local bioavailability of L-arginine [63]. Interestingly, peroxinitrite and hydrogen peroxide have recently been shown to increase the expression and activity of arginase in endothelial cells, potentially contributing to endothelial dysfunction [64].

Diverse stimuli common to the hypertensive milieu, including Ang II, aldosterone, catecholamines, increased vascular stretch, and endothelin promote ROS production, which

then increases expression of proinflammatory molecules that cause rolling, adhesion, and transmigration of inflammatory cells [65, 66].

Innate Immunity

The innate immune system is the first line of defense against invading pathogens such as microbes, viruses or fungi. The innate immune system is composed of physical and chemical barriers to prevent infection as well as the recognition of invading pathogens by various cell types. Initial barriers include the epidermis, vascular endothelium, respiratory epithelium and mucosal surfaces [67]. Cellular components include antigen presenting cells (APCs) such as dendritic cells (DCs) and monocytes, phagocytic macrophages and granulocytes, natural killer (NK) cells and innate lymphoid cells. The innate immune system is important in that it detects foreign microbes early during infection by recognizing evolutionarily conserved structures on pathogens called pathogen-associated molecular patterns (PAMPs) through germline-encoded pattern-recognition receptors (PRRs) and begins clearance by employment of complement activation, phagocytosis, and autophagy [68].

PRRs on immune and nonimmune cells survey the extracellular and intracellular space for conserved microbial determinants that can indicate infection. Charles Janeway Jr. was the first to describe two features of innate immunity including the ability to distinguish self from non-self-molecules and the ability of the innate immune system to activate the adaptive immune system [69]. Innate immunity relies on the release of local mediators and phagocytes, while the adaptive immune system uses antigen-specific T and B cells. Phagocytes are responsible for clearing pathogens mainly by phagocytosis, but also by the release of proinflammatory cytokines and chemokines that allow recruitment of other immune cells to the site [70]. Further, in response to pathogens, phagocytes such as neutrophils and macrophages release respiratory or oxidative

burst, which helps destroy the internalized pathogen [71]. The expression of PRRs on these cells allow them to detect specific pathogens and in a way gives a degree of specificity like the adaptive immune system [72]. PRRs are classified into five different families based on their protein domain homology including: Toll-like receptors (TLRs), C-type lectin receptors (CLRs), nucleotide-binging domain, leucine-rich repeat (LRR)-containing or NOD-like receptors (NLRs), RIG-I-like receptors (RLRs) and the AIM2-like receptors [73]. There are two main classes of PRR families, distinguished by their membrane-bound receptors or unbound intracellular receptors. Membrane-bound receptors include TLRs and CLRs that survey the presence of microbial ligands in the extracellular space or the endosomal space. NLRs, RLRs and ALRs are located within the cytoplasm and survey the presence of intracellular pathogens such as viruses [74]. PRR activation initiates either a transcriptional or a non-transcriptional innate immune response, which ultimately leads to adaptive immune responses. The production of proinflammatory cytokines and interferons (IFNs) in response to a PRR-induced response is a critical component for initiating innate and adaptive immune responses [75]. Other responses include phagocytosis, autophagy, cell death and cytokine processing, which are linked to the tightly controlled signal transduction pathways [76].

TLRs are transmembrane glycoproteins that contain an extracellular domain, a transmembrane domain and an intracellular toll/interleukin-1 receptor (TIR) homology domain. The extracellular domain is essential for ligand recognition and has a horseshoe-like structure [77]. There are 13 types of TLRs, three of which are not expressed in humans, and they are distinct for their ligand specificity. TLR4 was the first toll-like receptor to be identified [78]. Poltorak et al. showed that mice with selective mutations in the TLR4 gene that detects Lipopolysaccharide (LPS) are resistant to endotoxin but are highly susceptible Gram-negative sepsis [79]. Thus, TLR4 requires

a multi-receptor complex in response to LPS binding that consists of LPS-binding protein (LBP), CD14 and MD-2 in order to extract LPS from bacteria and initiate signaling. [80].

Cluster of differentiation (CD) 14 is a membrane protein initially identified by its interaction with LPS and is expressed on myelomonocytic cells. CD14 displays a dimeric structure that resembles the TLR4 extracellular domain and can be released as a soluble factor or be a glycosylphosphatidylinositol (GPI)-anchored glycoprotein [81]. CD14 anchors to regions on the plasma membrane with high density of cholesterol called lipid rafts, which are essential regions for protein signaling, trafficking and endocytosis [82]. CD14 lacks an intracellular tail, however, with the aid of adaptive proteins it can initiate signaling that leads to calcium influx and gene regulation via nuclear factor of activated T cells (NFAT) activation independent of TLR4 signaling [83]. The proinflammatory signaling occurring in response to activated PRRs ultimately leads to activation, maturation and induction of the adaptive immune system. Major players in this signaling response include transcription factors NFκB, AP1 and IRF3/7 that stimulate the production of proinflammatory mediators such as cytokines and IFN [84]. Specifically, NFκB plays a central role in both innate and adaptive immunity by orchestrating the expression of multiple genes that are essential for an immune response. Many proinflammatory cytokines including IL-6, IL-1 and TNFα and chemokines such as RANTES and IL-8 can be induced in response to NFκB activity [85]. Further, many molecules involved in inflammation are upregulated in response to PRR activity and NFκB including cytokines, immunoreceptors and chemokine receptors, TLRs, major histocompatibility complex (MHC) molecules, costimulatory molecules and immunoglobulins [74]. All of these factors are essential for the activation and recruitment of leukocytes to sites of inflammation, enhanced phagocytosis and apoptosis by complement or NK cell-mediated lysis and enhanced antigen presentation.

Monocyte subsets and implications in disease

Monocytes are a relatively large circulating leukocyte with a diameter of 12-20 μm that are part of the mononuclear phagocyte system [86]. Monocytes originate from myeloid common progenitor, which gives rise to monocyte precursors (MPs) that give rise to monocytes that are then released from the bone marrow [87, 88]. Human monocytes are sub-classified on their cell surface expression of CD14 and CD16, the Fcγ (III)-receptor. Classical monocytes express CD14 and little to no CD16 and comprise 90-92% of all monocytes. Non-classical monocytes express lower levels of CD14 and high levels of CD16. In 2010, another subset of monocytes expressing both CD14 and CD16 was identified and named intermediate monocytes [89].

Monocytes survive in circulation up to 72 hours and can migrate into the tissue to act as phagocytes, differentiate into a different subset of cells or die [90]. In humans, ten percent of all nucleated cells in blood are monocytes and they concentrate in specialized tissues including spleen and lungs and they can be mobilized from these sites to other tissues in response to pathological stimulus [91]. Once monocytes reach the designated tissue, they can produce effector molecules and phagocytose microorganisms, lipids, other toxic molecules, and cells undergoing apoptosis [92]. Effector molecules of monocytes that can initiate inflammation include cytokines, chemokines, ROS, MMPs, MHC, costimulatory molecules and other T cell interacting factors.

Monocytes represent accessory cells that link the innate immune system with the adaptive immune system by acting as APCs to T cells to induce an immune response. Importantly, monocytes are heterogeneous and plastic cells that can serve as progenitors to different subset of cells including macrophages and DCs [93]. These latter two cell types can present antigen to

T cells. Recently, it has been recognized that monocytes can be activated to present antigen with minimal differentiation [94].

Monocytes have both beneficial and deleterious properties. Monocytes can clear antigen and generate a beneficial immune response when needed. However, they have detrimental effects when their activity is prolonged that can ultimately lead to end-organ damage. Monocytes play an important role in inflammation and are increased in the circulation and activated in many inflammatory diseases including different types of cancers, atherosclerosis, and coronary artery disease (CAD) [92, 95, 96]. Classical monocytes express a wide range of genes associated with the process of phagocytosis including CD64, CD14, and CD93. Additionally, classical monocytes have the highest expression of antimicrobial proteins making this subset one of the first lines of innate immunity [97]. Previous studies have indicated that loss of monocytes prevents development of vascular dysfunction and oxidative stress in atherosclerosis [98] and hypertension [99]. Recent studies using deuterium labeling have shown that intermediate and non-classical monocytes arise sequentially from the classical population. The circulating lifespan of intermediate and non-classical monocytes (4 and 7 days, respectively) is much longer than classical monocytes (1 day) [100]. In culture, classical monocytes acquire increasing levels of CD16 with time [101]. Classical monocytes can differentiate into various subtypes of monocytes, DCs or macrophages in response to stimulus such as growth factors, cytokines, and immune responses.

Non-classical monocytes ($CD14^{low}CD16^{++}$) have high levels of TNFα and IL-1β in response to LPS. In addition, non-classical monocytes have the highest expression of CX3CR1 and genes necessary for adhesion including integrin α [97], the integrin-associated protein CD47, sialophorin (CD43)-a ligand for ICAM-1, and PECAM-1, which triggers endothelial adhesion and

integrin-mediated migration to tissue [102]. Studies by Urbanski et al. have shown that the presence of non-classical monocytes corresponds with reduced vascular responses to acetylcholine, indicative of impaired endothelial function in patients with CAD [96]. Non-classical monocytes have been associated with increased body mass index (BMI) and carotid intimal medial thickening, a marker of early atherosclerosis in patients at low risk for cardiovascular diseases [103]. The number of circulating non-classical monocytes correlates with subclinical atherosclerosis in patients with systemic lupus erythematosus [104]. In addition, in patients with endothelial dysfunction non-classical monocytes exhibit high expression of CD11c, suggesting an increase in activation [96]. Also in this study, non-classical monocytes correlated with superoxide production of vessels removed from patients. Conversely, other studies have shown that the non-classical monocytes patrol capillaries after adoptive transfer, do not produce ROS and are weak producers of inflammatory cytokines after exposure to LPS or TLR1/TLR2 agonists [105]. These cells produce IL-1β and CCL3 in response to viruses and immune complexes via MyD88-MEK pathway [105].

In 1989, Passlick et al. described a new subset of blood monocytes characterized by the co-expression of CD14 and CD16 [101]. These were named intermediate monocytes ($CD14^{++}CD16^{+}$) and were found to comprise of approximately 2.2% of the mononuclear cells. Intermediate monocytes have been implicated in inflammatory diseases including Kawasaki disease [106], psoriasis [107] rheumatoid arthritis [108], sepsis [109], HIV [110], acute heart failure [111], and coronary artery disease [111]. Dialysis patients without infection have an increase in the number of circulating intermediate monocytes and those suffering from chronic infection have higher levels of these cells compared to healthy controls. In addition, intermediate monocytes express higher levels of MHC class II antigens including histocompatibility leukocyte

antigen (HLA)-DR,DP and –DQ compared to other monocyte subsets [112]. Intermediate monocytes also exhibit enhanced phagocytosis and produce high levels of ROS [97] and inflammatory mediators such as TNFα [113] and IL-1β [114]. Intermediate monocytes have higher levels of soluble ICAM-1 and, similar to non-classical monocytes, high levels of CD11a and CD11c [106], which bind to ICAM-1 on the endothelial cells promoting adhesion and migration into tissues [115] [116]. Rossol et al. showed that intermediate monocytes produce high levels of TNFα upon co-culture with pre-stimulated $CD3^+$ T cells from healthy individuals. Intermediate monocytes also have the highest expression of CCR5, CD68 and lower ABCA1 expression than classical monocytes in chronic kidney disease patients [117]. The ligand for CCR5, CCL5 or RANTES, is expressed in atherosclerotic plaques and genetic deletion of CCR5 protects against experimental atherogenesis suggesting a potential role of intermediate monocytes in atherosclerosis [118]. Further, intermediate monocytes take up oxidized low-density lipoprotein cholesterol, known to promote experimental atherosclerosis [117]. In addition, intermediate monocytes from dialysis patients have a high expression of membrane-bound angiotensin converting enzyme (ACE), the enzyme that converts Ang I to Ang II [119]. Intermediate monocytes have been shown to independently predict cardiovascular events in subjects referred for elective coronary angiography [120]. Classical, intermediate and non-classical monocytes are defined by their expression of different markers in mice and humans and these are summarized in Table 1-1 [121].

Calzada-Wack and colleagues found that blood monocytes spontaneously undergo maturation in culture and this is evident by the decrease in expression of CD33, a myelomonocytic stem cell marker [122]. This group found that addition of IL-10 to these monocytes in culture further reduced the expression of CD33 and gained the expression of CD16. In addition, Eligini et al.

showed similar results in that human monocytes spontaneously differentiate into macrophage after 7 days in autologous serum and that these cells have an overexpression of CD163, IL-10, TGFβ-2 and higher lipid content [123]. Thus, monocytes can have both beneficial and deleterious effects.

Table 1-1. Human vs mouse monocyte subset of cells and their markers.

Human	Mouse
Classical monocytes: $CD14^{++}CD16^{-}$	Classical monocytes: $Ly6C^{++}CD43^{+}$
Intermediate monocytes: $CD14^{++}CD16^{+}$	Intermediate monocytes: $Ly6C^{++}CD43^{++}$
Non-classical monocytes: $CD14^{low}CD16^{++}$	Non-classical monocytes: $Ly6C^{low}CD43^{++}$

Immune system in hypertension

As early as 1954, Heptinstall described the presence of lymphocytes in kidneys of humans with hypertension [124]. In the 1960s, Okuda and Grollman showed that transfer of lymphocytes from rats with unilateral renal infarction transferred hypertension to recipient rats. In 1972, Olsen described an inflammatory reaction adjacent to the small arteries and arterioles of humans with hypertension consisting of T cells and monocytic cell [10]. In the 1970s, Svendsen discovered mice that were thymectomized do not maintain hypertension after renal infarction. In the last 12 years, there has been a reemerging interest in the role of the immune system in hypertension. In the early 2000s, our group showed that recombination-activating gene 1 ($RAG1^{-/-}$)-deficient mice, which lack both T and B cells, are protected against Ang II-induced and DOCA-salt hypertension and maintain vascular endothelial function [125]. Adoptive transfer of T cells, but not B cells, restored the hypertensive response and vascular dysfunction similar to wildtype (WT) mice. In addition, the deletion of RAG1 gene in Dahl-salt-sensitive rats attenuated hypertension

and renal damage upon high-salt feeding, again showing the role of adaptive immunity in the development of hypertension [20]. Crowley et al. showed that mice deficient in lymphocytes or *SCID* mice are also protected against high blood pressure and cardiac hypertrophy during Ang II-induced hypertension [126].

Several studies address the types of T cells involved in hypertension. Specifically, our laboratory found that $CD8^+$ T cells and not $CD4^+$ T cells play a crucial role in this disease. Mice lacking CD8 ($CD8^{-/-}$) and OT1xRAG1$^{-/-}$, which only have one T cell receptor, were protected against Ang II-induced hypertension; while, mice lacking CD4 and MHCII were not [127]. Adoptive transfer of $CD8^+$ T cells but not $CD4^+$ T cells restored the hypertensive phenotype in RAG1$^{-/-}$ mice. Youn et al. examined circulating T lymphocytes in hypertensive patients and age- and sex-matched non-hypertensives. They found an increase number in senescent circulating $CD8^+$ T cells in humans with hypertension [128].

There is also evidence that $CD4^+$ T cells are activated in hypertension. An important cytokine seems to be interleukin 17a (IL-17A). Mice lacking IL-17A, a cytokine largely produced by $CD4^+$ T cells, are protected against Ang II-induced hypertension, and infusion of the soluble IL-17C receptor lowers blood pressure and prevents oxidative stress in rats with experimental pre-eclampsia [129, 130]. IL-17A raises blood pressure when administered to normal mice and it can induce phosphorylation of eNOS at threonine 495, which is an inhibitory site that leads to impaired endothelium-dependent vasodilation [131]. Our groups also found that IL-17A production is increased in circulating $CD4^+$ T cells of humans with hypertension [132]. In addition, our group found that effector memory T cells accumulate in the kidney and bone marrow in response to L-NAME/high salt or repeated Ang II stimulation in mice [17]. This increase in

effector memory T cells is associated with an increase in the surface expression of the costimulatory molecule CD70 by antigen presenting cells such as macrophages and monocytes. CD70 is a costimulatory factor that reacts with CD27 on T cells and is important for formation of memory T cells. Mice lacking CD70 were protected against repeated hypertensive challenges. Another T lymphocyte subset, the T regulatory (reg) cells, have immune suppressant roles and have been shown to lower BP in Ang II-induced hypertension. Adoptive transfer of T cells from Scurfy mice, which lack T reg cells, to RAG1$^{-/-}$ mice worsen microvascular remodeling and stiffening in Ang II-induced hypertension [133]. Another cell type from the adaptive immune system that plays a role in hypertension is the B cell. Previous research in preeclampsia, an illness that affects 2-8% of pregnancies, has shown the presence of circulating autoantibodies against the angiotensin AT1 receptor [134]. These antibodies are agonistic such that when they bind to the AT1 receptor they promote vasoconstriction and renal sodium retention. Further, B cell-activating factor receptor deficient mice (BAFF-R$^{-/-}$ mice), which lack mature B cells, have blunted systolic blood pressure in response to Ang II as well as a reduction of the initial increase in circulating IgG observed in WT mice [135].

The innate immune system also plays an essential role in the development of hypertension. De Ciuceis et al. performed studies in Op/Op mice, which are deficient in the macrophage colony-stimulating factor and therefore cannot form these cells, and showed that these mice are protected against Ang II-induced hypertension [136]. Wenzel et al. showed that depletion of lysozyme M-positive (LysM^{+}) myelomonocytic cells by diphtheria toxin attenuated Ang II-induced hypertension, vascular endothelial dysfunction and reduced vascular superoxide formation [99]. This group further found that adoptive transfer of WT CD11b^{+}Gr-1^{+} monocytes to depleted LysM^{+}

mice reestablished the Ang II-induced hypertension, vascular dysfunction and oxidative stress confirming an important role of monocytes in the development of hypertension.

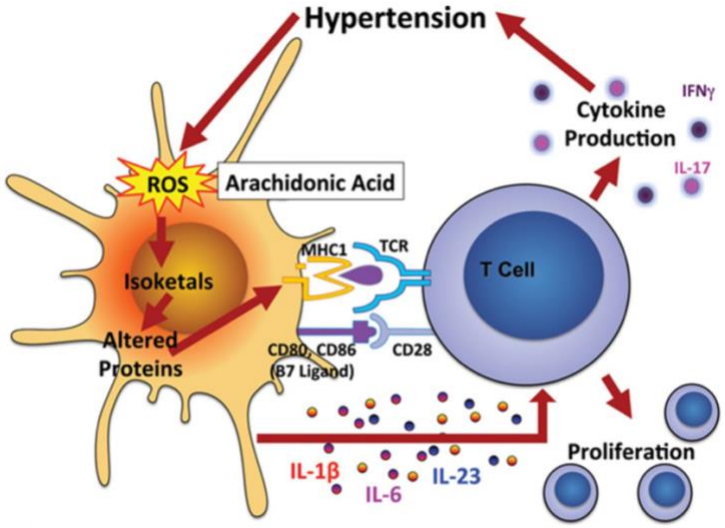

Figure 1-1: The role of dendritic cells in hypertension. Hypertension induces production of reactive oxygen species in dendritic cells, leading to oxidation of arachidonic acid and formation of isolevuglandins (IsoLG). IsoLGs rapidly ligate to protein lysines in the dendritic cell, forming proteins that are recognized as non-self. Peptides from these are presented to T cells, leading to T cell proliferation. IsoLG formation also promotes DC production of cytokines including IL-1β, IL-6 and IL-23, which polarize T cells to produce specific cytokines. Adapted from McMaster et al. [137]

Our laboratory also showed a link between the adaptive and innate immune system in which the B7 ligands that include CD80 and CD86 on antigen presenting cells are essential for the development of hypertension [138]. The B7 ligands interact with the T cell co-receptor CD28, in turn, promoting T cell activation. We showed that blocking the B7 ligands with CTLA4-Ig reduced both Ang II and DOCA-salt induced hypertension. We showed that mice lacking the B7 ligands are protected against hypertension and this protection is lost after transplant of WT bone marrow. Dendritic cells (DCs) are another cell type from the innate immune system that our group and others have found to be important in hypertension. In a study that I participated in, we found that DCs from Ang II-induced hypertensive WT mice have increased amounts of ROS and accumulate isolevuglandin (IsoLG) protein adducts [139]. Compared to macrophages and other

DC subsets, the myeloid or monocyte derived DCs had the highest accumulation of these IsoLG-adducts in hypertensive mice suggesting a potential role of monocytes in differentiation and activation in this disease. The formation of these IsoLG-adducts corresponds to the production of IL-6, IL-1β and IL-23. Further, these modified proteins in DCs seem to act as neoantigens that promote T cell proliferation and production of cytokines including IL-17 and IFN-γ. A schematic of the main findings in this study are illustrated in Figure 1-1. Transfer of DCs from a hypertensive mouse primes hypertension in recipients in response to low dose of Ang II. I showed that exposure of DCs from WT mice with prooxidant *tert*-butyl hydroperoxide (t-BHP) promotes formation of IsoLG-adducts in the myeloid-derived DC populations, which in turn can promote $CD8^+$ T cell proliferation. Adoptive transfer of t-BHP-treated DCs to WT mice exposed to a subpressor dose of Ang II leads to a hypertensive response in these mice (Figure 1-2).

In another study that I participated in, we found that a major stimulus for IsoLG-adduct formation is sympathetic nerve activity, and in particular, renal sympathetic nerves. While controversial, renal sympathectomy has been used to treat hypertension. We sought to determine if renal sympathectomy would prevent immune activation in hypertension. We performed bilateral renal denervation using phenol and shows that this markedly reduced IsoLG-adducts formation in DCs, not only in the kidney, but also in the spleen [140]. As part of this paper, we showed that stimulation of DCs with norepinephrine promoted formation of IsoLG-adducts in these cells. Thus, a factor present in the hypertensive milieu that can cause immune activation is increased catecholamines. Immune cells possess adrenergic receptors and can be activated by innervation not only the kidney, but also the spleen and lymph nodes [141] [142]. The source of peripheral sympathetic activity originates from the central nervous system. We addressed this by using CRE-lox technology to delete the NADPH oxidase subunit $p22^{phox}$ in the subfornical

organ (SFO). This reduced sympathetic nerve activity, markedly blunted the hypertensive response to Ang II, prevented vascular inflammation and reduced T cell activation [143]. We also performed anteroventricular third ventricle (AV3v) lesions in mice and showed that this had a similar effect [144]. In contrast, we increased sympathetic outflow by deleting a key anti-oxidant from the subfornical organ (ECSOD) using CRE-lox technology and showed that this enhanced hypertension and T cell activation [145]. In keeping with these findings, Carnevale et al. showed that sympathetic enervation of the spleen showed placental-like growth (PlGF) production [146]. These data provide strong evidence that the central nervous system plays a central role in immune activation in hypertension.

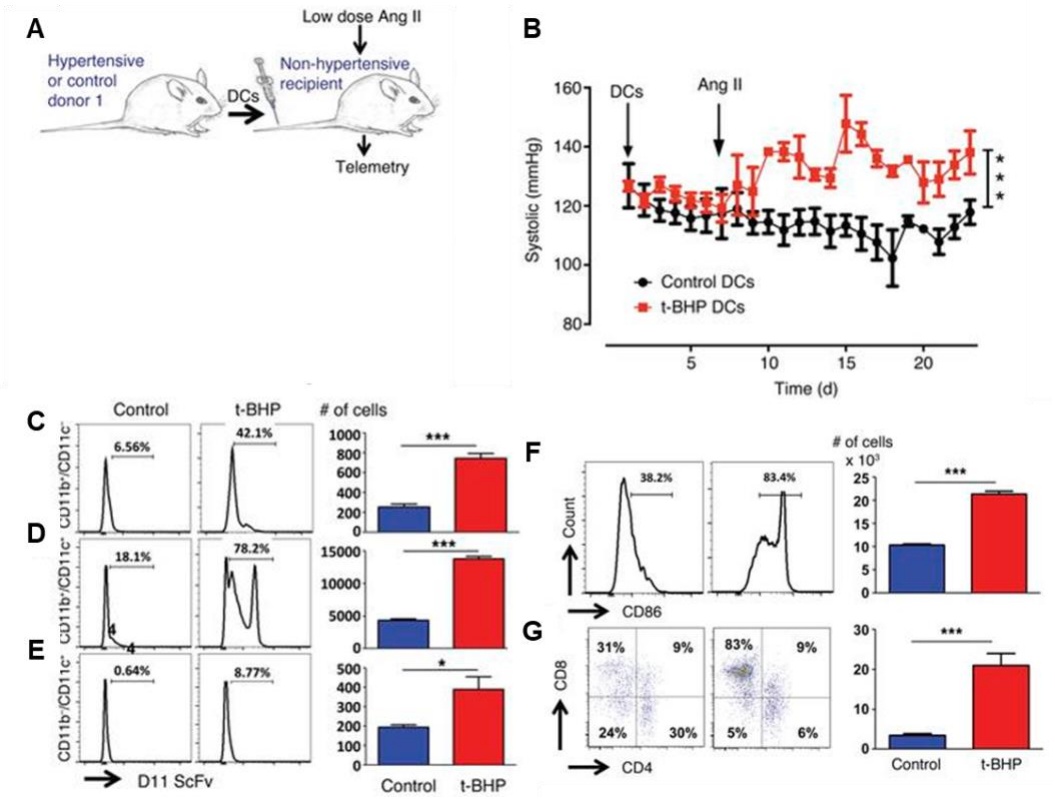

Figure 1-2: Transfer of hypertension by dendritic cells. A. DCs were obtained from WT mice and treated with 1 mM t-BHP. One million of these treated DCs were adoptively transferred to recipient WT mice and blood pressure was monitored using telemetry. **B.** Systolic blood pressure in response to low-dose Ang II infusion (140 ng/kg/min) 10 days after DC adoptive transfer. **C**. DCs were treated with 1 mM t-BHP and IsoLG-adducts were measured by flow cytometry using Alexa Fluor 488-tagged D11 antibody in $CD11b^{+}CD11c^{-}$, (**D**) $CD11b^{+}CD11c^{+}$ and (**E**) $CD11b^{-}CD11c^{+}$ cells. **F**. Expression of CD86 in DCs. G. Co-culture of t-BHP-treated DCs with T cells promoted survival of $CD8^{+}$ T cells (n = 4-7, **p*<0.05, ** *p*<0.01, *** *p*<0.001). Adapted from Kirabo et al. [139].

Another stimulus of immune activation in hypertension is increased sodium. Hypertensive animals and humans have interstitial tissue concentrations of sodium that can exceed the blood plasma concentration by 40 mmol/liter [147]. These concentrations of sodium can stimulate IL-17A production by T cells through the salt-sensing kinase serum and glucocorticoid-related kinase 1 (SGK1) [148]. We have found that deletion of T cell SGK1 blunts hypertension and reduces end-organ damage in response to Ang II or DOCA-salt [13]. I participated in a study in which we found that exposure of DCs to elevated sodium concentrations similar to that observed

in hypertensive humans increases formation of ROS and IsoLG-adducts in DCs [149]. We found that sodium enters DCs via an amiloride-sensitive channel and that this ultimately leads to activation of the NADPH oxidase. Further, these DCs exposed to high levels of sodium can stimulate T cells to proliferate and to produce IL-17A as well as transfer hypertension to a naïve recipient mouse exposed to the subpressor dose of Ang II.

As discussed above, the kidney plays an essential role in the genesis of hypertension. Accumulating evidence supports a role of immune activation in renal dysfunction in this disease. Mice that lack the ability to produce IFN-γ and IL-17 are protected against activation of the sodium transporters described above [150]. Norlander et al. showed that IL-17 treatment of distal convoluted tubular cells caused phosphorylation of SGK1, which can in turn regulate ENAC [13]. Zhang et al. showed that mice lacking the IL-1 receptor 1 are protected against Ang II hypertension and this is associated with a reduction of the NKCC2 [151]. INF-γ released by adjacent T cells can stimulate angiotensinogen production by proximal tubular cells, thus, allowing formation of intrarenal Ang II further enhancing sodium reabsorption [152]. Multi genome-wide association studies identified a polymorphism in the *Sh2b3* gene that encodes the adaptor protein LNK, which correlates to cardiovascular diseases including hypertension as well as other autoimmune disorders. Saleh et al. found that mice lacking LNK have higher inflammation in the kidney and vessels at baseline and that this is further exacerbated with Ang II infusion [153]. LNK deficient mice also develop exaggerated hypertension, ROS production, albuminuria and increased sodium and water retention in response to Ang II infusion. Thus, these animals that have an exaggerated immune response exhibit markedly renal damage and hypertension [154-156].

Recently it has been recognized that the gut microbiome is altered in hypertension that can lead to end-organ damage. Karbach et al. found that germ-free mice were protected against Ang II hypertension and had lower renal and vascular leukocyte infiltration compared to normal mice [157]. This reduction in leukocyte infiltration was associated with a reduction in mRNA expression of monocyte chemoattractant peptide 1 (MCP-1) and reduced endothelial leukocyte rolling. Further, germ-free mice had a reduction in cardiac infiltration of monocytes. More recently, Wilck et al. found that a 14-day challenge with high salt diet increased blood pressure and circulating IL-17A/TNFα positive T cells in humans and that this is associated with a reduction of fecal *Lactobacilus* species [158]. These data confirm an essential role of the immune system in hypertension as well as the interplay between various organs linked by both innate and adaptive immunity.

Leukocyte recruitment to the vascular endothelium

The process of leukocyte recruitment to the site of inflammation involves interaction with the vascular endothelium via a series of complex mechanisms that involves the activity of integrins, selectins and their ligands that initiate the capture and rolling of immune cells. In addition, chemokines released by vascular cells and resident immune cells further promote the transmigration of the adherent cells. ICAM-1 and VCAM-1 that are expressed by endothelial cells binds to lymphocyte function-associated antigen 1 (LFA1) and very late antigen 4 (VLA4), respectively, to allow the process of leukocyte rolling, a process that is triggered by cytokines and chemokines [159, 160]. Another integrin CD11b/CD18 integrin (MAC1) plays an important role in both neutrophil and monocyte crawling during inflammation [161]. The binding of integrins on leukocytes to endothelial cell receptors initiates a signaling event that begins through the activation of phospholipase C (PLC), activation of GTPases and integrin conformational changes

that allow the process of adhesion and transmigration to continue [162]. The process of crawling is the last step before leukocytes undergo transmigration. This process involves the binding of integrins such as MAC1 to endothelial cell molecules like ICAM-1 [163]. Leukocyte transmigration through the endothelial cell barrier occurs at a rapid rate (<2-5 minutes). However, leukocytes take longer to penetrate the endothelial cell basement membrane (>5-15 minutes) [162]. This process can be facilitated or delayed according to the composition of the endothelial cell basement membrane, which is composed in part of pericytes. Leukocytes adherent to the endothelium can induce the formation of docking structures on the endothelium, which are projections rich in ICAM-1 and VCAM-1 [164]. In addition, platelet/endothelial-cell adhesion molecule-1 (PECAM-1) and junctional adhesion molecule A (JAM-A) exist at endothelial cell interphases and creates an adhesive gradient that helps promote transmigration [165]. The transmigration of leukocytes is a process that is stabilized by actin and vimentin [166]. Randolph et al. has shown that human monocytes can become DCs when they reverse-transmigrate an endothelium that is stimulated with LPS, IL-1β, and zymosan [167]. Monocytes that remain in the subendothelium become macrophages. A schematic from a previous review article [162] of the process of leukocyte recruitment to the endothelium, the rolling and transmigration is illustrated in Figure 1-3.

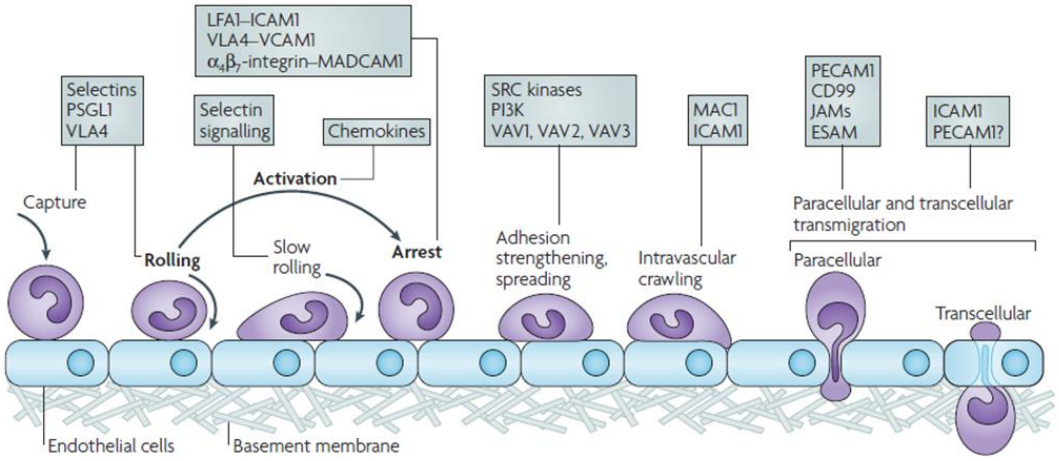

Figure 1-3: The process of leukocyte transmigration through the endothelium. Adapted from Ley et al. [162].

Vascular endothelium and mechanical stretch in disease

Vascular endothelial cells are subjected to various hemodynamic forces including mechanical stretch and shear stress that occur in response to the nature of blood flow. Under physiological conditions, these hemodynamic forces play an important role in modulating vascular homeostasis, cell structure, vascular angiogenesis, proliferation and vascular tone. Hypertension leads to excessive or high levels of mechanical stretch on vessels that lead to pathological consequences including formation of ROS, production of pro-inflammatory factors and lead to apoptosis [168]. Mechanical stretch is modeled *in vivo* through regulation of stretch intensity by the percent of cell elongation from the cell's original dimensions. A low magnitude or elongation of stretch that is considered physiological ranges from 5%-10%, while high elongation pathological levels of stretch range from 10% and above and these are proposed to occur in hypertension [169]. Blood vessels are composed of different layers including the tunica intima, the tunica media and the tunica adventitia. The innermost tunica intima is the layer that contains the endothelial cells, the tunica media contains elastin, collagen and smooth muscle cells, and the outermost layer is the tunica adventitia that is composed of connective tissue,

collagen and elastic fibers. Blood vessels are exposed to two types of stresses in response to the pumping motion of the heart that includes sheer stress and mechanical stretch. Shear stress is the tangential drag of blood over the surface of the endothelium, while mechanical stretch is the longitudinal and circumferential deformation caused by elevations of distending pressure throughout the cardiac cycle.

Mechanical stretch on vessels initiates a series of biochemical signaling cascades that begin from mechanoreceptors on the plasma membrane and ultimately lead to gene expression and protein synthesis that promote angiogenesis, proliferation, inflammation, apoptosis, vascular tone and cell survival. Three known mechanoreceptor proteins that detect mechanical stretch are stretch activated (SA) channel, integrin proteins and PECAM-1 [170]. The membrane-bound SA channel participates in calcium influx in response to stretch, which initiates PI3K and Rho-associated kinase (ROCK) activation that is involved in cellular orientation [171]. Integrins transmit stretch signals from the extracellular matrix (ECM) into the cell and human umbilical vein endothelial cells (HUVECs) exposed to stretch express high levels on integrin $\alpha V\beta_3$ through PI3K activation, which suggests an increase adhesiveness of the cells to RGD (tripeptide of L-arginine, glycine, and –aspartic acid)-containing ECM substrates [172]. Further, the ECM contains a mixture of molecules including collagen, elastin, laminin and fibronectin among others that provides a structural support, adhesion sites, and is essential for vascular remodeling and homeostasis. PECAM-1 also known as CD31, is a cell adhesion molecule highly expressed in regions of cell-cell contact that can sense the change in cell morphology and induce MAP and extracellular signal-regulated kinase (ERK) 1/2 signaling leading to cellular reorientation [173].

Endothelial cells develop morphological changes in response to mechanical stretch that occur due to cytoskeleton and focal adhesion complexes and in response to the emergence of stress

fibers, a bundle of 10-30 actin filaments [174]. Under static conditions, endothelial cells have a polygonal shape and random orientation. Endothelial cells become elongated and perpendicularly aligned in response to the stretch [168]. The ECM plays a role in physiological and pathological stretch in the vasculature. The synthesis and degradation of the ECM is essential for the process of vascular remodeling and for homeostasis of the tissue. MMPs produce zinc-dependent endopeptidases that can breakdown the ECM [175]. During normal levels of stretch, bovine arterial endothelial cells (BAEC) express MMP-2, while in pathological stretch levels HUVECs express increased levels of MMP-2 and MMP-14 and is mediated through TNFα and c-Jun amino-terminal kinases (JNK) pathways [176, 177]. Further, physiological stretch upregulates key tyrosine kinase receptors like FLT-1, Tie-2 and Tie-1 in HUVECs, which are genes involved in angiogenesis and the formation of new blood vessels [178]. Physiological stretch in BAECs induces cell proliferation by PI3K-dependent mammalian target of rapamycin (mTOR) pathway, which regulates cell cycle, proliferation and growth. Uncontrolled proliferation of endothelial cells that occurs in response to pathological stretch can lead to intimal thickening that increases vascular resistance and BP leading to vascular disease [179].

Endothelial cell activation in response to mechanical stretch and other stimuli has long term effects including changes in mRNA and protein expression. Among the genes altered by stretch are cytokines, ROS producing-enzymes, adhesion molecules and MMPs. Further, 10% levels of cyclical stretch on human aortic endothelial cells (HAECs) lead to superoxide production, mediated initially by the NADPH oxidase and subsequently by the NO synthase depending on the presence of tetrahydrobiopterin compared to endothelial cells in static cultures [180]. Superoxide can be dismutated to H_2O_2 either spontaneously or via the enzymatic action of the

superoxide dismutases. ROS formation can in turn activate NFκB and transcription of adhesion molecules. Excess production of ROS or their impaired removal regulates many of the endothelial responses in a pro-inflammatory environment including monocyte adhesion and impaired endothelium-dependent relaxation. NO is a vasodilator that has anti-atherogenic properties and inhibition of NO results in severe hypertension and renal vasoconstriction [181]. Under physiological levels of stretch, endothelial cells increase NO release and reduce ROS formation having a “vasoprotective” effect [182]. Pathological or hypertensive levels of stretch can phosphorylate $p66^{Shc}$ in HAECs, which is an adaptor protein that increases superoxide anion formation that reacts with NO to generate $ONOO^-$ [183-185]. This mechanism will then reduce NO bioavailability that in turn contributes to endothelial dysfunction during hypertensive levels of stretch [186].

Immune cells from the innate and adaptive immune system accumulate in the blood vessel within the perivascular fat and adventitia during cardiovascular disease. These cells communicate with the vessel wall and can promote a series of events that ultimately lead to infiltration and activation of immune cells and the endothelium. Humoral or mechanical stimuli on endothelial cells can activate the NADPH oxidase and initiate signals that cause lymphocyte infiltration and T cell homing [154]. The cytokines released by T cells diffuse to vascular cells promoting further NADPH oxidase activation and, thus, ROS formation, as well as activation of MMPs in the endothelium and vascular smooth muscle cells. The chemokine RANTES, which is released by the endothelium, is detected by its receptor CCR5, that is expressed on T cells and in turn, initiates the process of infiltration. Inflammatory cytokines can also lead to reduction of NO, collagen synthesis and recruitment of more inflammatory cells [137]. We have shown that treatment of mice with etanercept, a TNFα antagonist, increases vascular ROS and enhances

endothelium-dependent vasodilation in Ang II-induced hypertension [125]. Vascular fibrosis occurs in response to vascular inflammation in hypertension. Hypertension increases cyclic stretch in large vessels and as proximal vasculature stiffens this increases the PWV to the distal vasculature and further enhances the end-organ damage. This stretch increases endothelial production and release of IL-6, IL-8, endothelin, ROS and other proinflammatory mediators [168]. Further increased endothelial stretch increases the expression of VCAM-1, ICAM-1 and CD40. We found that RAG1$^{-/-}$ mice and IL-17A$^{-/-}$ mice exposed to Ang II hypertension are protected against aortic stiffness [7]. Further, IL-17A produced by CD4^{+} T cells and γδ T cells play an important role in vascular dysfunction that occurs in response to hypertension [187]. We have shown that increased in endothelial cyclical stretch promotes monocyte activation and differentiation to its various proinflammatory subsets. This will be discussed in more detail on Chapter II.

Signal transducer and activator of transcription and its implications in disease

Signal Transducer and Activator of Transcription (STAT) are a family of cytoplasmic transcription factors that mediate intracellular signaling generated from the cell membrane to the nucleus and control many physiological processes and are exacerbated during inflammatory state [188]. In mammals, the STAT family has seven members including STAT1, 2, 3, 4, 5A and 6 and their structure is composed of six conserved domains. STATs structural domains have a helical N-terminal, a coiled-coil four helix bundle, a central Ig-like DNA-binding domain, a helical liker, a Src-homology 2 (SH2) domain and a C-terminal transactivation domain [189]. STAT activation occurs by phosphorylation of a critical tyrosine residue located in the SH2 domain and C-terminal transactivation domain [STAT1 (Y701), STAT2 (Y690) and STAT3 (Y705)]. Upon cytokine stimulation, Janus kinases (JAKs) are recruited to the receptor and is phosphorylated at specific

residues that constitute docking sites for STAT monomers. Following this, STATs are recruited to the receptor via their SH2 domain and are phosphorylated by JAKs on the respective residues [190]. This phosphorylation enables STATs to either homodimerize or heterodimerize via their SH2 domains and translocate to the nucleus and interact with DNA motifs to promote gene transcription [191]. In STAT3, a second phosphorylation occurs at a single serine 727 that in some cases is necessary for maximal transcriptional activity of STAT3, but is not necessary for DNA binding [192-194]. In particular, STAT3 phosphorylation in the S727 occurs in response to members of mitogen activated protein kinases (MAPK) and JNK family of serine kinases [195].

The entire STAT family can be divided into two groups; the first comprises of STAT2, STAT4 and STAT6 that are involved in T cell development and IFN-γ signaling and the second comprises of STAT1, STAT3 and STAT5, which are also involved in IFN-γ signaling, development of mammary glands and embryogenesis [188]. In response to IL-6, IFN-α/β and IFN-γ activation STAT1 or STAT3 can form homodimers or heterodimers, which then promote expression of many genes. STAT1 and STAT2 are considered pro-inflammatory, while STAT3 has pro-inflammatory and anti-inflammatory properties [189]. STAT3 and NFκB are constitutively active in many human tumors and they cooperate to induce the expression of many genes including CCL5, IL-1β, lL-6, IL-21, IL-17, P2, ICAM-1 and nitric oxide synthase [196].

STATs play an important role in cardiovascular diseases. STAT1 is important for foam-cell formation, atherosclerotic lesion development, promotion of oxidative stress and neointimal hyperplasia [197, 198]. STAT1 activation in DCs is required for induction of MHC and co-stimulatory molecules and, thus, antigen presentation and cross-presentation to activate $CD8^+$ T cells [199, 200]. STAT1-depleted DCs have impaired regulation of MHC and costimulatory molecules as well as reduced Th1 cell priming in responses to *Leishmania major* [201]. STAT2

is involved in regulation of type I IFN signaling and gene expression [202], while STAT3 is involved in vascular SMC de-differentiation, lesion formation and recruitment of inflammatory cells to vessel wall in cardiovascular diseases [203]. In particular, STAT3 is involved in many oncogenic signaling pathways and in cardiovascular diseases as well as other inflammatory diseases. Cytokines like IL-6 and EGF family members and hematopoietic growth factor mediate STAT3 activation and phosphorylation. IL-6 and TGF-β costimulation activate STAT3 and this interaction is required for T helper 17 (T_H17) differentiation and expression of IL-21 [204]. The cytokine IL-21 acts as autocrine factor that sustains STAT3 activation and promotes expression of RORγt that upregulates IL-23R expression, which in turn leads to STAT3-dependent induction of IL-17 [205]. STAT3 is also implicated in B cell differentiation and CD40 expression, which can stimulate activation of JAK3 and STAT3 [206]. Further, STAT3 phosphorylation is increased in atherosclerotic lesions of $ApoE^{-/-}$ mice fed a cholesterol-rich diet [207]. STAT3 signaling induces a large number of genes that are pro-inflammatory including IL-6, 10, 11, 17, 23, CXCL12, and cyclooxygenase-2 (COX-2) [208].

Investigators have used several approaches to inhibit STAT3-mediated events. These include blocking receptors upstream of STAT3 activation, use of a variety of small molecules that directly block STAT3 and blocking downstream signaling events [189]. Some small molecule inhibitors of STAT bind to STAT monomers and/or dimers inhibiting dimerization, oligomerization or disrupt the SH2 domain where the tyrosine is phosphorylated by kinases. Some compounds that target STAT3 phosphorylation of tyrosine 705 in the SH2 domain include STA-21, Stattic, STX-0119 and OPB-31121, all of which are currently in clinical trials and show promising results on experimental mice. In particular, Stattic is a small-molecule that inhibits activation, dimerization, nuclear translocation of STAT3 and selectively inhibits the function of STAT3 SH2 domain [209].

Johnson et al. showed that Stattic prevents alterations of murine carotid arteries vasodilatation and superoxide production caused by Ang II-infusion [210]. This group also found that administration of the STAT3 inhibitor, S31-201, prevented the hypertension and endothelial dysfunction caused by Ang II. Further, mice with reduced STAT3 activity due to mutations in the S727 (SA/SA) had similar levels of systolic BP and mean arterial pressure compared to WT mice, but had reduced cytokines levels associated with heart failure [211]. The SA/SA mice had more fibrosis and they had loss of myocytes compared to WT controls. Thus, loss of STAT3 impairs cardiac function in hypertensive hearts due to a defective myofibrillar structure. Nitric oxide has an important role in modulating STAT3 signaling. Kielbik et al. found that addition of an NO donor, DETA NONOate, to ovarian cancer cell lines inhibited STAT3 and AKT3 phosphorylation and down regulated their cytosolic levels [212]. STATs play pivotal roles in various inflammatory disorders including cancer, autoimmune disease, cardiovascular disease and hypertension. The interplay between STATs and many other signaling pathways makes this a complex area to study.

This dissertation aims to address several outstanding questions that surround vascular stimuli and its involvement in immune activation, specifically in monocytes, which are precursors to many immune cells in hypertension. During hypertension, vessels are exposed to mechanical forces including cyclical stretch that alter the microenvironment of the endothelium and lead to the development of pro-inflammatory events. In Chapter II, we test the hypothesis that hypertensive levels of mechanical stretch on endothelial cells promotes human monocyte activation and differentiation. In Chapter III, we test the hypothesis that hypertension in mice promote activation and differentiation of monocyte and DCs in a similar fashion to human cells. Finally, in Chapter IV, we attempted to engineer human induced-pluripotent stem cells to create

a more personalize method to study the effects of mechanical stretch on cells from the same patients. The findings from the various studies in this dissertation enhance our understanding of how hypertensive stimuli on vessels such as increased mechanical stretch can lead to the activation of immune cells and their differentiation to more specialized subsets, and thus can sustain inflammatory events that are prevalent in hypertension.

Chapter II

Hypertension and increased endothelial mechanical stretch promote monocyte differentiation and activation: Roles of STAT3, interleukin 6 and hydrogen peroxide

Roxana Loperena[1], Justin P. Van Beusecum[2], Hana A. Itani[2], Noah Engel[3], Fanny Laroumanie[2], Liang Xiao[2], Fernando Elijovich[2], Cheryl L. Laffer[2], Juan S. Gnecco[5], Jonathan Noonan[6], Pasquale Maffia [4, 6, 7], Barbara Jasiewicz-Honkisz[8], Marta Czesnikiewicz-Guzik[4], Tomasz Mikolajczyk[8], Tomasz Sliwa[8], Sergey Dikalov[2], Cornelia Weyand[9],Tomasz J. Guzik[4], and David G. Harrison[1,2]

[1]Department of Molecular Physiology and Biophysics, Vanderbilt University, Nashville, TN

[2]Division of Clinical Pharmacology, Department of Medicine, Vanderbilt University Medical Center, Nashville, TN

[3]Department of Biological Sciences, Vanderbilt University, Nashville, TN

[4]Institute of Cardiovascular and Medical Sciences, University of Glasgow, Glasgow, UK

[5]Department of Pathology, Microbiology and Immunology, Vanderbilt University, Nashville, TN

[6]Institute of Infection, Immunity & Inflammation, University of Glasgow, Glasgow, UK

[7]Department of Pharmacy, University of Naples Federico II, Naples, Italy

[8]Department of Internal Medicine and Department of Immunology Jagiellonian University School of Medicine, Cracow Poland

[9]Division of Immunology and Rheumatology, Department of Medicine, Stanford University School of Medicine, Palo Alto, CA

The contents of this chapter have been published in the Journal of Cardiovascular Research

Introduction

In 2016, hypertension was ranked as the leading risk factor for global burden of disease in both developed and underdeveloped countries [213]. Hypertension affects 30% of Western populations and is a major source of morbidity and mortality by promoting atherosclerosis, renal disease, stroke and heart failure [125]. In the past 10 years, it has become evident that activated immune cells infiltrate the kidney and other organs and that these cells contribute to the end-organ damage. In particular, monocytes seem to play a particularly important role in hypertension. Wenzel et al. showed selective ablation of $LysM^+$ myelomonocytic cells in mice completely prevented Ang II induced hypertension and prevented the endothelial dysfunction and vascular oxidative stress generally observed in this model [99].

The mechanism by which monocytes promote hypertension remains undefined but likely involves transformation into activated states or into other cell types, including macrophages and monocyte-derived DCs. Indeed, De Ciuceis et al. found that mice lacking macrophage colony-stimulating factor, required for stimulation of macrophage formation from monocytes, are protected against blood pressure elevation [136]. Further, these mice are protected from vascular remodeling, vascular superoxide production and the alteration of endothelium-dependent vasodilation that normally accompanies hypertension [136]. Likewise, monocyte-derived DCs seem to play a critical role in hypertension. DCs potentially activate T cells, which are essential for full development of hypertension [125]. We have shown that in hypertension, DCs accumulate isolevuglandin-adducted proteins that are immunogenic, and that adoptive transfer of DCs from hypertensive mice primes hypertension in recipient mice. DCs of hypertensive mice produce large quantities of cytokines including IL-6, IL-23 and TNFα and exhibit enhanced ability to drive proliferation of T cells from other hypertensive mice [139]. These

cytokines are activated in response to the phosphorylation of STAT3, which is known to skew T cells towards T_H17 differentiation [214]. The production of IL-17 by such cells is critical for maintenance of Ang II-induced hypertension and vascular dysfunction [129]. Indeed, we have observed increased IL-17A producing T cells in the circulation of hypertensive humans [132].

Circulating monocytes in humans have been classified into three subpopulations depending on their surface expression of the TLR4 co-receptor CD14 and the FcγIII receptor CD16 [101]. Most circulating monocytes are classified as “classical” and exhibit surface expression of CD14 and little or no CD16 ($CD14^{++}CD16^{-}$). These are thought to represent cells newly released from the bone marrow, and they circulate for approximately one day before either dying, transmigrating or transforming into another phenotype [100]. Non-classical monocytes, characterized by their expression of CD16 and low levels of CD14 or $CD14^{low}CD16^{++}$, and are known to expand in inflammatory states. Upon stimulation, these $CD14^{low}CD16^{++}$ cells exhibit increased production of TNFα [113]. In 1988, a small population of monocytes expressing both CD14 and CD16 was identified [215], subsequently termed intermediate monocytes or $CD14^{++}CD16^{+}$ [121]. These cells are also expanded in inflammatory states such as rheumatoid arthritis, psoriasis and peripheral artery disease [107, 108, 216, 217]. Recent deuterium labeling studies indicate that intermediate and non-classical monocytes arise sequentially from the CD14 population [100]. When placed in culture, classical monocytes acquire increasing levels of CD16 with time [215]. The population of monocytes that gives rise to human monocyte-derived DCs remains poorly defined, but includes $CD16^{+}$ cells [89]. Another population are monocytes that express the dendritic cell-specific ICAM-3 grabbing nonintegrin (DC-SIGN) or CD209 DC receptor, which interacts with the leukocyte cell-derived chemotaxin 2 (LECT2). LECT2 is crucial for the process of adhesion and rolling of DCs on endothelial cells and can mediate macrophage activation and

protection against bacterial sepsis [218]. The expression of CD209 on DCs is considered a marker of maturation [219].

A potential source of monocyte activation in hypertension is interaction of these cells with the vascular endothelium. In this regard, Randolph et al. showed that monocytes cultured with endothelial cells that had been stimulated with IL-1β, LPS or zymosan particles differentiate into either DCs or macrophages depending on reverse transmigration through the endothelium [167]. These investigators further showed that $CD16^+$ cells are more likely to reverse transmigrate and that reverse transmigration of monocytes promotes the formation of a $CD16^+$ population [220]. A feature of hypertension that can activate the endothelium is increased mechanical stretch. Indeed, increased cyclic stretch activates transcription factors including AP1, the cAMP responsive binding protein, NFκB in human endothelial cells [221], and a variety of signaling molecules including ERK1/2, the focal adhesion kinase pp125fak, PI3 kinase and p21Ras [222-224]. Gene array studies have indicated that endothelial stretch increases expression of inflammatory mediators including IL-6, IL-8, MCP-1 and VCAM-1 [169]. These events promote monocyte adhesion, rolling and transmigration through the endothelium [92], and some are redox sensitive [225]. Hishikawa and Luscher showed that 10% stretch of human aortic endothelial cells enhances superoxide production, mediated initially by the NADPH oxidase and subsequently by the NO synthase depending on the presence of tetrahydrobiopterin [180].

In the present study, we examined the role of endothelial mechanical stretch and STAT3 in promoting transformation of co-cultured human monocytes to the intermediate phenotype and to cells bearing DC properties. We also examined monocyte subsets and STAT phosphorylation status in humans with hypertension. Our findings provide new insight into how altered mechanical forces in the vessel can promote immune activation.

Material and Methods

Human subjects

We performed three studies: one involved obtaining monocytes from normotensive subjects to analyze their response to endothelial stretch. For this analysis, we included male and female normotensive participants who had blood pressures between less than 135/80 mmHg. In a second study, we examined the phenotype of circulating monocytes from 20 normotensive subjects, 52 subjects with mild hypertension (systolic BP from 130 mmHg to 140 mmHg), and 60 subjects with more severe hypertension (systolic BP >140 mmHg). In a third study, we recruited 15 normotensive subjects and 12 hypertensive subjects for analysis of phospho-STAT levels in circulating monocytes. For this third study, participants were considered hypertensive if they had a systolic blood pressure higher than 140 mmHg, a diastolic blood pressure higher than 90 mmHg or had a diagnosis of hypertension and were currently treated with anti-hypertensive agents. Normal and hypertensive volunteers were included between ages 18-55.

Exclusion criteria included the following: 1) Autoimmune disease or history of inflammatory diseases; 2) Recent vaccinations, within the last 3 months; 3) Confirmed or suspected causes of secondary hypertension; 4) Severe psychiatric disorder; 5) HIV/AIDS; 6) Current treatment with steroids or antihistamines; 7) Liver or renal disease and 8) History of cancer. Protocol 1 and 3 were approved by the Vanderbilt Institutional Review Board and conformed to standards of the US Federal Policy for the Protection of Human Subjects. The Ethics Committee of Jagiellonian University approved protocol two. Written informed consent was obtained from all participants. Demographic and clinical characteristics are shown in Table 2-1 and Table 2-2.

Table 2-1: Clinical characteristics of patients studied for comparison of circulating monocytes

	NT	HTN well controlled	HTN poorly controlled	P value (ANOVA or Chi-Sq)
Age	58.1+/-12	59.8+/-10.9	62+/-10	NS
Race	20/0	52/0	60/0	-
Sex (M/F)	7/13	24/28	27/33	NS
BMI	26.1+/-2.7	28.8+/-5.7	28.0+/-4.7	NS
SBP	120+/-10	127+/-8	147+/-13	<0.001
DBP	77+/-10	81+/-7	90+/-8	<0.001
Cholesterol	5.6+/-1.4	5.2+/-1.5	5.5+/-1.3	NS
Smoking	5/20	16/52	16/60	
Hypercholesterolemia	11/20	35/52	48/60	
Medications (n)				Pearson ChiSq
ACEi	3	41	55	<0.002
CCB	1	14	36	<0.01
BB	5	33	39	0.4
Diuretic	1	25	50	<0.001
ARB	0	5	5	0.7
α1B	0	2	12	<0.02
Statin	8	26	31	0.8

ACEi = angiotensin converting enzyme inhibitor
ARB = angiotensin AT1-receptor blocker
BB = beta-blocker
α1B= alpha-1 adrenergic receptor antagonist
CCB + BB = nifedipine and metoprolol
CCB + α1B = amlodipine and doxazosin

Table 2-2: Demographics of patients studied for analysis of phospho-STAT in circulating monocytes

	Normotensive	*P*	Hypertensive
n	15		12
Age (y)	44.8±3.9	NS	51.3±2.6
Race (W/B)	15/0	NS	9/3
Gender (F/M)	11/4	NS	9/3
BMI (Kg/m^2)	26.6±1.3	<0.03	34.7±2.9
SBP (mmHg)	110.8±3.7	<0.00003	140.5±4.1
DBP (mmHg)	64.4±1.6	<0.003	78.7±3.6
Drug Rx:			
None	15		2
ACEi	0		4
ARB	0		1
HCTZ + ACEi	0		2
HCTZ + ARB	0		1
CCB + BB	0		1
CCB + α1B	0		1

ACEi = angiotensin converting enzyme inhibitor
ARB = angiotensin AT1-receptor blocker
HCTZ = hydrochlorothiazide
BB = beta-blocker
α1B = peripheral alpha-1 adrenergic receptor antagonist
CCB + BB = nifedipine and metoprolol
CCB + α1B = amlodipine and doxazosin

Human aortic endothelial cells

Human aortic endothelial cells (Lonza, Walkersville, MD, USA) were plated on T-75 plates with an initial passage ranging from 3 to 7 and fed every other day with EBM-2 medium (Lonza) containing EGM-2 growth factors and supplements (Lonza) and 2% fetal bovine serum (FBS) or Vascular Cell Basal Medium (ATCC®) with Endothelial Cell Growth Kit-VEGF (ATCC® PCS-100-041) and 5% anti-anti (100X, Gibco). Once cells reached 100% confluency, they were split with 0.25% Trypsin-EDTA (1X) (Gibco) and cultures were kept in 37°C incubators with 5% CO_2.

Monocyte isolation and monocyte-human aortic endothelial cells cultures

HAECs (Lonza, Walkersville, MD, USA) were grown to confluency on flexible 6-well culture plates that permit uniaxial stretch (Flexcell® International Corporation, Burlington, NC, USA). These were coated with collagen I and 1% gelatin cross-linked with 0.05% of glutaraldehyde.

Peripheral blood mononuclear cells (PBMCs) were isolated from blood collected in preparation tube with sodium heparin by Ficoll-density gradient centrifugation (400 rpm, 30 minutes, room temperature). $CD14^+$ monocytes were further isolated from PBMCs using negative selection with the monocyte isolation kit (Miltenyi Biotec 130-096-537; Miltenyi Biotec, Auburn, CA, USA) as previously described [149]. Monocyte purity was confirmed by flow cytometry using an anti-CD14 conjugated antibody and an 80 percent or higher purity was considered viable for experimental purposes. Monocytes from each volunteer were added to the endothelial cells previously grown on Uniflex® 6-well culture plates so that we could simultaneous examine the response of one million monocytes to endothelial cells undergoing 5% and 10% uniaxial stretch. In indicated experiments, 6% and 8% stretch was applied. In some experiments, one million human monocytes were added to Uniflex® 6-well culture plates coated with collagen I and Pronectin® (RGD) (Flexcell® International Corporation) in the absence of HAECs.

Cyclic stretch application

The FX-5000 (Flexcell® International Corporation), a computer-driven strain unit, was used to induce the cyclic mechanical stretch on the monocyte-HAEC monolayers. Uniflex® culture plates are placed on BioFlex® gaskets and placed on greased Arctangle™ Loading Stations™ on the BioFlex® baseplate where cells can be exposed to either 5% (normal) or 10% (hypertensive) uniaxial stretch. This unit is then placed in the culture incubator and provides mechanical stretch that is applied to the flexible membranes on the plates by applying a vacuum that deforms such membranes downward. Compressed air with 30% or lower level of humidity was also applied to the Flexcell® Tension FlexLink® for 48 hours. The loading regimen was for 48 hours of uniaxial cyclical, 5% and 10% elongation stretch, 1 Hz, and ½ sine curve using the Flexcell® Stretch Unit.

Transwell and conditioned media experiments

Transwells® (Costar) permeable 24 mm insert for 6-well plates with 0.4 µM polyester membrane were placed on Flexcell® Transwell Holders for Uniflex® 6-well culture plates coated with collagen I (Flexcell® International Corporation) and 1% gelatin cross-linked with 0.05% of glutaraldehyde. Using this set-up, monocytes were added to the transwells limiting the direct cell contact with confluent HAECs. Once monocytes were added, HAECs were exposed to either 5% or 10% cyclical stretch for 48 hours. In other experiments, HAECs cultured on Uniflex® 6-well culture plates coated with collagen I and 1% gelatin cross-linked with 0.05% of glutaraldehyde were exposed to 5% or 10% cyclical stretch for 48 hours and conditioned media was extracted from these cultures and supplemented with 2% FBS. Conditioned media was stored in -80°C until use and within 6 months of storage. Monocytes isolated from PMBCs of

normotensive humans were cultured with the conditioned media from HAECs for 48 hours in static conditions.

Flow cytometry

Single cell suspension and surface staining: Monocyte populations were collected from the HAEC co-culture by including the cells in suspension and those that adhered to the endothelial cell layer. Adhered monocytes and endothelial cells were released in suspension by digesting the collagen I and 1% gelatin coating with Collagenase A (1 mg/ml, Roche), Collagenase B (1 mg/mL, Roche) and DNase I (0.1 mg/mL, Sigma) in RPMI 1640 medium with 10% FBS for 30 minutes at 37°C. Adhered monocytes cultured on non-coated plates were detached using 1X PBS with 2 mM of EDTA for 10 minutes and placed on ice. In other experiments, PBMCs were isolated by Ficoll-density gradient centrifugation from 20 milliliters of blood of normotensive and hypertensive individuals and directly stained with various markers for flow cytometry. Single cell suspensions were stained for flow cytometry using the following directly conjugated antibodies purchased from Biolegend (San Diego, CA), BD Bioscience (San Jose, CA) and EBioscience/Thermofisher (San Diego, CA): Pacific LIVE/DEAD™ Fixable Violet Dead Cell Stain (Life Technologies); PECy7-conjugated anti-CD209 (BioLegend); APC-CY7-conjugated anti-CD83 (BioLegend); APC-CY7-conjugated anti-CD163 (BioLegend); PerCPCY5.5-conjugated anti-CD14 (eBioscience); AmCyan-conjugated anti-CD16 (BD Bioscience). A known quantity (50 µL) of calibration or counting beads (123count eBeads, eBioscience) was added to each sample prior to analysis. BD FACSCanto II system was used to run the samples and FlowJo® was used for data analysis. Gates for each antibody stain were determined by Fluorescent minus one (FMO) controls and confirmed using isotype controls. We employed live/dead stains to eliminate non-viable cells and selected only single cells for analysis (Figure

2-1B). For freshly isolated human monocytes, we used a gating strategy as described by Urbanski et al. [96]. Results were normalized using bead count and expressed as total number of cells.

Intracellular staining for phosphorylated STAT3, STAT1 and Isolevuglandin-adducts: Human cells were washed and stained first with Pacific LIVE/DEAD™ Fixable Violet Dead Cell Stain (Life Technologies). Human single cell suspensions were then washed and stained with indicated surface antibodies (described above) for 15 minutes at 4°C. Cells were immediately fixed and permeabilized after staining with FIX & PERM® Cell Fixation & Permeabilization Kit (ThermoFisher) by adding 100 µL of Reagent A and incubating for 15 minutes in the dark at room temperature. Cells were washed with 3 mLs of wash medium (1XPBS + 0.1% NaN_3 + 5% FBS). Cells were permeabilized using 100 µL of Reagent B and 3 µLs of either PE-conjugated anti-pSTAT3 (S727) (BD Bioscience), FITC-conjugated anti-pSTAT3 (Y705) (eBioscience), APC-conjugated anti-pSTAT1 (eBioscience) or APC-conjugated anti-pSTAT3 (Y705) (eBioscience) and incubated for 20 minutes at room temperature in dark. In other experiments, the D11 ScFv antibody was used to identify isolevuglandin-lysine adducts independent of protein backbone [139], which was labeled with a fluorochrome using the Fluor 488 Antibody Labeling kit (APEX™, Invitrogen). Cells were permeabilized using 100 µL of Reagent B and 5 µLs of Alexa-fluor 488 conjugated-D11 and incubated for 20 minutes. Cells were washed with 3 mLs of wash medium and resuspended in MACS buffer for flow cytometry analysis. Results were normalized using bead count and expressed as total number of cells or mean fluorescent intensity (MFI).

FlowSight® Imaging Flow Cytometer: Human monocytes and HAECs cultures undergoing 5% or 10% stretch for 48 hours were released in suspension by digesting plate coating with

Collagenase A (1 mg/ml, Roche), Collagenase B (1 mg/mL, Roche) and DNase I (0.1 mg/mL, Sigma) in RPMI 1640 medium with 10% FBS for 30 minutes at 37°C. Cells were then stained with surface markers PerCPCY5.5-conjugated anti-CD14 and PeCy7-conjugated anti-CD83 at a 1:10 concentration in MACS buffer (Miltenyi). Cells were then washed and fixed using the FIX & PERM® Cell Fixation & Permeabilization Kit (ThermoFisher). Intracellular staining was done along with 100 uL Reagent B (permeabilization) and PE-conjugated anti-pSTAT3 (Y705) (1:5 concentration) and Sytox® Green Nucleic Acid Stain (Life Technologies, 1:5000 concentration) for 20 minutes at room temperature. Cells were washed and imaged using FlowSight® Imaging Flow Cytometer at the Flow Cytometry Shared Resources core at Vanderbilt University.

Co-Immunoprecipitation and Western Blotting

For the following experiments, monocytes were isolated from the monocyte-HAEC cultures using the negative selection for human CD31 MicroBeads Kit human (Miltenyi Biotec). Co-immunoprecipitation (co-IP) and Western blotting were performed as previously described [149], cells were lysed in 150 uLs of the lysis buffer solution, 10 mLs of RIPA buffer (Sigma) and one tablet of complete Tablets protease inhibitor cocktail (Roche) and one tablet of the PhosSTOP EASYpack phosphatase inhibitor cocktail (Roche). Protein was quantified using the Pierce™ BCA Protein Assay Kit (ThermoScientific). For co-IP, samples (20 µg of protein) were incubated with total STAT3 antibody (124H6, Cell Signaling Technology) at 1:150 concentration for 1 hour at 4°C and 15 µLs of Protein A/G PLUS-Agarose (sc-2003) were added to lysates and gently rocked at 4°C overnight. Immunoprecipitated samples or protein samples (20 µg) were separated by SDS-PAGE and transferred to a nitrocellulose membrane and blocked with 5% milk and 1% BSA in 1X TBS-T as previously described [226]. Membranes were probed with primary antibody total STAT1 antibody (D1K9Y, Cell Signaling). Membranes were labeled using

horseradish peroxidase (HRP)-conjugate and detected with chemiluminescence solution using the SuperSignal™ West Femto Maximum Sensitivity Substrate (Thermo Scientific). Membranes were imaged with a BioRad ChemiDoc Imager. Blots were then stripped for 15 minutes and re-probed using an antibody for total STAT3 (Cell Signaling). Densitometry was performed using the BioRad Image Lab software and bands of interest were normalized to total STAT3.

Quantitative RT- PCR

Monocytes were lysed in RLT buffer with 1% of β-mercaptoethanol and RNA was extracted using the RNeasy Mini Kit (Qiagen). RNA quantity and purity was measured using a spectrophotometer. RNA was used for reverse transcriptase cDNA synthesis using both iScript cDNA synthesis kit (BioRad, Hercules, CA, USA) or the High Capacity cDNA reverse transcriptase kit (Applied Biosystems). Samples were evaluated for human IL-6, IL-1β, IL-23, TGF-β, CD168, $p22^{phox}$, CCL4, IL-18, CCL2, MMP8 and TNFα using Taqman primers. Relative quantification was determined using the comparative CT method where samples were normalized to GAPDH and calibrated to the average of the control group (5% stretch).

Visualization of monocytes with endothelial cells in co-cultures

One to two million human monocytes isolated from PBMCs of normotensive people were incubated with 12 μM of CellTracker™ Green CMFDA Dye (C2925, ThermoFisher Scientific, Waltham, MA, USA) in EBM2 medium (Lonza) for 30 minutes at 37°C according to manufacturer's instructions. After incubation, cells were washed with medium and one million fluorescently tagged with monocytes were added to wells containing either confluent HAECs on collagen I/gelatin coated 6-well stretch plates or without the presence of endothelial cells in 6-well stretch plates coated with collagen I or Pronectin® (RGD, Flexcell® International Corporation). Endothelial-containing cultures or monocytes alone were exposed to either 5% or

10% levels of continuous uniaxial stretch for 24 hours. Cells were subsequently washed with 1X PBS and the remaining cells were fixed with 4% paraformaldehyde (PFA) solution for 15 minutes at room temperature. The cells were then permeabilized with 0.5% Triton X-100 (Sigma) in 1X PBS for 30 minutes at room temperature. Cells underwent several washes in PBS and were blocked with goat serum solution (5% goat serum and 2.3 % glycine in PBS) for 1 hour at room temperature. Cultures with endothelial cells were then stained with the primary purified anti-human CD54 (ICAM-1, HA58, Biolegend, San Diego, CA, USA) at a 1:100 concentration in goat serum solution for 1 hour at room temperature followed. Cells were then stained with the ReadyProbes secondary antibodies conjugated with Alexa Fluor™ 594 dyes goat anti-mouse antibody (R37121, ThermoFisher Scientific) using one drop per mL of PBS and incubation for 30 minutes at room temperature. Finally, all plates' flexible membranes were mounted unto glass slides and ProLong® Gold antifade reagent with DAPI (ThermoFisher Scientific) was used to stain for cells' nucleus before adding the coverslip. Imaging of the slides was performed using an EVOS™ FL Imaging System (ThermoFisher Scientific). Adhered monocytes were counted using ImageJ software in three random fields and an average was calculated and used as a graphing representative.

For imaging with confocal microscopy, membranes were fixed in 4% PFA for 15 minutes at room temperature, washed with PBS and then blocked for one hour in Dako Serum Free Protein Block (DSFPB) (Agilent Technologies, Santa Clara, CA). Membranes were incubated with purified anti-CD83 antibody (BioLegend; category number 305301) or isotype matched control (Biolegend; category number 400102) in DSFPB overnight at 4^{o}C, washed in PBS, and then probed with Alexa Fluor 647 labeled anti-Murine IgG raised in goat (ThermoFisher Scientific) for 30 minutes. Following washing in PBS, membranes were stained with anti-CD31-FITC (BioLegend; category

number 303103) and anti-CD14-Alexa Fluor 594 (BioLegend; category number 325630) for two hours at room temperature. Samples were washed in PBS and counterstained with DAPI for 10 minutes. Membranes were washed in PBS and then mounted on glass-bottomed dishes. Immunofluorescent images were then acquired using a Zeiss Cell Observer SD confocal fluorescent microscope (Zeiss, Oberkochen, Germany).

Compounds

Several compounds were used to determine the mechanisms of processes including STAT3 inhibitor, Stattic (5 µM, Sigma), tofacitinib citrate (100 ng/µL, Sigma), tocilizumab (100 ng/mL, Genentech), neutralizing antibody anti-IL-6 (10 µg/mL, BioLegend) and an IL-6/IL-6R fusion protein (hyper IL-6, 100 ng/mL) provided by Dr. Stefan Rose-John. In addition, we used DETA NONOate (300 µM/1000 µM, Cayma), Nω-Nitro-L-arginine methyl ester hydrochloride (L-NAME) (ab120136, 100/ 300/1000 µM, ABCAM) and IsoLG-adducts scavenger, 2-hydroxybenxylamine (2-HOBA) (10 µM, Vanderbilt). Additional pharmacological inhibitors were used including tempol (100 µM, Sigma), ebselen (1 µM, Sigma), mito-ebselen (1 nM, Dikalov laboratory), catalase (20 µg/µL, Sigma), PEG-catalase (500 U/mL, Sigma), valdecoxib (100 nM, Cayman) and napabucasin (1 µM/L, MedChem). All these concentrations were determined by dose-curve experiments or previously published literature tested at *in vitro* cell culture conditions.

Enzyme-Linked Immunosorbent Assay (ELISA)

Human aortic endothelial cells were exposed to 5% or 10% cyclic mechanical stretch for 48 hours. Conditioned media from these cell cultures was collected and spun down to eliminate cellular debris. IL-6, LECT 2, and High Mobility Group Box-1 (HMGB-1) proteins were quantified using ELISA kits from LS-Bio, Affymetrix and IBL International, respectively. ELISAs were performed according to manufacturers' instructions. A standard curve was created using the

standards provided and serial dilutions were performed (1:2, 1:10, 1:20, 1:50, 1:100) and added to each well. Samples were also added to the appropriate wells and incubated for the indicated time points. ELISA plates were washed in wash buffer and detection antibody was added. Avidin-HRP was added to each for detection and a substrate for HRP was added for color change and to be read at a 450 nm wavelength.

Statistics

All data are expressed as mean ± SEM. One tailed- paired and unpaired Student's *t*-tests were used to compare two groups. In case of the non-normality, the nonparametric test one-tailed Mann-Whitney U test was used. When examining the effect of varying endothelial percent stretch on monocyte transformation to the intermediate phenotype, we employed one-way ANOVA with Student Newman Keuls post-hoc test. When examining the effect of DETA-NONOate, we employed the Friedman's multiple comparison test followed by the Dunn's post-hoc test. To compare the distribution of monocyte subtypes in normotensive humans vs humans with mild or severe hypertension, we employed one-way ANOVA. To compare pSTAT levels in monocytes from normotensive and hypertensive subjects, we employed two-way ANOVA with Student Newman Keuls post-hoc test. *P* values are reported in the figures and were considered significant when less than 0.05. Power analyses for the various experiments are provided in Table 2-3.

Table 2-3. Power achieved for each experimental condition

Experimental Condition	Number per group	Experimental Design	Effect Size	Achieved Power
5% vs. 10% Stretch	10	Paired	1.87*	1.00*
Effect of Stattic	7	Paired	1.05*	0.79*
DETA - NONOate	10	Nonparametric	1.3*	0.84 for Nonparametric*
Human monocyte distribution	20 to 60	ANOVA	0.69	0.80*
pSTAT3 MFI in NT humans	15	ANOVA	1.22	0.90ŧ

* For intermediate monocytes; ŧ for pSTAT3 (Y) MFI from normotensive human intermediate vs classical monocytes.

Results

Hypertensive mechanical stretch in human endothelial cells promotes monocyte activation and differentiation: It has been previously reported that endothelial cells activated by zymosan, LPS or IL-1β promote conversion of monocytes to DCs [167]. A feature of hypertension that activates endothelial cells is increased mechanical stretch. We therefore isolated $CD14^{+}$ monocytes from PBMCs of normotensive humans and co-cultured these with HAECs undergoing 5% or 10% mechanical stretch for 48 hours as shown by the illustration in Figure 2-1A. The intermediate monocyte $CD14^{++}CD16^{+}$ population (Figure 2-1B, 1C) and the $CD14^{++}CD209^{+}$ population (Figure 2-1B, 1D) were significantly increased in the co-cultures with HAECs undergoing 10% vs. 5% stretch. The non-classical monocyte population defined as $CD14^{low}CD16^{++}$ displayed a trend to increase in response to 10% endothelial stretch (Figure 2-1E). The macrophage population defined as $CD14^{+}CD163^{+}$ (Figure 2-1F) and the classical monocyte population defined as $CD14^{++}CD16^{-}$ (Figure 2-1G) were not different between experimental groups. Another marker of monocyte activation and DC development is CD83 [227], however only a few monocytes expressed $CD83^{+}$ after co-culture (Figure 2-1H) and these were not changed by endothelial stretch. In keeping with the state of monocyte activation, 10% endothelial stretch promoted a striking upregulation of monocyte mRNA for the cytokines IL-6, IL-1β, IL-23, TNFα, and CCL4 compared to 5% stretch (Figure 2-1I). In contrast, stretch did not affect monocyte expression of TGFβ–1, MMP8, CCL2, IL-18, or CD168 (Figure 2-2). Intermediate levels of endothelial stretch ranging from 6% to 8% failed to alter the phenotype of human monocytes (Figure 2-3A). There was also no difference in the percent of live cells between 5% and 10% endothelial stretch (Figure 2-3B).

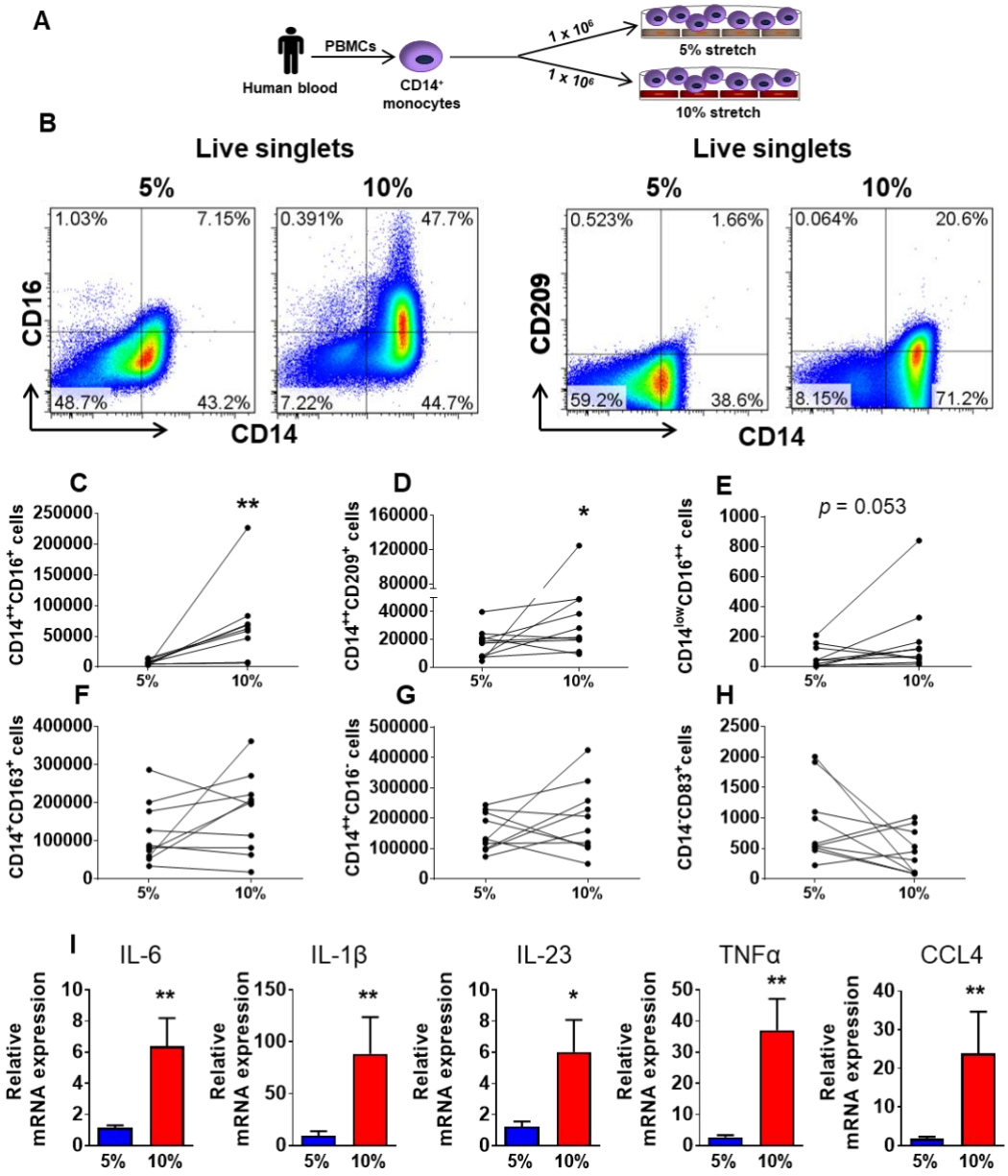

Figure 2-1: Hypertensive mechanical stretch in human endothelial cells promotes monocyte activation and differentiation. Human $CD14^{+}$ monocytes were isolated by magnetic sorting from PBMCs of normal human volunteers and cultured with HAECs exposed to cyclical stretch. **A.** Schematic of methods and (**B**) gating strategy for phenotyping human monocyte subsets including classical ($CD14^{++}CD16^{-}$), intermediate ($CD14^{++}CD16^{+}$), non-classical monocytes ($CD14^{low}CD16^{++}$) and the $CD14^{++}CD209^{+}$ cells comparing 5% and 10% stretch are shown. **C.** Changes in numbers of cells for each subject are depicted by connected lines for $CD14^{++}CD16^{+}$ (n = 9) and (**D**) $CD14^{++}CD209^{+}$, (**E**) $CD14^{low}CD16^{++}$ (**F**) macrophage population ($CD14^{+}CD163^{+}$), (**G**) $CD14^{++}CD16^{-}$, (**H**) $CD14^{-}CD83^{+}$ (n=10). **I.** Relative monocyte mRNA expression of IL-6, IL-1β, IL-23, TNFα and CCL4 in adhered and monocytes in suspension (5%, n=15; 10%, n=16). Comparisons were made using one-tail paired *t*-tests (**p*<0.05, ***p*<0.01).

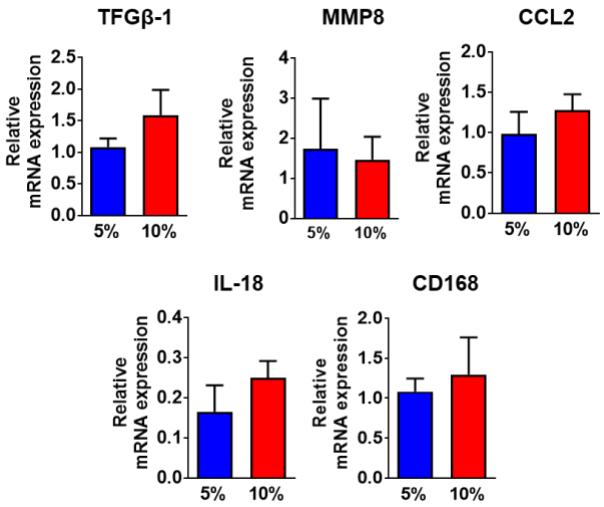

Figure 2-2: Hypertensive mechanical stretch in human endothelial cells effects on monocyte gene profile. Human CD14^{+} monocytes were isolated from PBMCs of normal human volunteers and cultured with HAECs exposed to 5% or 10% stretch for 48 hours. Relative monocyte mRNA expression of TGFβ-1 (n=8), MMP8 (5%, n=3; 10%, n=4), CCL2 (n=5), IL-18 (n=5) and CD168 (n = 8) in monocytes. Statistical differences were determined using one-tailed unpaired *t*-tests (***p*<0.01).

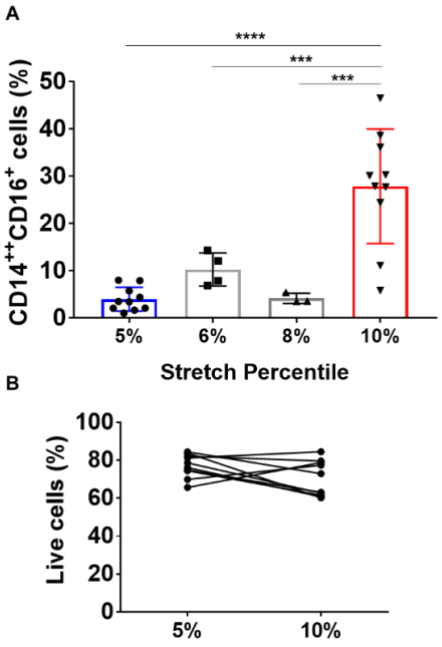

Figure 2-3: Intermediate levels of endothelial stretch and effects on monocyte phenotype. A. Human CD14^{+} monocytes were isolated from PBMCs of normal participants and cultured with HAECs undergoing 5% (n = 10), 6% (n = 4), 8% (n = 3) and 10% (n = 10) cyclical stretch for 48 hours. Mean data showing the percent number of intermediate monocytes in response to each stretch percentile. **B.** Mean data showing the percent number of live cells after 48 hours of endothelial 5% and 10% stretch. Comparisons were made using one-way ANOVA with Student Newman Keuls post-hoc test and one-tailed paired *t*-tests (****p*<0.001, *****p*<0.0001).

Hypertensive mechanical stretch on endothelial cells promotes STAT3 activation in co-cultured monocytes: Increased expression of IL-6, IL-1β and lL-23 resemble a cytokine response typical of STAT3 signaling [228]. In addition, STAT3 activation has been identified as a checkpoint for FLT-3-regulated DC development [229]. We therefore sought to determine whether STAT3 plays a role in monocyte activation and differentiation when exposed to HAECs undergoing stretch. STAT3 activation occurs upon phosphorylation of tyrosine (Y) 705 and/or serine (S) 727. When activated, STAT3 can also form a heterodimer with STAT1. Using intracellular staining, we found that the $CD14^{++}CD16^{+}$ intermediate (Figure 2-4A, 4C-E) and the $CD14^{++}CD209^{+}$ populations (Figure 2-4B, 4F-H) had a significant increase in pSTAT3 (Y705), pSTAT3 (S272) and pSTAT1 when cultured with endothelial cells undergoing 10% stretch. We also observed an increase in STAT3 and STAT1 phosphorylation in cells that remained $CD14^{++}CD16^{-}$, but not in the non-classical monocytes (Figure 2-5A-B). Given that both STAT3 and STAT1 are activated in monocytes that underwent transformation, we considered the possibility that this involved heterodimerization of the two STAT isoforms, however, we were unable to detect association of the two using co-immunoprecipitation (Figure 2-5C). Moreover, we were unable to detect fluorescence resonance energy transfer between STAT1 and STAT3 using flow cytometry-based method (data not shown).

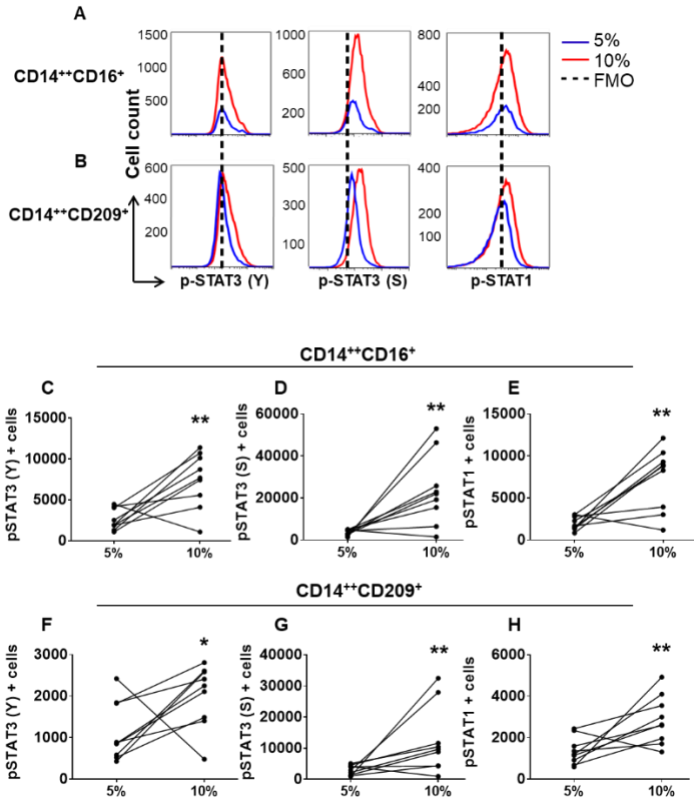

Figure 2-4: Effect of endothelial stretch on STAT3 activation in co-cultured monocytes. Human $CD14^{+}$ monocytes were isolated from buffy coats of normal human volunteers and cultured with HAECs exposed to 5% or 10% cyclical stretch. **A**. Representative flow cytometry plots are shown for intracellular staining of STAT3 phosphorylation in the tyrosine (Y) 705 and the serine (S) 727 and STAT1 phosphorylation in the Y701 in the $CD14^{++}CD16^{+}$ intermediate monocytes and (**B**) the $CD14^{++}CD209^{+}$ cells in the 5% stretch (blue), 10% stretch (red), and the dashed line represents FMO control. **C-E.** Changes in numbers of intermediate monocytes between 5 and 10% endothelial cell stretch expressing pSTAT3 (Y), pSTAT3 (S), and pSTAT1 are depicted by connected lines. **F-H.** Changes in numbers of $CD14^{++}CD209^{+}$ cells expressing pSTAT3 (Y), pSTAT3 (S), and pSTAT1 between 5% and 10% endothelial cell stretch. Comparisons were made using one-tail paired *t*-tests (n = 9, * $p<0.05$, ** $p<0.01$).

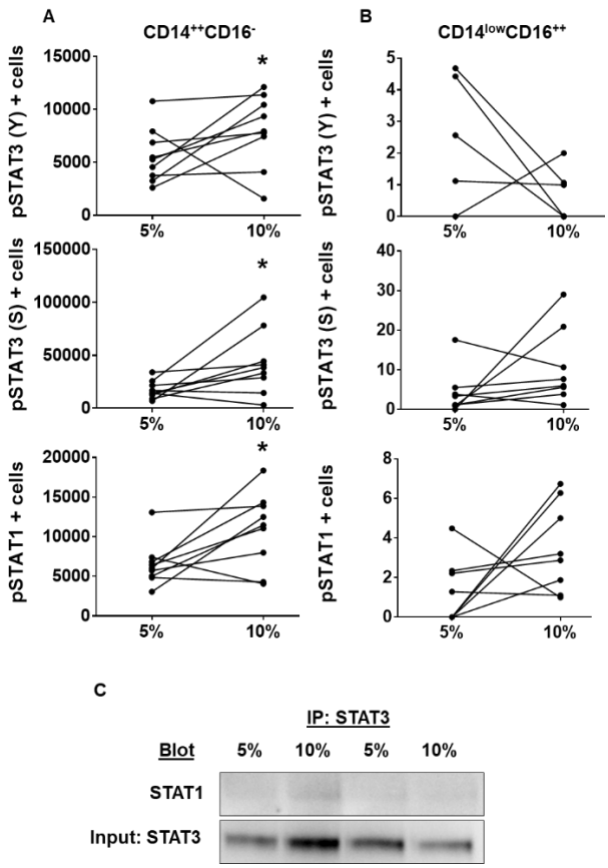

Figure 2-5: STAT3 and STAT1 expression in other monocyte subpopulations when culture with endothelial cells undergoing mechanical stretch. Human $CD14^{+}$ monocytes were isolated from PBMCs of normal human volunteers and cultured with HAECs exposed to 5% or 10% stretch for 48 hours. **A**. Individual values for number of cells within the classical monocyte population expressing p-STAT3 (Y), p-STAT3 (S), and p-STAT1 for each subject are indicated by connected lines (n= 9). **B**. Values for total number of cells within the $CD14^{low}CD16^{++}$ non-classical population expressing p-STAT3 (Y), p-STAT3 (S), and p-STAT1 for each participant (n = 8). **C.** Proteins from monocyte cell lysates (20 µg) in cultures with HAECs exposed to 5% or 10% stretch after 48 hours were immunoprecipitated with total STAT3 and subjected to Western Blot detection of total STAT1 protein. Representative of two independent experiments are shown (n=8). Statistical differences were determined using one-tailed paired *t*-tests (*p<0.05).

STAT3 plays a role in monocyte differentiation and activation during hypertensive mechanical stretch of endothelial cells: To determine a specific role of STAT3 in differentiation of monocytes during stretch, we employed Stattic, a nonpeptidic small molecule that selectively inhibits the function of the STAT3 SH2 domain [209]. Addition of Stattic to the cell culture reduced formation of the $CD14^{++}CD16^{+}$ intermediate monocyte population (Figure 2-

6A, 6C) and $CD14^{++}CD209^{+}$ DC population in response to 10% stretch (Figure 2-6B, 6D). Likewise, Stattic reduced pSTAT3 (Y), pSTAT3 (S), and pSTAT1 in the $CD14^{++}CD16^{+}$ intermediate (Figure 2-6E-G) and the $CD14^{++}CD209^{+}$ monocyte populations (Figure 2-6H-J). Further, we found that addition of Stattic to monocyte-HAEC cultures undergoing 10% stretch reduced upregulation of mRNA for the cytokines IL-6, IL-1β, and IL-23 (Figure 2-6K).

Next, we sought to determine mechanisms by which endothelial cells undergoing stretch could activate monocytes and promote STAT3 phosphorylation in adjacent monocytes. Our group has reported an increase formation of IsoLG-adducts in monocytes and DCs of hypertensive mice and humans [139]. IsoLGs adduct to protein lysines and can potentially act as a neoantigen, which induce T cell activation and formation of cytokines. To examine IsoLG-adduct formation in monocyte populations in response to endothelial mechanical stretch, we used flow cytometry and intracellular staining using an Alexa Fluor 488-tagged single-chain antibody specific for IsoLG-adduct, D11 [230]. We found that the $CD14^{++}CD209^{+}$ population had the highest accumulation of IsoLG-adducts compared to the classical monocytes, macrophages and $CD83^{+}$ DCs when cultures with endothelial cells undergoing 10% stretch (Figure 2-7).

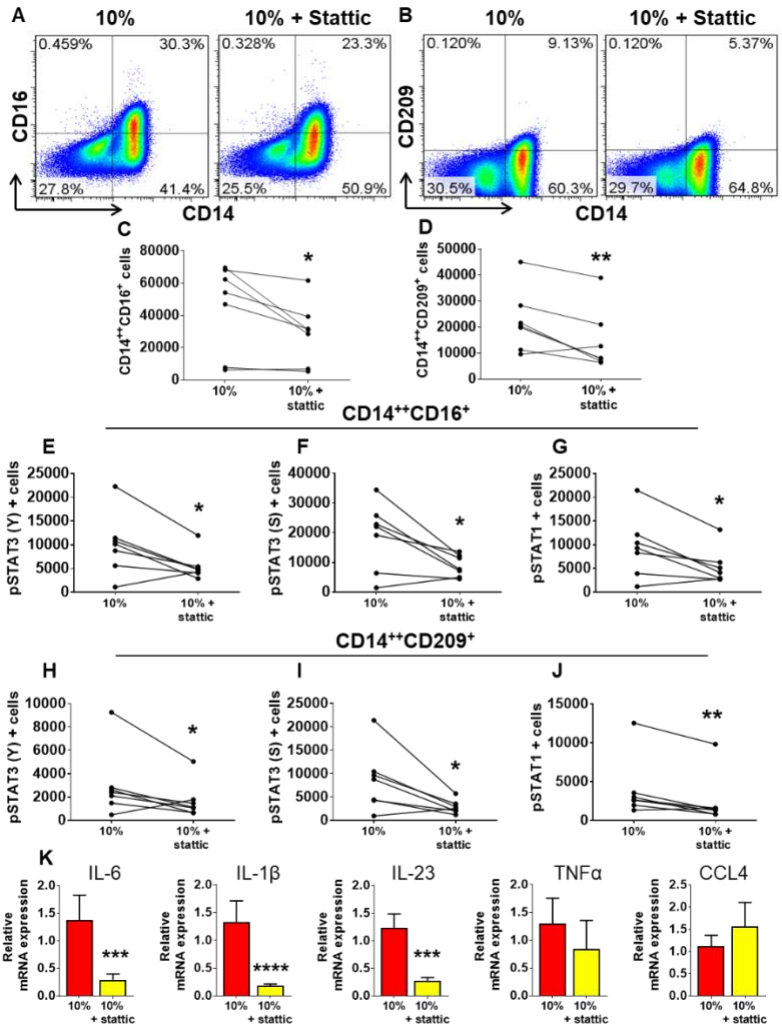

Figure 2-6: STAT3 contributes to monocyte differentiation and activation during hypertensive mechanical stretch of endothelial cells. Human CD14^{+} monocytes were isolated from PBMCs of normal human volunteers and cultured with HAECs exposed to 10% or 10% stretch plus STAT3 inhibitor (5 µM), Stattic, for 48 hours. **A.** Flow cytometry gating examples are shown for the CD14^{++}CD16^{+} intermediate monocyte population and (**B**) the CD14^{++}CD209^{+} cells. **C.** Individual data point for the effect of Stattic on the number intermediate monocytes and (**D**) CD14^{++}CD209^{+} cells for each subject. **E-G.** Effect of Stattic on total number of cells expressing pSTAT3 (Y), pSTAT3 (S), and pSTAT1 within the intermediate monocyte population and (**H-J**) the CD14^{++}CD209^{+} population. A total of n=7 participants per group were used. **K.** Relative monocyte mRNA expression of IL-6, IL-1β, IL-23 (10%, n= 11; 10% + Stattic, n = 9), TNFα (n = 7), and CCL4 (n =4) in monocytes. Comparisons were made using one-tail paired *t*-tests (*p<0.05, ** p<0.01, *** p<0.001, **** p<0.0001).

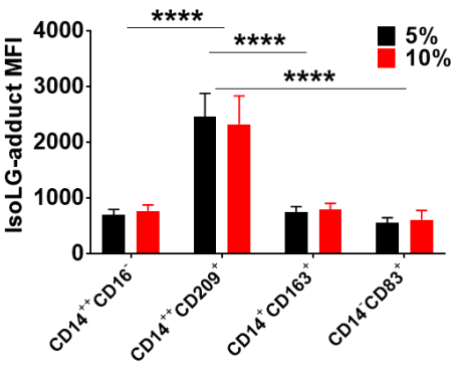

Figure 2-7: Accumulation of IsoLG-adducts in different monocyte-derived populations exposed to endothelial cells undergoing stretch. Monocytes isolated from PBMCs of normal subjects was added to endothelial cells, which underwent 5% and 10% stretch for 48 hours. IsoLG-adducts were measured by intracellular staining flow cytometry using Alexa Fluor 488-tagged D11 antibody. Mean fluorescent intensity (MFI) for IsoLG-adducts are shown for the classical, CD209 population, macrophage population and the DCs comparing 5% vs 10%. Two-way ANOVA with Student Newman Keuls post-hoc test was used (n = 8; *** p<0.001).

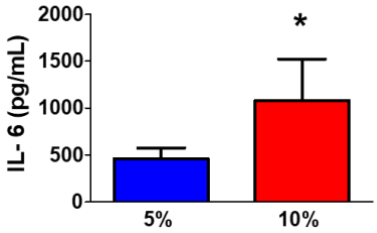

Figure 2-8: Interleukin 6 is released by endothelial cells undergoing hypertensive mechanical stretch. Human aortic endothelial cells were grown to confluency and exposed to either 5% or 10% stretch for 48 hours. Conditioned media from HAECs exposed to various levels of stretch was used to detect IL-6 by ELISA and normalized according to a concentration curve. Mean values for IL-6 are shown as pictogram per milliliter. Statistical difference was determined using a one-tailed unaired *t*-test (n= 9; *p<0.05).

Others have reported that stretch stimulates expression of IL-6 by endothelial cells, and we confirmed a 2-fold increase in IL-6 protein production by HAECs undergoing 10% cyclical stretch (Figure 2-8). IL-6 has been shown to both stimulate STAT3 activation and to be produced in response to STAT3 in a feed-forward fashion [231]. Addition of an IL-6 neutralizing antibody to the endothelial/monocyte co-cultures markedly reduced formation of intermediate monocytes (Figure 2-9A-B), while having no effect on the $CD14^{++}CD209^{+}$ population (Figure 2-9C).

STAT3 can also be activated by ROS, including hydrogen peroxide [228]. ROS, in turn can stimulate IL-6 production by the endothelium [232]. Increased endothelial stretch can stimulate ROS formation and, thus, we performed additional experiments using Tempol, a superoxide dismutase mimetic, or PEG-Catalase, to scavenge hydrogen peroxide. While Tempol had no effect (data not shown), we found that PEG-Catalase markedly reduced formation of intermediate monocytes in response to 10% endothelial stretch (Figure 2-9D). Similar to anti-IL-6, PEG-Catalase did not inhibit formation of the CD209 population (Figure 2-9E). In keeping with these results with anti-IL-6 and PEG-Catalase, we found that these interventions also inhibited pSTAT3 (S727) and pSTAT1 (Y701) and exhibited a trend to inhibit pSTAT3 (Y705) (Figure 2-9F-G) within the intermediate monocytes.

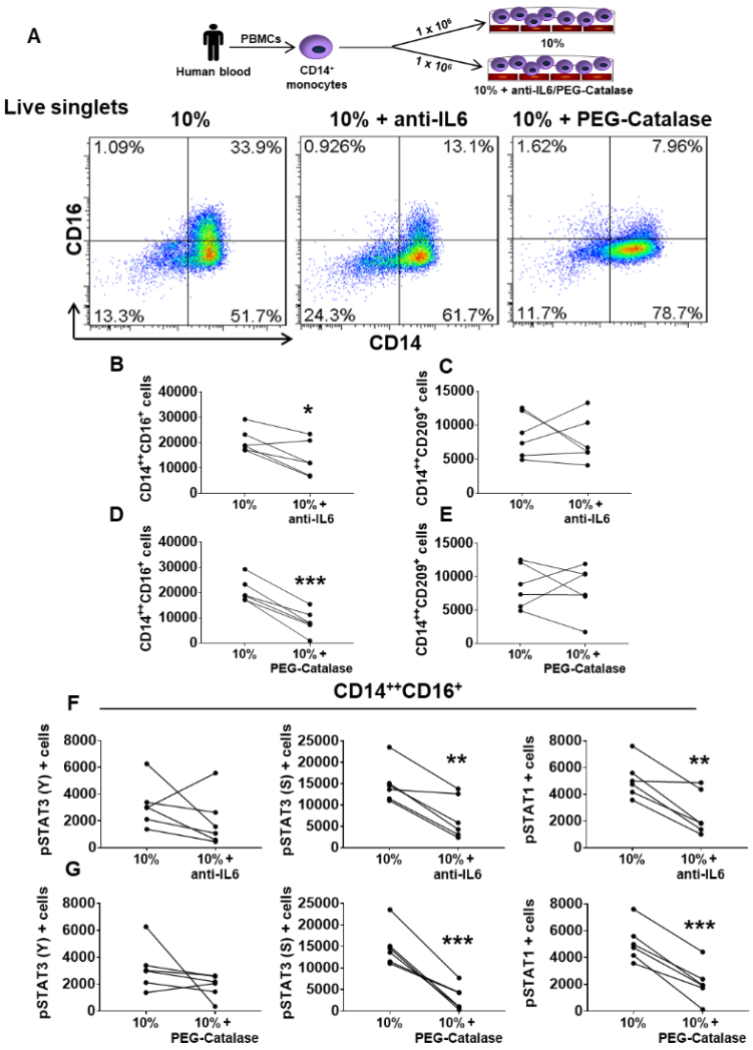

Figure 2-9: IL-6 and hydrogen peroxide play a role in monocyte transformation and activation. Human $CD14^{+}$ monocytes were isolated from PBMCs of normal human volunteers and cultured with HAECs exposed to 10% stretch, 10% plus anti-IL-6 neutralization antibody (10 µg/mL) or 10% plus PEG-Catalase (500 U/mL) for 48 hours. **A.** Schematic of methods and **f**low cytometry gating representatives are shown for the $CD14^{++}CD16^{+}$ intermediate monocyte population exposed to 10%, 10% + anti-IL-6, and 10% + PEG-Catalase. **B**. Effect of anti-IL-6 on the total number of intermediate monocytes and (**C**) the $CD14^{++}CD209^{+}$ cells for each subject. **D**. Effect of PEG-Catalase on total number of intermediate monocytes and (**E**) the $CD14^{++}CD209^{+}$ cells for each participant. **F.** Effects of anti-IL-6 and **G.** PEG-Catalase on number of cells expressing pSTAT3 (Y), pSTAT3 (S), and pSTAT1 within the intermediate monocyte population for each subject. Data with and without these interventions for each subject are shown by the connected lines. A total of n=6 participants per group and per experimental treatment were used. Comparisons were made using one-tail paired *t*-tests (*p<0.05, ** p<0.01, *** p<0.001).

Increased endothelial stretch has also been shown to uncouple the endothelial NO synthase and to reduce stimulatory phosphorylation of eNOS in endothelial cells [180, 233]. Likewise NO has been shown to suppress IL-6-induced STAT3 activation in ovarian cancer cells [234]. We therefore hypothesized that a loss of bioavailable NO might promote STAT3 activity. In keeping with this hypothesis, we found the NO donor DETA-NONOate (DETA NONO) dramatically reduced formation of intermediate monocytes (Figure 2-10A, 10C) and the activation of STAT3 (Y), STAT3 (S), and STAT1 when added to monocytes cultures in the absence of endothelial cells (Figure 2-10D-F). Further, addition of this NO donor also reduced formation of $CD14^{++}CD209^{+}$ cells (Figure 2-10B, 10G) and activation of STAT3 (Y05), STAT3 (S727), and STAT1 (Figure 2-10H-J). We further found that addition of the NO synthase inhibitor L-NAME to monocytes undergoing 5% stretch significantly increased pSTAT3 (Y705), pSTAT3 (S272), and pSTAT1 levels in intermediate monocytes (Figure 2-10K).

We considered the possibility that LECT2, a ligand for CD209, might be released by endothelial cells, however, we were unable to detect LECT2 released from HAECs undergoing either 5% or 10% stretch using ELISA (data not shown). We were also unable to detect release of the HMGB-1 chromatin binding protein, which has been shown to activate STAT3 [235], from stretched endothelial cells (data not shown).

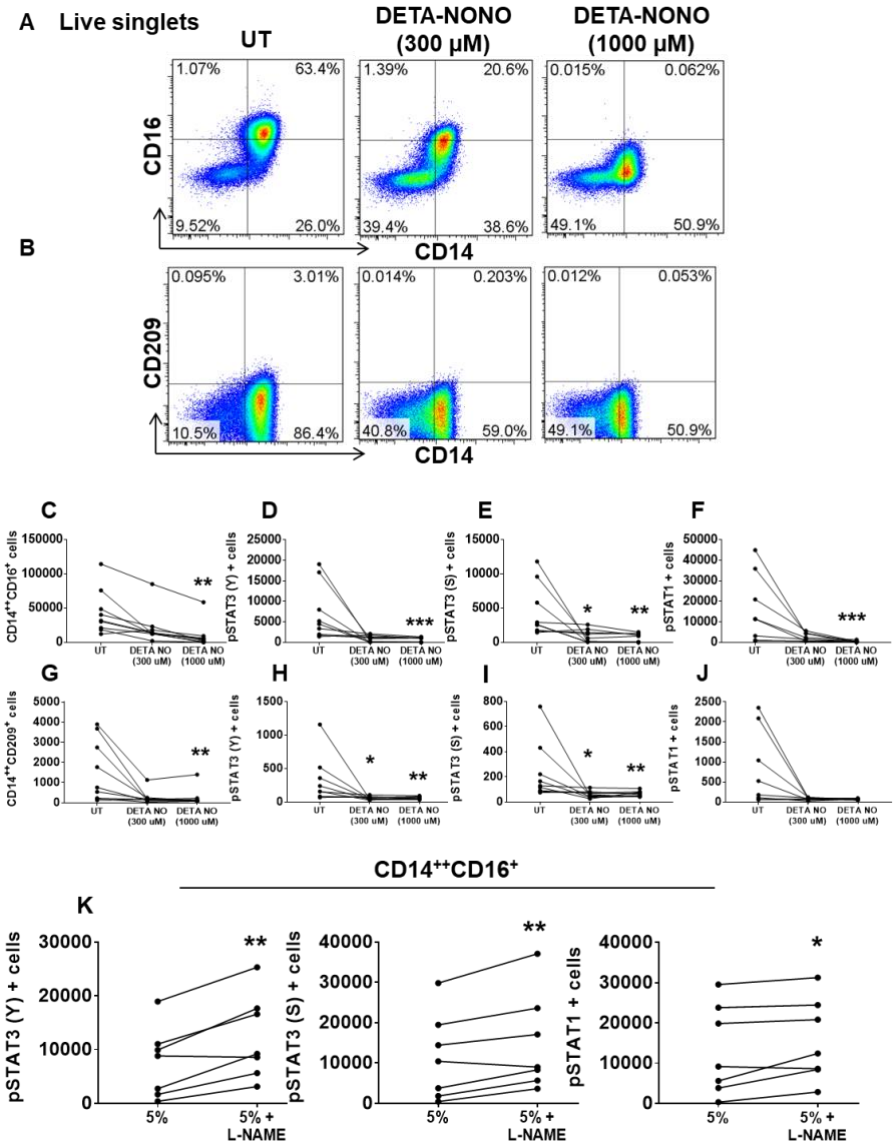

Figure 2-10: Exposure of monocytes to NO donor inhibits human monocyte conversion and activation to its derived populations. Human $CD14^{+}$ monocytes were isolated from buffy coats of normal human volunteers and cultured alone in untreated (UT) conditions, DETA-NONOate (DETA-NONO), an NO donor, at 300µM or DETA-NONO at 1000µM concentrations in static conditions for 48 hours. **A.** Flow cytometry representatives are shown for the $CD14^{++}CD16^{+}$ intermediate monocyte and (**B**) the $CD14^{++}CD209^{+}$ population. **C.** Values for each subject without and with DETA-NONO are shown for the total number of cells from the $CD14^{++}CD16^{+}$ intermediate monocytes and for the total number of cells expressing (**D**) pSTAT3 (Y), (**E**) pSTAT3 (S), and (**F**) pSTAT1 within this population. **G.** Effect of DETA-NONO on the number of $CD14^{++}CD209^{+}$ cells and the expression of (**H**) pSTAT3 (Y), (**I**) pSTAT3 (S), and (**J**) pSTAT1 for each subject. A total of n= 9 participants per group were used for these experiments. **K**. Human $CD14^{+}$ monocytes were cultured with HAECs exposed to 5% stretch or 5% plus NO synthase inhibitor, L-NAME, (1000 µM) for 48 hours. The number of $CD14^{++}CD16^{+}$ intermediate monocyte population expressing pSTAT3 (Y), pSTAT3 (S), and pSTAT1 for each subject are connected by lines. A total of n=7 participants per group were used. For panel **C-J** the nonparametric Friedman's test followed by Dunn's multiple comparison tests was employed. For panel **K** a one-tailed paired *t*-tests was used (*p<0.05, ** p<0.01, *** p<0.001).

We considered the possibility that the factor promoting this process of monocyte transformation and activation could be released from endothelial cells undergoing increased stretch and not necessarily require direct cell contact. We obtained evidence suggesting that the factors potentially mediating monocyte transformation are likely short-lived and do in fact require direct cell contact. Thus, we collected conditioned media from HAECs stretched alone to 5% or 10% for 48 hours and added this to monocytes for another 48 hours in static conditions. We found no differences in monocyte transformation when these were cultured with 5% or 10% stretch conditioned media. However, monocytes underwent transformation into the intermediate phenotype and the CD209 population at the same rate than the co-culture system undergoing stretch (Figure 2-11A-D). In addition, we tested the hypothesis that monocytes require direct cell contact with the endothelium to undergo transformation by using a transwell system, which eliminated the cell contact but allowed the transfusion of smaller compounds. Similar to the conditioned media experiment, we observed the same rate of monocyte transformation in the transwell system when endothelial cells were undergoing 5% and 10% stretch (Figure 2-11E-H) compared to the co-culture system. These experiments suggest that physiological levels of stretch on vessels might release a short-lived factor that prevents monocyte activation and transformation.

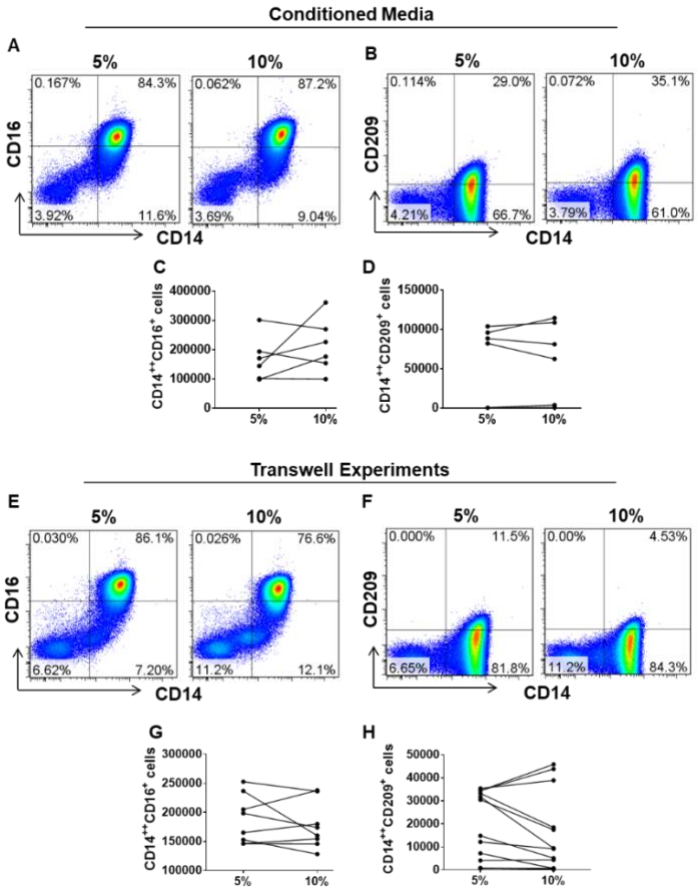

Figure 2-11: Exposure of monocyte to stretched endothelial cells in a transwell set-up or to conditioned media. A. Human $CD14^+$ monocytes were isolated from PBMCs of normal human subjects and cultured in conditioned media supplemented with 2% FBS from HAECs that underwent stretching of 5% and 10% for 48 hours. These cells were kept under static conditions for another 48 hours. Flow cytometry representatives are shown for the $CD14^{++}CD16^+$ intermediate monocyte and (**B**) the $CD14^{++}CD209^+$ population. **C.** Values for each subject exposed in 5% or 10% conditioned media are shown for the total number of cells from the $CD14^{++}CD16^+$ intermediate monocytes and (**D**) $CD14^{++}CD209^+$ population (n = 6). **E**. Isolated monocytes were added to transwells that were on top of confluent endothelial cells and these were stretched to 5% and 10% for 48 hours. Flow cytometry representatives are shown for the $CD14^{++}CD16^+$ intermediate monocyte and (**F**) the $CD14^{++}CD209^+$ population. **G.** Values for each subjects' monocytes placed on transwells and exposed to HAECs undergoing 5% or 10% stretch are shown for the total number of cells from the $CD14^{++}CD16^+$ intermediate monocytes and (**H**) $CD14^{++}CD209^+$ population (n = 8, n = 12, respectively). One-tailed paired *t*-tests was used.

Further, we examined the hypothesis that monocytes might adhere to the endothelium and themselves undergo cyclical stretch. In keeping with this, we found that 10% stretch increased ICAM-1 expression on endothelial cells and increased adhesion of monocytes to the HAECs compared to the 5% stretch controls (Figure 2-12A) after 24 hours. We also employed confocal

microscopy with Z stacking to interrogate the endothelial layer and the subendothelial collagen to visualize $CD31^+$, $CD14^+$ and $CD83^+$ cells. Using this approach, we observed $CD14^+$ monocytes on the surface of endothelial cells in the co-culture (Figure 2-12B). Moreover, $CD83^+$ cells were observed on the surface of the $CD31^+$ endothelial cells exposed to 10% stretch, while none was detected in cultures exposed to 5% stretch. We observed no monocyte or CD83 expressing cells in the collagen/gelatin sub-endothelial space in either the 5% or 10% stretch experiments.

To determine if stretch could directly activate monocytes we cultured monocytes in arginylglycylaspartic acid (RGD) -covered Pronectin® or collagen I coated stretch plates in the absence of HAECs, and exposed these to either 5% or 10% levels of stretch. Both Pronectin® and collagen I-coated stretch plates promoted monocyte adhesion (Figure 2-12C) after 24 hours, but neither supported monocyte transformation when exposed to stretch (Figure 2-12D) after 48 hours. To confirm the nuclear translocation of p-STAT3 in monocytes in response to endothelial mechanical stretch, we performed FlowSight® techniques. We have previously shown that all monocyte populations have at least some degree of cells that are positive for p-STAT3, but the intermediate monocytes and the CD209 population express the highest amount of p-STAT3 in response to hypertensive stretch. We found that p-STAT3 in classical monocytes, $CD14^+CD83^+$ cells, and $CD83^+$ DCs co-localizes with the nuclear stain Sytox (Figure 2-13). Thus, endothelial mechanical stretch promote monocyte phosphorylation of STAT3 and translocation to the nucleus where it can act as a transcription factor for various pro-inflammatory genes of which are the ones we found to be increased. has pathophysiological implications.

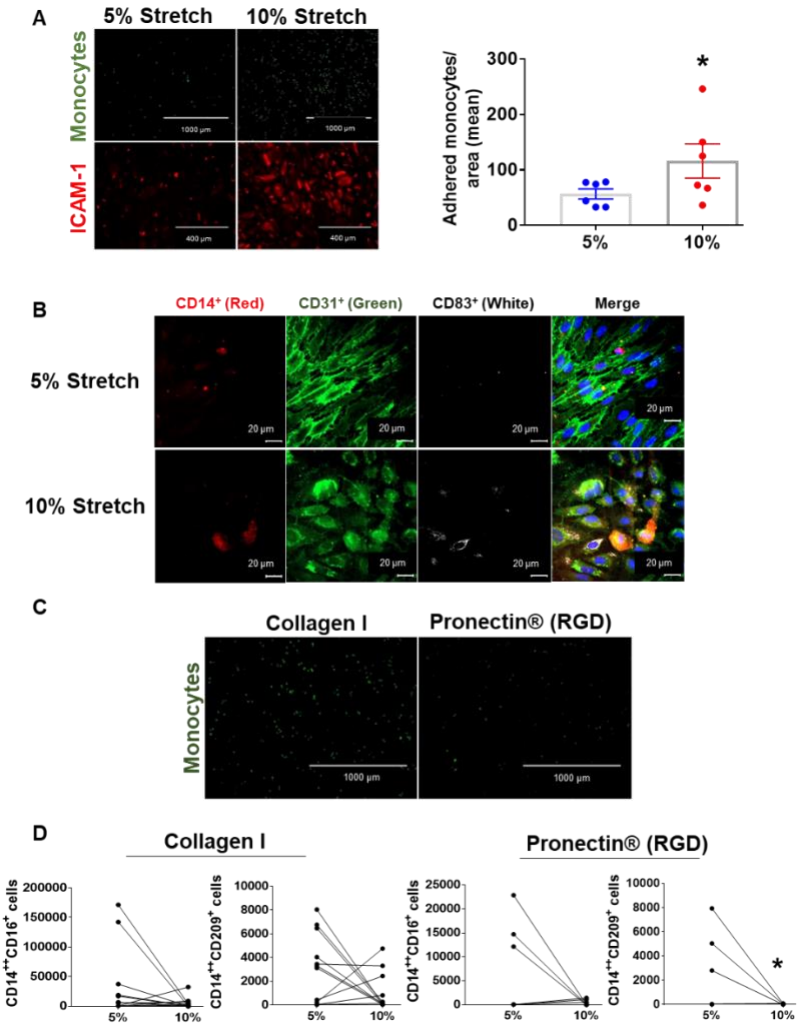

Figure 2-12: Human monocytes require endothelial cell contact for their differentiation and activation during hypertensive mechanical stretch. A. Human monocytes from normal volunteers were isolated from buffy coats and labeled with 12µM of CellTracker™ Green CMFDA dye for 30 mins at 37°C in medium and added to HAEC cultures exposed to either 5% or 10% stretch for 24 hours. Plates were washed with 1X PBS and fixed with 4% PFA. Adhered monocytes were counted. Immunofluorescent microscopic images show monocytes adhered to the endothelial cells (green) and expression of ICAM-1 on the endothelial cell monolayer (red). Mean data showing the number of adhered monocytes per three random fields are illustrated (n=6). **B**. Human monocytes from normal volunteers were isolated from buffy coats and added to HAEC cultures exposed to either 5% or 10% stretch for 24 hours. Plates were washed with 1X PBS and fixed with 4% PFA. Confocal microscopy with Z stacking was used to visualize $CD31^+$ (green), $CD14^+$ (red) and $CD83^+$ (white) in different surfaces including the subendothelial space. Cells were counterstained with DAPI (n=4). **C.** Human $CD14^+$ monocytes labeled with 12 µM of CellTracker™ Green CMFDA dye were placed on either collagen I or Pronectin® (RGD) coated plates without the presence of endothelial cells and were exposed to 5% or 10% cyclical stretch for 24 hours. Immunofluorescent microscopic images show monocytes that adhered to the collagen I and Pronectin® coated membranes after exposure to hypertensive mechanical stretch (n= 4). **D.** Human $CD14^+$ monocytes were cultured alone on collagen I (n=11) or Pronectin® (n=6) coated plates and stretched to either 5% or 10% for 48 hours. Individual values are shown for each participant of the number of cells expressing $CD14^{++}CD16^+$ and $CD14^{++}CD209^+$ cells in each experimental condition. Statistical differences were determined using one-tailed unpaired or paired *t*-tests (*p<0.05).

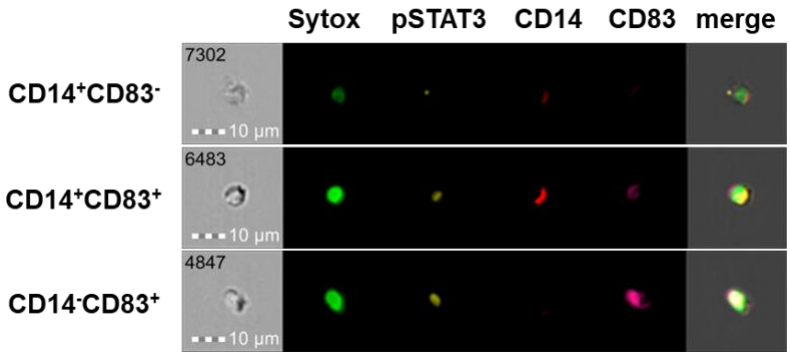

Figure 2-13: Phosphorylated STAT3 localizes to the nucleus of activated monocytes and dendritic cells. Normal human monocytes were cultured with HAECs undergoing stretch for 48 hours. Two days later, cells were harvested and stained for the surface markers CD14 and CD8 and for the intracellular markers pSTAT3 (Y705) and Sytox, which is a nuclear stain. FlowSight® technique was used to visualize the cells real-time and determine the localization of phosphorylated STAT3 within the $CD14^{+}CD83^{-}$, $CD14^{+}CD83^{+}$ and $CD14^{-}CD83^{+}$ populations.

Hypertension affects the distribution of circulating mononuclear cells in humans: In additional experiments, we sought to determine if hypertension is associated with an alteration of the phenotype of circulating monocytes. The demographics of the 132 subjects enrolled for this analysis are shown in Table 2-1. Using a gating strategy as published previously [236], we found that there is a progressive decline in the classical monocytes and a concomitant increase in the percent of intermediate and non-classical monocytes with increasing levels of hypertension (Figure 2-14A-C). In additional studies, we sought to determine if intermediate monocytes or non-classical monocytes exhibit evidence of STAT activation. We recruited an additional 15 normotensive and 12 hypertensive subjects for this analysis. The demographics of these subjects are shown in Table 2-2 and a representative dot plot for the different monocyte populations is shown in Figure 2-14D. Example histograms for STAT phosphorylation in normotensive and hypertensive individuals are shown in Figure 2-14E. Intermediate monocytes exhibited increased phosphorylation of STAT3 Y705, STAT3 S727 and STAT1 Y701 compared

to other monocyte populations (Figure 2-14F-H). No differences between normotensive and hypertensive groups were observed.

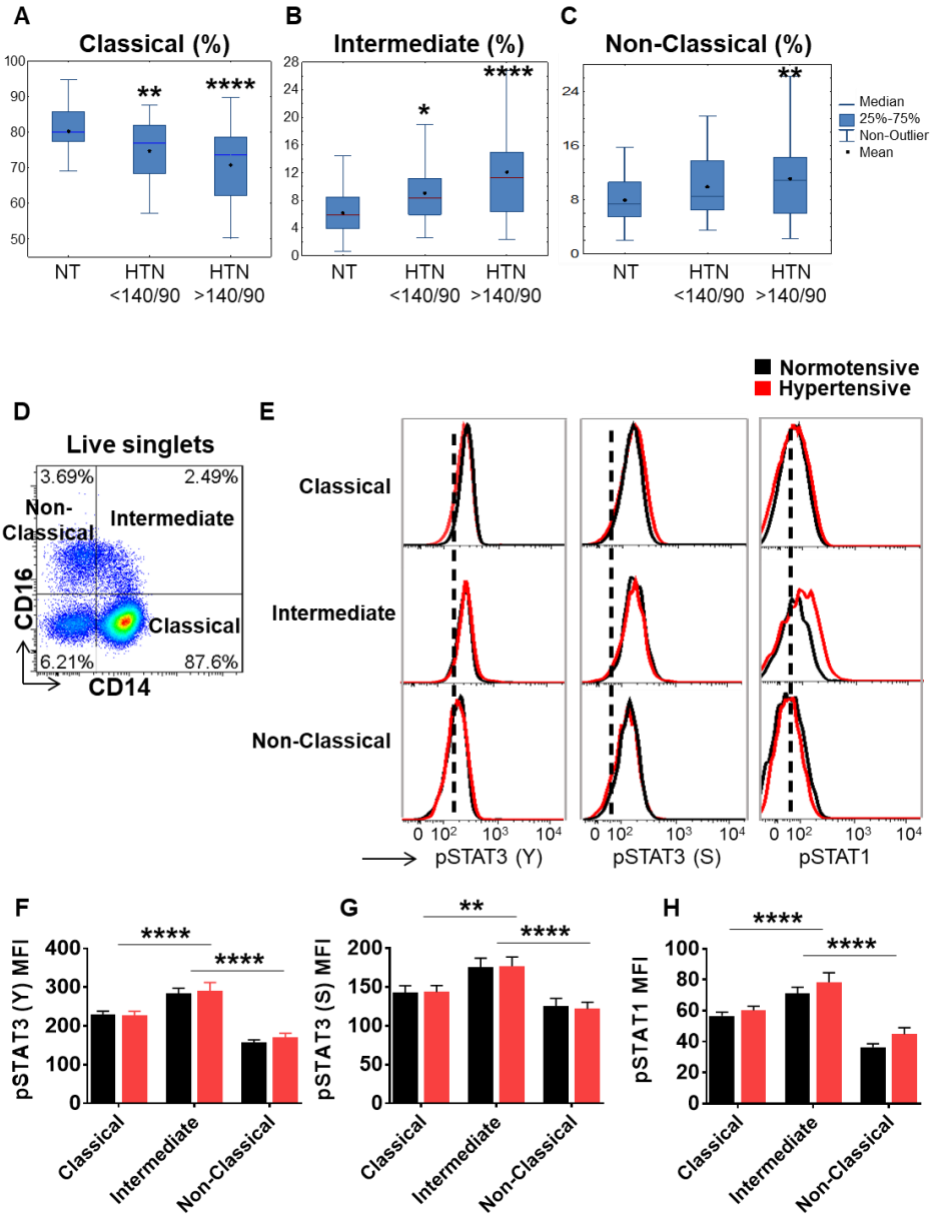

Figure 2-14: Hypertension affects the distribution of circulating monocytes in humans. A. A cohort of normotensive (n = 20), mildly hypertensive (systolic BP ~130-140 mmHg, n = 52), and severely hypertensive (systolic BP >140 mmHg, n = 60) subjects were recruited and flow cytometry was used to analyze various monocyte populations. A. Mean values are shown for the percent of positive $CD14^{++}CD16^{-}$ classical, (**B**) $CD14^{++}CD16^{+}$ intermediate and (**C**) $CD14^{low}CD16^{++}$ non-classical monocytes comparing normotensive, mild and severely hypertensive subjects. Data were analyzed using one-way ANOVA. **D.** Representative flow cytometry dot plots showing classical, intermediate, and non-classical subset distribution are shown. **E.** Histograms showing the $CD14^{++}CD16^{-}$ classical, $CD14^{++}CD16^{+}$ intermediate, non-classical monocyte population comparing normotensive (black) and

hypertensive (red) subjects. The dashed line represents the Mean fluorescent intensity (MFI) for the FMO control. **E.** MFI for pSTAT3 (Y), pSTAT3 (S) (**F**), and pSTAT1 (**G**) in various monocyte subgroups in both normotensive (n=15) and hypertensive (n = 12) subjects. Two-way ANOVA with Student Newman Keuls post-hoc test was used (*p<0.05, ** p<0.01, *** p<0.001, **** p<0.0001).

Discussion

In this study, we demonstrate that exposure of human monocytes to endothelial cells undergoing 10% mechanical stretch increases differentiation into $CD14^{++}CD16^{+}$ intermediate monocytes and $CD14^{++}CD209^{+}$ cells. We further show that monocytes cultured with endothelial cells exposed to hypertensive mechanical stretch markedly increase expression of IL-6, IL-1β, IL-23, CCL4, and TNFα. In addition, we found that endothelial cells undergoing hypertensive mechanical stretch stimulate an increase in pSTAT3 (Y), pSTAT3 (S), and pSTAT1 within these monocyte populations. Inhibition of STAT3 by Stattic prevented conversion of monocytes into the intermediate and the DC phenotype and normalized the cytokine production of these monocytes cultured with endothelial cells undergoing 10% stretch. Our data implicate a role of hydrogen peroxide and IL-6 as mediators of monocyte differentiation. We also show that hypertension is associated with an increase in the percentage of circulating intermediate and non-classical monocytes and that circulating intermediate monocytes exhibit higher levels of pSTAT3 (Y), pSTAT3 (S), and pSTAT1. Thus, altered mechanical forces affecting the endothelium can modify monocyte differentiation and activation and likely contribute to immune activation in hypertension.

Intermediate monocytes are the least characterized of the monocyte subtypes in humans, however, these cells have been implicated in inflammatory diseases such as Kawasaki disease [106], rheumatoid arthritis [108], sepsis [109], HIV [110], acute heart failure and coronary artery disease [111]. Using deuterium labeling in humans, Patel and colleagues recently showed a sequential transition of classical monocytes that emerge from the bone marrow to the

intermediate and subsequently the non-classical phenotype [100]. Compared to classical monocytes, intermediate monocytes exhibit enhanced phagocytosis, produce higher levels of ROS and inflammatory mediators such as TNFα and IL1-β [97, 113, 114]. They also have the highest expression of the major histocompatibility complex class II antigens, including HLA-DR, -DP and -DQ indicating that they also possess antigen presentation functions [112]. Thus, the presence of high numbers of intermediate monocytes in humans with hypertension likely has pathophysiological implications.

Our data are compatible with findings by Randolph et al. showing that activated endothelial cells can modify monocyte phenotype. They demonstrated that monocytes that transmigrate the endothelium convert to macrophages that remain in the subendothelial space or DCs expressing CD83 that reverse transmigrate the endothelium [167]. In a subsequent study, this group also showed that a subpopulation of $CD16^+$ monocytes have a propensity to reverse transmigrate the endothelium and, upon doing so, increase their expression of $CD86^+$ and HLA-DR. In keeping with this, the authors showed these monocytes potently induced allogenic T cell proliferation [220]. The investigators assumed cells had transmigrated the endothelial monolayer if they were not removed by washing the monolayer 2 hours after addition of the cells. In our study, we found that 10% stretch markedly enhanced monocyte binding to the endothelial surface. Our analysis included adhered cells and those potentially within the subendothelial space and it also demonstrated the presence of macrophage-like cells expressing the CD163 marker; however, these were not altered by the degree of endothelial stretch.

In these experiments, we not only examined intermediate and non-classical monocytes, but also $CD14^+$ cells bearing the markers CD209 and CD83. These have been employed as dendritic cell markers, but can be expressed on a variety of activated myeloid cells. CD209 is a C-type

Lectin receptor that promotes the production of IL-1β and IL-23 that can ultimately skew T cells to a T_H17 phenotype. Levels of CD209 on whole leukocytes correlate with disease severity in Behçet's Disease [237]. LECT2 acts on CD209 to induce JNK signaling in monocytes and endothelial cells [218]. CD209 forms a complex with TLR4 and promotes NFκB activation in response to oxidized low-density lipoprotein (LDL) confirming the role of CD209 in innate immunity and antigen presentation [238]. While we were not able to detect LECT2 levels in our co-culture system, the increase in CD209 on monocytes could arm these cells to respond to signals like LECT2 or oxidized LDL *in vivo*. CD83 is a type-I lectin transmembrane protein expressed on monocyte-derived DCs and small subsets of other immune cells [239]. The presence of CD83 on DCs enhances their ability to evoke T cell calcium transients and proliferation [227]. Thus, surface expression of CD209 and CD83 may have functional consequences in enhancing immunogenicity of monocyte-derived cells in hypertension.

There are a number of factors in the hypertensive milieu that could activate both endothelial cells and monocytes, including cytokines and oxidative stress [240, 241]. In this investigation, we focused on the role of increased endothelial stretch, which is known to stimulate endothelial cell cytokine production, ROS formation and expression of adhesion molecules [180]. The vessels affected by stretch in hypertension likely vary depending on the duration of the disease. Early in hypertension, there is increased stretch of large vessels; however, as hypertension is sustained, large vessel become stiff leading to propagation of the forward PWV into smaller resistance vessels [242]. Our present data therefore might explain how increased cyclic stretch in small vessels could promote immune activation. Consistent with this, we have previously shown that aortic stiffening precedes renal accumulation of T cells, monocyte and macrophages ultimately leading to renal dysfunction [7].

In these experiments, we found evidence for STAT activation in intermediate monocytes of humans and in monocytes exposed to endothelial cells undergoing 10% cyclical stretch as evidenced by phosphorylation of STAT1 at Y701 and STAT3 at S727 and Y705. Of interest, STAT3 is required for FLT-3-dependent formation of DCs from bone marrow derived cells [229], and plays an important role in production of IL-1β, IL-6 and TNFα in macrophages of humans with coronary artery disease [228]. We also found that exposure of monocytes to endothelial cells undergoing 10% stretch markedly enhanced mRNA expression of these cytokines and STAT3 activation in these. Inhibition of STAT3 with Stattic not only inhibited cytokine production by human monocytes, but also reduced their conversion to intermediate monocytes and $CD14^{++}CD209^{+}$ cells. Thus, STAT-signaling seems to play an important role in monocyte differentiation and activation in hypertension.

We made substantial efforts to identify factors released by the endothelium that would mediate STAT3 activation. STAT3 can be activated by myriad factors, including growth factors, numerous cytokines, JAK, ROS, heat shock proteins and xenobiotics [188]. IL-6 is both upstream and downstream of STAT3 activation, and we found that endothelial cells undergoing 10% stretch produced increased amounts of this cytokine. This is compatible with prior gene profiling studies showing that cyclical stretch increases IL-6 expression in endothelial cells [169]. We found that immune-clearing of IL-6 inhibited STAT3 activation and monocyte transformation to the intermediate phenotype suggesting a scenario in which IL-6 released by the endothelium stimulates STAT3 activation in adjacent monocytes, and ultimately greater amounts of IL-6 production by these latter cells in a feed-forward fashion. Of note, IL-6 quartiles were found to be strongly associated with the risk of developing hypertension in the Nurses Health Study [243], and mice lacking this cytokine are protected against Ang II-induced hypertension [244].

We also found that PEG-Catalase, which scavenges hydrogen peroxide, prevents monocyte transformation and STAT3 activation. This finding is compatible with prior studies showing that cyclical stretch activates production of ROS by endothelial cells, initially via activation of the NADPH oxidase and subsequently from uncoupled NO synthase [180]. In preliminary studies, we confirmed that superoxide production, as measured by detection of 2-hydroxyethidium formation from dihydroethidium, was increased in both monocytes and endothelial cells when the latter cells were exposed to 10% vs. 5% stretch (data not shown). Our data suggest that superoxide is unlikely the mediator of monocyte transformation, as the superoxide dismutase mimetic Tempol failed to prevent formation of intermediate cells or STAT3 activation. It is therefore likely that hydrogen peroxide, formed by dismutation of superoxide, mediates these effects. Hydrogen peroxide is relatively stable and thus likely to serve a paracrine-signaling role in mediating cross talk between the endothelium and adjacent monocytes. Of interest, the expression of heme oxygenase, which has anti-oxidant properties, inversely correlates with monocyte expression of CD14 in humans [245].

In our experimental setup, we cannot exclude the possibility that IL-6 and hydrogen peroxide also have effects on the endothelium. Activation of the IL-6 receptor has been shown to stimulate the JAK-STAT pathway that can lead to further IL-6 production [246]. Likewise, hydrogen peroxide can activate the NADPH oxidase, which could ultimately lead to additional hydrogen peroxide production in a feed forward fashion [247]. We have also shown that ROS released from the mitochondria can stimulate the NADPH oxidase in endothelial cells [40]. Thus, production of IL-6 and hydrogen peroxide in a milieu of endothelial cells and monocytes could have actions on both cell types, but ultimately lead to monocyte differentiation.

Another potential mediator of STAT activation is loss of NO signaling. NO has been shown to inhibit STAT3 activation in ovarian cancer cells and endothelial NO bioavailability is commonly lost in hypertension and related diseases [212, 248]. Monocytes in the circulation are constantly exposed to endothelial-derived NO, however when placed in culture, spontaneously acquire CD16. We confirmed this in our studies and found that this was associated with STAT3 phosphorylation and that the NO donor, DETA-NONOate, markedly inhibited monocyte transformation and STAT activation. We also found that the addition of L-NAME to HAECs undergoing 5% stretch promoted monocyte STAT activation, in a fashion similar to 10% stretch. L-NAME exposure did not cause monocyte transformation during this 48 hour exposure, suggesting that other signals like IL-6 and hydrogen peroxide might also be needed for this response.

In keeping with our findings in the co-culture experiments, we found that hypertensive humans have an increase in circulating intermediate and non-classical monocytes, and that this seems dependent on their severity of hypertension. It is likely that this shift in monocyte population predisposes to further inflammatory responses, including production of cytokines and T cell activation. Of note, we also confirmed that intermediate monocytes of both hypertensive and normotensive subjects exhibit STAT1 and STAT3 activation. This is compatible with a scenario in which intermediate monocytes consistently exhibit and likely require STAT activation for their transformation from the classical precursors, but that this transformation is higher in hypertension, perhaps due to encounter with activated endothelium.

In summary, our current study provides a previously unrecognized link between mechanical forces affecting the endothelium and activation of monocytes (Figure 2-15). This provides new insight into how the immune system can be activated in hypertension and for the first time

implicates intermediate monocytes as potentially important in this disease. Intermediate monocytes are not only a biomarker of inflammation in hypertension, but their acquisition of CD16 arms these cells to possess cytotoxic function and to produce TNFα. The production of cytokines like IL-6, IL-23 and IL-1β can also skew T cells to produce IL-17A, which we have previously shown to be involved in hypertension [129]. It is therefore likely that altered endothelial mechanical forces have important effects on immune cell function, leading to end organ dysfunction and worsening hypertension.

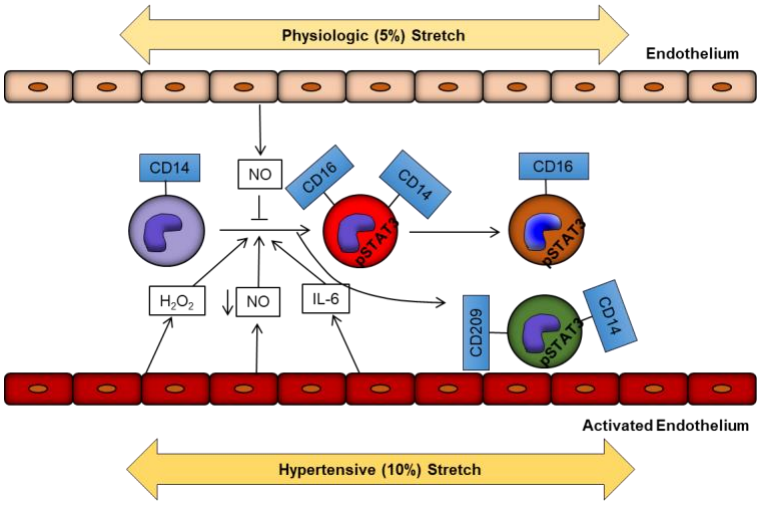

Figure 2-15: Model: Increased endothelial stretch promotes monocyte transformation and activation.

Chapter III

Interplay between Signal transduction and activation of transcription factors, ROS and inflammation during hypertension

Introduction

One third of the population in United States has hypertension, and its prevalence increases with age. Current treatments for hypertension include ACE inhibitors, β- blocking drugs, calcium-blocking drugs, and thiazide diuretics [249]. Despite treatment with these agents, up to 20% of patients continue to have poorly controlled BP. Recent studies in our laboratory and others have shown a critical role of the innate and adaptive immune system in BP elevation caused by several stimuli including pro-inflammatory cytokines, Ang II, DOCA-salt hypertension and norepinephrine [12]. The vasculature also plays an essential role in hypertension. Ang II promotes vascular disease and hypertension partly by formation of pro-inflammatory cytokine IL-6. IL-6 is upstream of STAT3 and binds to its receptor on the plasma membrane to initiate the JAK/STAT cascade. Johnson et al. found that isolated carotid arteries from WT mice incubated with Ang II had increased levels of superoxide and that this was prevented by addition of STAT3 inhibitors, Stattic or S3I-201 [210]. Further, this group found that Ang II-induced hypertension in WT mice was reduced by 40 mmHg in mice treated with S3I-201, confirming a role of STAT3 in hypertension. STAT3 can be activated via many mechanisms apart from IL-6/JAK pathways. Mitochondrial ROS can promote dimerization of the glycolytic enzyme pyruvate kinase M2 (PKM2) and this enables nuclear translocation [228]. Nuclear PMK2 acts as a protein kinase that phosphorylates nuclear STAT3.

Reactive oxygen species play a role in the genesis of hypertension. Ang II can activate the NADPH oxidase to induce superoxide production, which can lead to endothelial dysfunction and

reduction of NO bioavailability. Dikalov et al. showed that depletion of NOX2, but not NOX1, NOX4, or NOX5 inhibits Ang II-induced superoxide production [250]. This group found that NOX2 knockout mice ($NOX2^{-/-}$) displayed blunted Ang II-induced hypertension and the superoxide production associated with it. NO is a vasodilator and essential for normal endothelial functionality. Inhibition of NO results in severe hypertension and renal vasoconstriction [181]. Our group found that aortas from mice exposed to DOCA-salt hypertension had increased ROS production by NO synthase and tetrahydrobiopterin oxidation, which leads to reduction of NO bioavailability [51]. Conversely, treatment with oral tetrahydrobiopterin to DOCA-salt infused mice leads to a reduction of vascular ROS and an increase in NO production. NO also plays a role in STAT3 activation. Kielbik et al. found that addition of NO donor, DETA NONOate, to ovarian cancer cells inhibits STAT3 and AKT3 phosphorylation and downregulated their cytosolic levels [212]. These data suggest that NO plays a role in STAT3 signaling and that this process could be evident in hypertension.

An emerging paradigm is that activated immune cells enter the kidney and blood vessels and release cytokines that cause renal and vascular dysfunction [137]. Work from our laboratory has established a critical role of DCs in hypertension. We showed that either blockade or genetic deletion of B7 ligands on antigen presenting cells such as DCs that are essential for T cell signaling reduces blood pressure [138]. In addition, we showed that Ang II-induced hypertension causes a 5-fold increase in superoxide production in DCs [139]. A major finding in this study is that this leads to formation of IsoLG, which rapidly ligate lysines on proteins. These IsoLG-protein adducts accumulate in DCs of hypertensive mice and in monocytes of hypertensive humans [139]. Another stimulus of immune activation in hypertension is increased sodium. We found that DCs exposed to high concentrations of sodium have increased levels of ROS and

IsoLG-adducts and they are able to induce T cell proliferation [149]. Recently, we have identified that monocyte-derived DCs ($CD11b^+CD11c^+MHC\text{-}II^+$) have the highest accumulation of these IsoLG-adducts and are more pro-inflammatory having the ability to promote T cell proliferation in comparison to other DC subsets.

In this study, we examined the role of STAT3 in hypertension *in vivo*. As we have previously shown in Chapter II, increased endothelial stretch promotes human monocyte activation and transformation into the intermediate monocytes and the CD209 DC-like cells. We showed that this process occurs via STAT3 and, thus, in this chapter we sought to determine whether this is true using various mouse models. In this study, we also determined the role of hematopoietic and somatic NOX2 in hypertension and STAT3 activation in response to Ang II treatment. Therefore, this study gives insight into the potential role of dendritic cell STAT3 and NOX2 in the genesis of hypertension.

Materials and Methods

Animals

Mouse Strains: WT C57Bl/6 mice, WT SJL CD45.1 mice, $tg^{CRE/CD11C}$ mice, $STAT3^{loxp/loxp}$ mice and $NOX2^{-/-}$ mice were obtained from The Jackson Laboratory, Bar Harbor, ME, USA. STAT3/CD11c KO mice were made by crossing $STAT3^{loxp/loxp}$ with $tg^{CRE/CD11C}$ mice. The resultant offspring were heterozygotic for loxP sites and for these were crossed to create mice that were homozygotic for $STAT3^{loxp/loxp}$ genotype. Male mice of approximately 10-12 weeks of age were used.

All animal procedures were approved by Vanderbilt University's Institutional Animal Care and Use Committee (IACUC) where the mice were housed and cared for in accordance with the Guide for the Care and Use of Laboratory Animals, US Department of Health and Human Services.

Surgical Procedures and Blood Pressure Measurements

Angiotensin II infusion: Mice were anesthetized with 1% isoflurane in 100% oxygen in a specialized anesthetizing chamber. Two week osmotic mini-pumps were implanted subcutaneously in mice to infuse high-dose Ang II (490 ng/kg/min) or vehicle (sham, 0.08 M sodium chloride/1% acetic acid solution) for 6 to 14 days (Alzet, Model 2002; DURECT Corporation, Cupertino, CA, USA) as previously described [125, 139].

Tail Cuff Blood Pressure Measurements: This method of blood pressure measurement is non-invasive. For these measurements, we used the MC4000 Blood Pressure Analysis System (Hatteras Instruments). The person performing the blood pressure measurement was blinded for the genotype and treatment of the animal. Four mice were placed on pre-warmed platforms,

which promotes vasodilation of the tail artery. A magnetic black cover was used to cover the mice and tails from mice were threaded through a small blood pressure cuff and gently taped down. The machine measures systolic blood pressure in cycles of 10 and gives an average. To allow the mice to acclimate to this device, the first two rounds of 10 cycles are eliminated from the analysis and rounds 3 and 4 are averaged together to generate a final systolic blood pressure value for the day. The blood pressure of the mice is measured two days per week and averaged to produce a final weekly value [13].

Carotid Radiotelemetry Blood Pressure Measurement: This method of blood pressure measurement is invasive. Mice were anesthetized with ketamine/xylazine (90-120 mg/kg + 10 mg/kg; 1:1 volume ratio). The catheter that is connected to the transducer was inserted into the isolated left common carotid artery and advanced until the tip was inside the thoracic aorta. The transmitter was then positioned under the skin on the right flank close to the hind limb [139]. After telemetry implantation, mice were allowed 10 days to recover prior to baseline measurements followed by the implantation of osmotic mini-pumps as described above. Measurements of blood pressure were obtained daily or three consecutive days per week for a total of three weeks.

Stattic treatment in mice: Animals were administered vehicle or Stattic (5 mg/mL) every two days by oral gavage. Stattic treatment began two days before initial administration of Ang II and continued through the rest of Ang II treatment (14 days).

Euthanasia of mice: All mice were sacrificed at the end of each experiment by CO_2 inhalation. Organs were transcardially perfused by physiological pressure with saline solution prior to organ collection.

Measurement of Vascular Reactivity

Third-order mouse mesenteric arterioles were dissected free of perivascular fat and 2 mm segments were used to perform isometric tension studies. Studies were performed in a small vessel horizontal wire myograph (Danish Myo Technology, models 610M and 620M) with a physiological salt solution (130 mM NaCl, 4.7 mM KCL, 1.2 mM $MgSO_4$, 1.2 mM KH_2PO_4, 25 mM $NaHCO_3$, 5 mM glucose and 1.6 mM CaCl2). LabChart Pro v7.3.7 (AD Instruments) was used to record isometric tone for each vessel. Vessels were equilibrated over a 20 minute period at 37°C. To determine optimal passive tension to simulate an *in vivo* transmural pressure of 100 mmHg, a passive circumference-tension curve was generated for each vessel [251]. Endothelium-dependent and endotheluml-independent vascular relaxations were tested using increasing concentrations of acetylcholine or sodium nitroprusside, respectively, following pre-constriction with norepinephrine (10 µM).

Flow Cytometry

Flow cytometry for mice tissues: Single cell suspensions were prepared from aortas, kidneys, spleen and mesenteric lymph nodes as previously described [153]. Single cell suspensions of thoracic aorta with surrounding perivascular fat were digested using RPMI 1640, 5% FBS, Collagenase A (1mg/mL), Collagenase B (1 mg/1mL) and DNase I (0.1 mg/mL). Aortas were homogenized by hand in 1.5 mL Eppendorf tubes using scissors and incubated in rotator at 37°C for 30 minutes [44]. Tissue homogenates were filtered through a 40 µM cell strainer after digestion. Kidneys were placed in digestion media containing RPMI 1640, 5% FBS, Collagenase D (2mg/mL) and DNase I (0.1 mg/mL) and homogenized using AutoMACS Dissociator (Miltenyi Biotech). Homogenized tissues were incubated and shaking at 37°C for 20 minutes. Single cell suspensions were stained for flow cytometry using the following antibodies: Pacific

LIVE/DEAD™ Fixable Violet Dead Cell Stain (Life Technologies); APC-CY7-conjugated anti-F4/80 (Biolegend); AmCyan-conjugated CD11b; AmCyan-conjugated Ly6C (Biolegend); FITC-conjugated CD44 (BD Bioscience); APC-conjugated CD4 (Biolegend); PE-conjugated CD8a (Biolegend); AmCyan-conjugated CD45 (Biolegend); PE-conjugated anti-MerTK; PerCPCy5.5-conjugated anti-MHC-II; PECy7-conjugated anti-CD64; FITC-conjugated anti-CD11c (Biolegend); AmCyan-conjugated anti-CD45.1 (BD Bioscience) and anti-CD45.2 (BioLegend). A known quantity (50 µL) of calibration or counting beads (123count eBeads, eBioscience) was added to each sample prior to analysis. BD FACSCanto II system was used to run the samples and FlowJo® was used for data analysis. Gates were set using FMO controls. Results were normalized using bead count and expressed as number of cells per kidney, spleen, lymph nodes or per thoracic aorta.

Intracellular staining for phosphorylated STAT3 and Isolevuglandin-adducts: Murine cells were washed and stained first with Pacific LIVE/DEAD™ Fixable Violet Dead Cell Stain (Life Technologies). Mouse single cell suspensions were then washed and stained with indicated surface antibodies (described above) for 15 minutes at 4°C. Cells were immediately fixed and permeabilized after staining with FIX & PERM® Cell Fixation & Permeabilization Kit (ThermoFisher) by adding 100 µL of Reagent A and incubating for 15 minutes in the dark at room temperature. Cells were washed with 3 mLs of wash medium (1XPBS + 0.1% NaN_3 + 5% FBS). Cells were permeabilized using 100 µL of Reagent B and 3 µLs of APC-conjugated anti-pSTAT3 (Y705) or 5 µLs of Alexa 488-conjugated anti-D11 ScFv and incubated for 20 minutes at room temperature in dark. Cells were washed with 3 mLs of wash medium and resuspended in MACS buffer for flow cytometry analysis. Gates were set using FMO controls. Results were normalized using bead count and expressed as total number of cells.

Western Blotting

For the following experiments, DCs were isolated from spleens of STAT3/CD11c KO mice and STAT3$^{loxp/loxp}$ mice using the positive selection for mice CD11c MicroBeads Ultrapure Kit (Miltenyi Biotec). Western blotting were performed as previously described [149], cells were lysed in 150 uLs of the lysis buffer solution, 10 mLs of RIPA buffer (Sigma) and one tablet of complete Tablets protease inhibitor cocktail (Roche) and one tablet of the PhosSTOP EASYpack phosphatase inhibitor cocktail (Roche). Protein was quantified using the Pierce™ BCA Protein Assay Kit (ThermoScientific). Protein samples (20 µg) were separated by SDS-PAGE and transferred to a nitrocellulose membrane and blocked with 5% milk and 1% BSA in 1X TBS-T as previously described [226]. Membranes were probed with primary antibody total STAT3 antibody (Cell Signaling). Membranes were labeled using horseradish peroxidase (HRP)-conjugate and detected with chemiluminescence solution using the SuperSignal™ West Femto Maximum Sensitivity Substrate (Thermo Scientific). Membranes were imaged with a BioRad ChemiDoc Imager. Blots were then stripped for 15 minutes and re-probed using an antibody for α-Actin (Abcam). Densitometry was performed using the BioRad Image Lab software and bands of interest were normalized to α-Actin.

Bone Marrow Transplants Studies

Two weeks prior to bone marrow transplant (BMT), 6 to 8 week old NOX2$^{-/-}$ or CD45.1 WT mice were transferred to sterile cages and fed sterile chow and acidified water (pH 2.0) containing 1 mg/ml of sulfamethazine-Na^{+} (Sigma-Aldrich) and 0.2 mg/ml of trimethoprim (Sigma-Aldrich) for prophylaxis. On the day of BMT, mice were lethally irradiated with a dose of 10 Gy 4 hours prior to BMT via a ^{137}Cs irradiator (J.L. Shepherd and Associates). Bone marrow (BM) cells were isolated from pooled femurs and tibias collected from mice and used to reconstitute the marrows

of recipient mice (~20 million cells per mouse). BM cells were transplanted to recipient mice via tail vein using a 25-gauge needle and mice were housed for 8 weeks to allow engraftment of the BM. Success of engraftment was determined by presence of CD45.1 or CD45.2 using Amcyan-conjugated anti-CD45.1 antibody (BD Bioscience) and anti-CD45.2 antibody (BioLegend).

Saline Challenge Study

Mice underwent a saline challenge and as a result, we examined the ability of mice to excrete water and sodium. Urination was stimulated by suprapubic compression. The mice were briefly anesthetized with isoflurane and intraperitoneally injected with normal saline using a volume equal to 10% of their body weight as previously described [153]. After awakening, mice were placed in metabolic cages for 4 hours and the volume-excreted urine was accurately recorded and presented as percentage of the volume injected. Sodium concentrations from excreted urine were measured with a flame photometer (Eppendorf EFOX 5053).

Nitric oxide measurements by Electron Spin Resonance

Mesenteric vessels were isolated and cleaned from any remaining fat. NO levels in vessels were quantified by electron spin resonance (ESR) and colloid $Fe(DETC)_2$ as previously described [252]. Following a 1 hour incubation, vessels were transferred to a 1 mL insulin syringe and snap-frozen in liquid nitrogen. ESR spectra were analyzed by EMX ESR spectrometer (Bruker Biospin Corp., Billerica, MA) with super high Q microwave cavity using liquid nitrogen Dewar flask (Wilmad-Labglass, Vineland, NJ). ESR settings for NO measurement include: field sweep, 100 Gauss; microwave frequency, 9.43 GHz; microwave power, 10 milliwatts; modulation amplitude, 2 Gauss; conversion time, 70 msec; time constant, 5.24 seconds; scan number, 4 [253].

Statistics

All data are expressed as mean ± SEM. One tailed- unpaired Student's *t*-tests were used to compare two groups. When examining the effect of bone marrow transplant from different recipients we employed one-way ANOVA with Student Newman Keuls post-hoc test. When examining the effect of bone marrow transplant from different recipients on blood pressure we employed two-way ANOVA with Student Newman Keuls post-hoc test. To compare telemetry blood pressure of STAT3/CD11c KO mice, we employed two-way ANOVA followed by Holm-Sidak's multiple comparisons test. To compare tail cuff blood pressure measurements on the Stattic treated mice, we employed two-way ANOVA with Student Bonferroni's post-hoc test. For vascular function studies, we employed a two-way ANOVA followed by Holm-Sidak's multiple comparisons test. *P* values are reported in the figures and were considered significant when less than 0.05.

Results

Angiotensin II-induced hypertension in Wildtype C57Bl/6 mice promotes accumulation of myeloid cells containing activated STAT3 in the kidney and aorta: In Chapter II, we defined some of the factors involved in mechanical stretch of vessels that promote monocyte transformation and activation in humans. In subsequent experiments, we sought to determine the role of hypertension *in vivo* on monocyte transformation in mice. We induced hypertension in C57Bl/6 WT mice by infusion of Ang II (490 ng/kg/min) for 6 days and analyzed single cell suspensions of the kidney, aorta, spleen and periaortic lymph nodes for the presence of monocytes, macrophages (MΦ) and DCs using a flow cytometry gating strategy that effectively allows discrimination of these cells (Figure 3-1A). We found a significant increase in the total number of macrophages (Figure 3-1B) and DCs (Figure 3-1C) and a trend of an increase in the monocytes (Figure 3-1D) within the aorta of Ang II treated mice. This increase in cell number was accompanied by an increase in STAT3 (Y705) activation (Figure 3-1E-F) and a trend of an increase in the monocyte population (Figure 3-1G). We also found an increase in macrophages, DCs and monocytes in the Ang II treated mice within the kidneys (Figure 3-1H-J) and an increase in STAT3 activation in each of these populations (Figure 3-1K-M). In the lymph nodes, only macrophages were increased in response to Ang II infusion (Figure 3-2A), while there was no change in DCs or monocytes. We also observed an increase in the STAT3 activation of monocytes in the lymph nodes (Figure 3-2B) of Ang II-treated mice. In the spleen, we found no major differences in the presence of macrophages or monocytes, but a significant decrease in DCs of hypertensive mice (Figure 3-2C). There was also a decrease in STAT3 activation within macrophages of spleen from Ang II-treated mice and no differences in the other cell types (Figure 3-2D). Further, we found that WT mice after 14 days of Ang II treatment had persistently

increased macrophages and DCs (Figure 3-3A) in the aorta accompanied by activation of STAT3 (Figure3-3B). To determine the location of monocytes infiltrating the aorta after 2 weeks of Ang II infusion in C57Bl/6 mice, we performed immunofluorescence of aortic sections for F4/80 (red), pSTAT3 (Y705, green) and DAPI. We found that after 2 weeks of Ang II infusion, monocytes and macrophages localize in the perivascular fat and adventitia segments of the aorta and these co-localize with pSTAT3 (Y705) (Figure 3-4). These data suggest that monocytes, DCs and macrophages leave secondary lymphoid organs in response to a hypertensive stimulus and accumulate in the vasculature and kidneys, which is associated with the end-organ damage and that these have STAT3 activation.

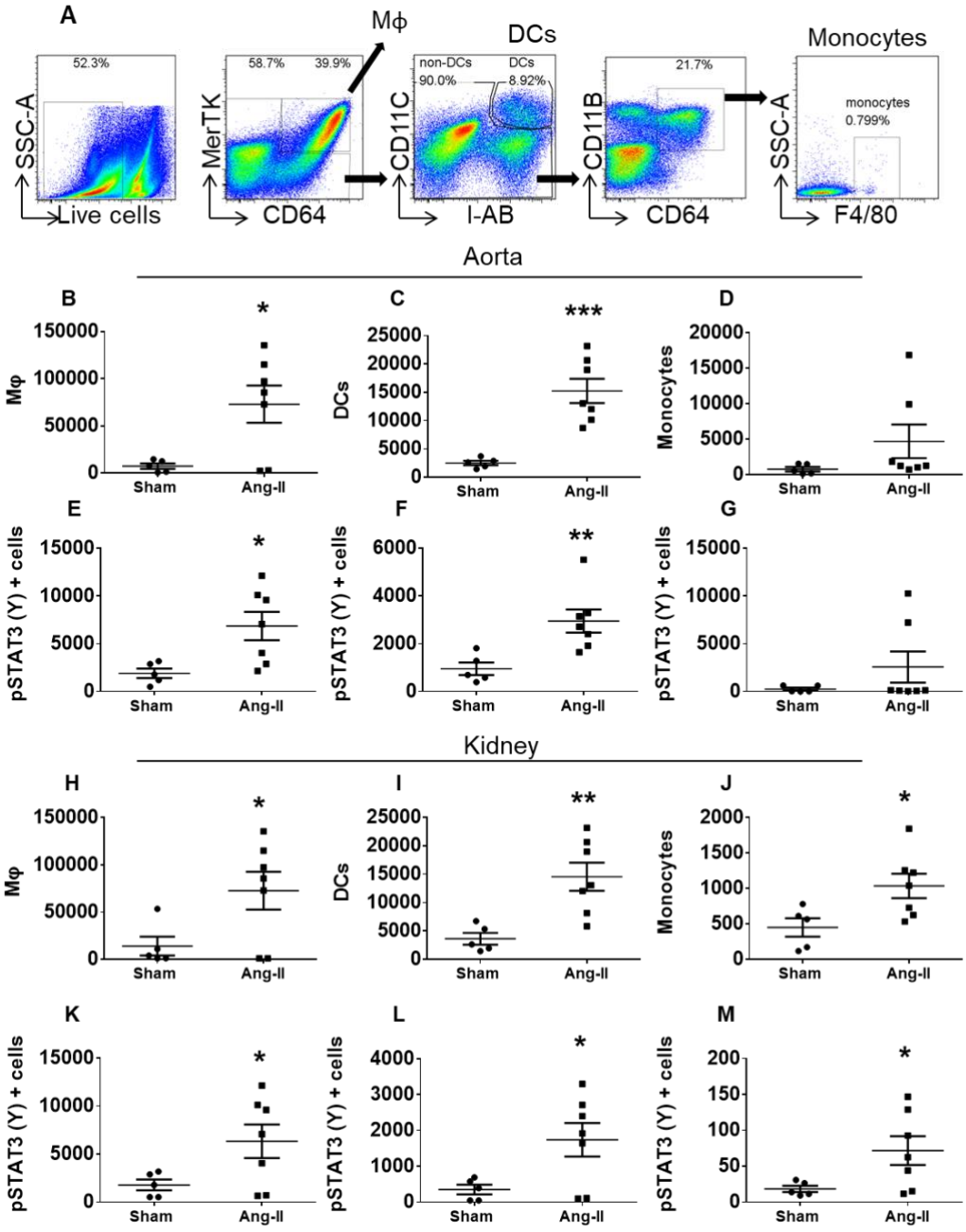

Figure 3-1: Angiotensin II-induced hypertension in wildtype C57Bl/6 mice promotes an increase in STAT3 phosphorylation in the immune cells from kidney and aorta. A. Representative flow cytometry dot plots showing the gating strategy to identify macrophages, DCs and monocytes from C57Bl/6 wildtype mice infused with Ang II (490 ng/kg/min) or sham for 6 days. **B-D.** Mean values of absolute numbers of indicated cell types per thoracic aorta. **E.** Mean values of pSTAT3 (Y) expression within the macrophage (Mϕ), (**F**) DC and (**G**) monocyte populations per thoracic aorta. **H-J.** Mean values of absolute numbers of indicated cell types per kidney. **K.** Mean values of pSTAT3 (Y) expression within the macrophage, (**L**) DC and (**G**) monocyte populations per kidney. A total of n=5, sham, and n =7, Ang II, treated mice per group were used. One-tail unpaired *t*-test was employed (*p<0.05, ** p<0.01, *** p<0.001).

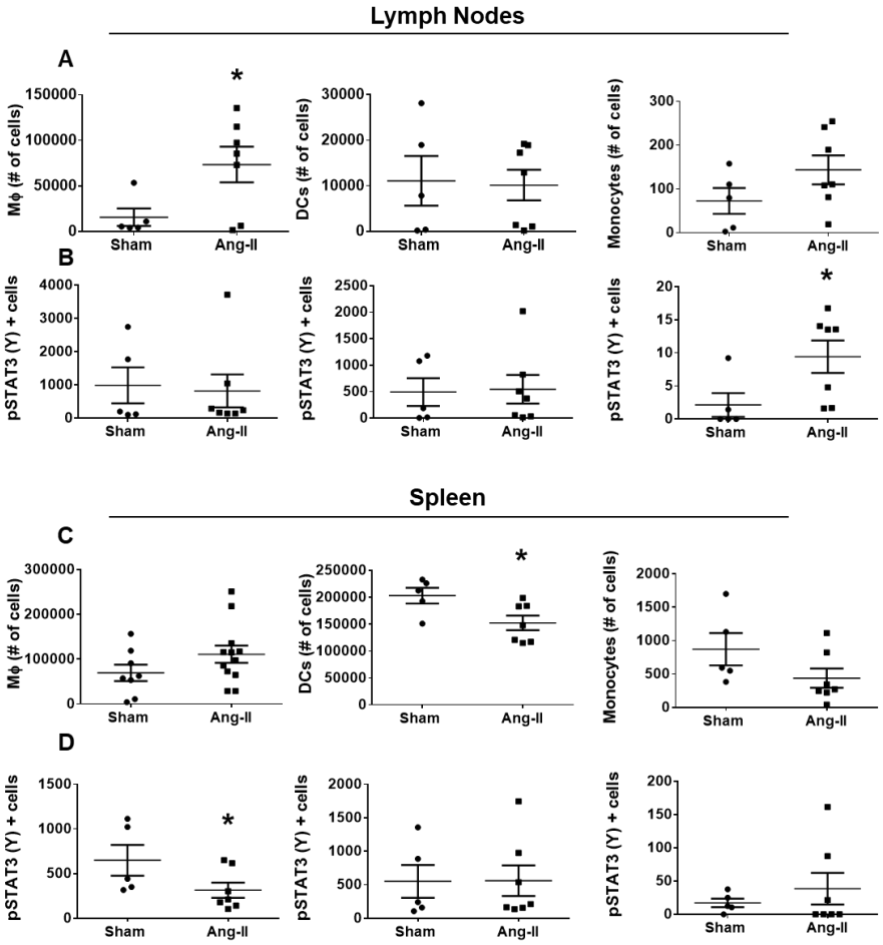

Figure 3-2: Angiotensin II-induced hypertension in wildtype C57 mice and the STAT3 phosphorylation in the immune cells from lymph nodes and spleen. C57Bl/6 wildtype mice were infused with Ang II (490 ng/kg/min) or sham for 6 days. **A.** Mean values of absolute numbers of indicated cell types per periaortic lymph nodes. Mean values of p-STAT3 (Y) expression within the macrophage (Mφ), DC and monocyte populations per periaortic lymph nodes. **B.** Mean values of absolute numbers of indicated cell types per spleen. Mean values of p-STAT3 (Y) expression within the macrophage, DC and monocyte populations per spleen. Statistical differences were determined using one-tailed unpaired *t*-tests (**p*<0.05).

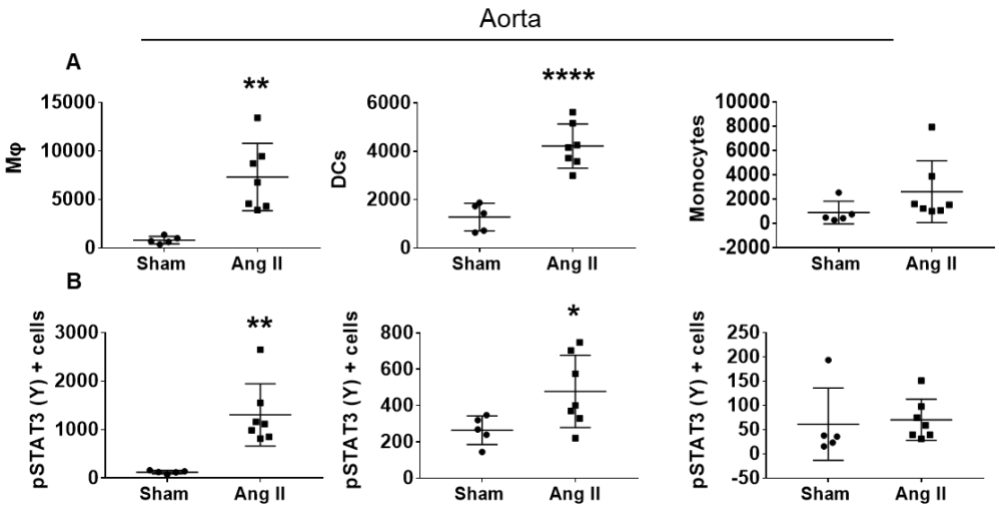

Figure 3-3: Angiotensin II-induced hypertension in wildtype C57Bl/6 mice promotes an increase in STAT3 phosphorylation in the immune cells from kidney and aorta after 14 days. C57Bl/6 wildtype mice were infused with Ang II (490 ng/kg/min) or sham for 14 days. **A.** Mean values of absolute numbers of macrophages (Mφ), DCs and monocytes per thoracic aorta. **B**. Mean values of p-STAT3 (Y) expression in the indicated cell type. Statistical differences were determined using one-tailed unpaired *t*-tests (**p*<0.05, ***p*<0.01, **** *p*<0.0001).

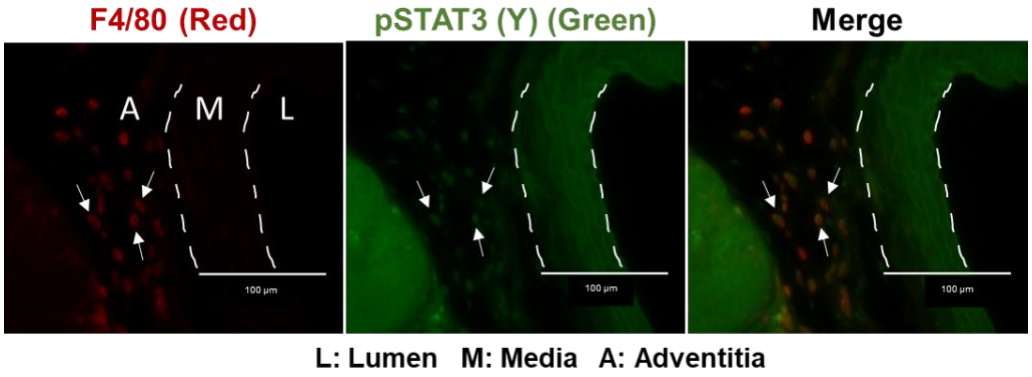

Figure 3-4: Monocytes and macrophages from Ang II hypertensive wildtype mice localize to the perivascular fat in the aorta and express STAT3. C57BL/6 mice were infused with Ang II (490 ng/kg/min) or sham for 14 days. Perfusion-fixed sections of the thoracic aortas were sectioned (6 mm) and immunofluorescence was performed to stain for F4/80 (red), pSTAT3 (Y705) (green) and counterstained with DAPI. Co-localization of F4/80 and pSTAT3 (Y) is shown.

Pharmacological STAT3 inhibition in Ang II-treated WT mice: Studies by Johnson et al. have shown the importance of STAT3 in the development of hypertension and that inhibition of STAT3 via treatment with the small molecule inhibitor, S3I-201, blunts the Ang II hypertensive response [210]. To determine whether *in vivo* inhibition of STAT3 will reduce transformation of monocytes to DCs and macrophages in hypertensive mice, we sought to inhibit STAT3 in hypertensive WT C57Bl/6 mice with the small molecule, Stattic (5 mg/mL). We administered Stattic or vehicle to mice by oral gavage every other day starting two days before Ang II infusion and continued treatment until mice were sacrificed (14-15 days after initial Ang II infusion). We measured systolic BP by tail cuff method and found no differences between Stattic or vehicle treated WT mice at baseline, day 7 and day 14 after Ang II infusion (Figure 3-5A). To determine whether Stattic-treated mice are protected against the endothelial dysfunction that occurs in response to hypertension, we assessed vascular function of resistance vessels by measuring endothelium-dependent and –independent relaxation of third order mesenteric arterioles from Stattic or vehicle-treated mice. Mesenteric arterioles from Stattic and vehicle-treated mice displayed no differences in relaxation in response to acetylcholine (Ach) (Figure 3-5B). Endothelium-independent relaxation in response to sodium nitroprusside (SNP) showed a trend for improvement in Stattic-treated mice (Figure 3-5C). However, when we measured the presence of monocytes, DCs and macrophages in the aorta of both experimental groups we found no differences in the presence of these or the levels of STAT3 activation indicating that treatment with Stattic and, thus, inhibition of STAT3 was not successful in these experiments (Figure 3-5D-E).

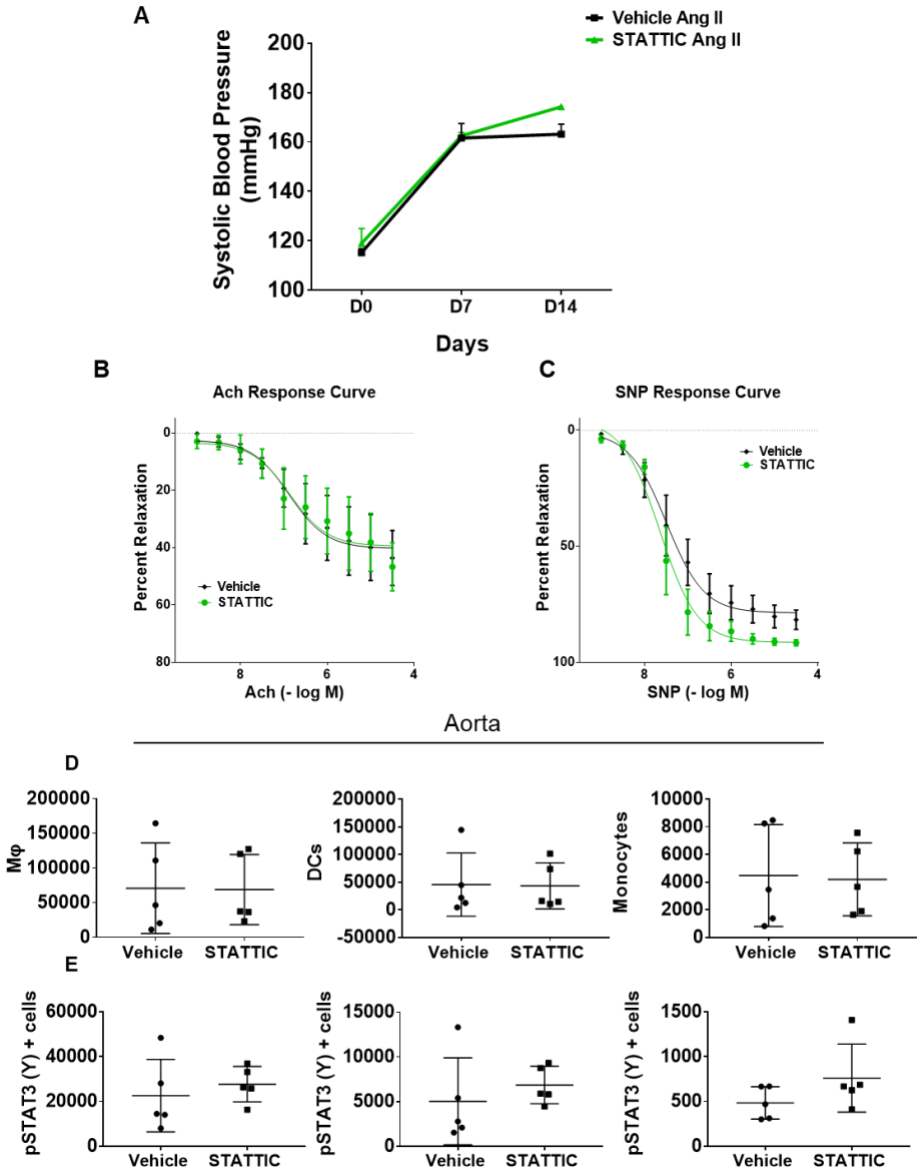

Figure 3-5: Systemic effects of the *in vivo* administration of STAT3 inhibitor, Stattic, in wildtype mice exposed to Ang II-induced hypertension. WT C57Bl/6 mice were given Stattic (5 mg/mL) or vehicle every two days by oral gavage starting two days before Ang II (490 ng/kg/min) infusion for 14 days. **A.** Systolic blood pressure measured noninvasively using the tail-cuff method over 14 days of Ang II infusion in Stattic- or vehicle-treated WT C56Bl/6 mice (n = 4 and n = 5, respectively). **B**. Endothelium-dependent relaxation in response to increasing doses of acetylcholine (Ach) in stattic- or vehicle-treated WT mice is shown. **C**. Endothelium-independent relaxation in response to increasing doses of sodium nitroprusside (SNP) is also shown (vehicle, n = 4; stattic, n = 3). **D.** Mean values of absolute numbers of Mφ, DC and monocyte populations per thoracic aorta. **E**. Mean values of p-STAT3 (Y) expression in the indicated cell type (n = 5). Statistical differences were determined using a two-way ANOVA followed by Bonferroni's multiple comparisons test for the tail-cuff experiments; a two-way ANOVA followed by Holm-Sidak's multiple comparisons test for the vascular function studies; and one-tailed unpaired t-tests for the flow cytometry on the aorta.

Effects of STAT3 inhibition in dendritic cells during hypertension: To assess the role of STAT3 in dendritic cells during hypertension, we created a knockout (KO) mouse using CRE-lox technology by crossing a $STAT3^{loxP/loxP}$ floxed mouse with the $CD11c^{tg/CD11cCRE}$ mouse. These STAT3/CD11c KO mice should have deletion of STAT3 within $CD11c^{+}$ cells including DCs, activated monocytes and activated macrophages. To confirm the inhibition of STAT3 in these mice, we isolated $CD11c^{+}$ cells from spleen of both $STAT3^{loxP/loxP}$ and STAT3/CD11c KO mice using magnetic sorting and extracted protein from these cells to perform Western blot techniques. As shown by the blots in Figure 3-6A, STAT3 protein expression was reduced by 5-fold compared to floxed controls (Figure 3-6B) after protein normalization to α-Actin. These STAT3/CD11c KO mice displayed mild colitis associated by presence of rectal prolapse in 75% of pups as well as impaired weight gain (Figure 3-6C). We implanted telemeters to measure blood pressure in these mice during baseline and two weeks after Ang II infusion. As shown in Figure 3-6D, the systolic blood pressure showed no differences at baseline between floxed controls and STAT3/CD11c KO mice, but there was a trend of a reduction towards the end of the Ang II treatment (> day 10) in the mice with STAT3 deletion in their DCs. There were no differences at baseline or after Ang II infusion in the diastolic blood pressure of both experimental groups (Figure 3-6E). We proceeded to look at the immune cells present within the aorta, spleen, kidney and blood at baseline levels in the STAT3/CD11c KO mice and the floxed controls. We found a significant reduction in the number of macrophages and DCs present in the spleen of the STAT3/CD11c KO mice accompanied by a reduction in the activation of STAT3 (Y705) in the macrophage, DCs and monocytes within this tissue (Figure 3-7A-B). In contrast, in the aorta, we found a significant increase in the number of macrophages and monocytes in the KO mice and the macrophages had an increase in STAT3 activation (Figure 3-7C-D). There was no

difference in the number of immune cells between KO and floxed controls in the kidney and blood (data not shown).

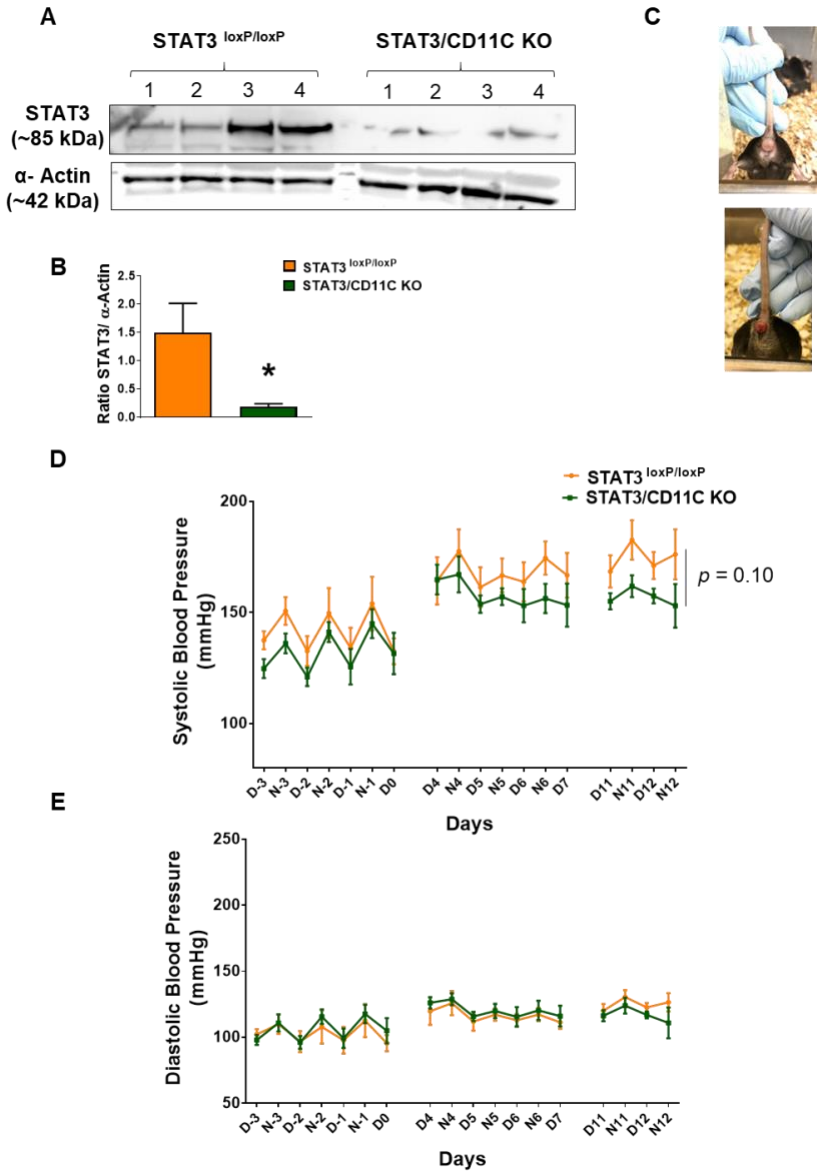

Figure 3-6: Effects of genetic deletion of STAT3 in dendritic cells in hypertension. STAT3/CD11c KO mice were made by crossing STAT3$^{loxp/loxp}$ with tg$^{CRE/CD11C}$ mice. **A**. DCs from STAT3/CD11c KO and STAT3$^{loxp/loxp}$ mice were isolated from the spleen by CD11c^{+} magnetic sorting and protein was isolated. Western blots for total STAT3 and normalized to α-Actin are shown. **B**. Normalized expression of STAT3 in DCs isolated from spleen of STAT3/CD11c KO and STAT3$^{loxp/loxp}$ mice (n = 4). **C**. Illustrations of rectal prolapse in STAT3/CD11c KO mice. **D**. Systolic blood pressures and (**E**) diastolic blood pressures using carotid radiotelemetry over 14 days of Ang II infusion in STAT3/CD11c KO and STAT3$^{loxp/loxp}$ mice (n = 6). Statistical comparison were made using unpaired t-tests for the Western blots and two-way ANOVA followed by Holm-Sidak's multiple comparisons test for the telemetry data (*p<0.05).

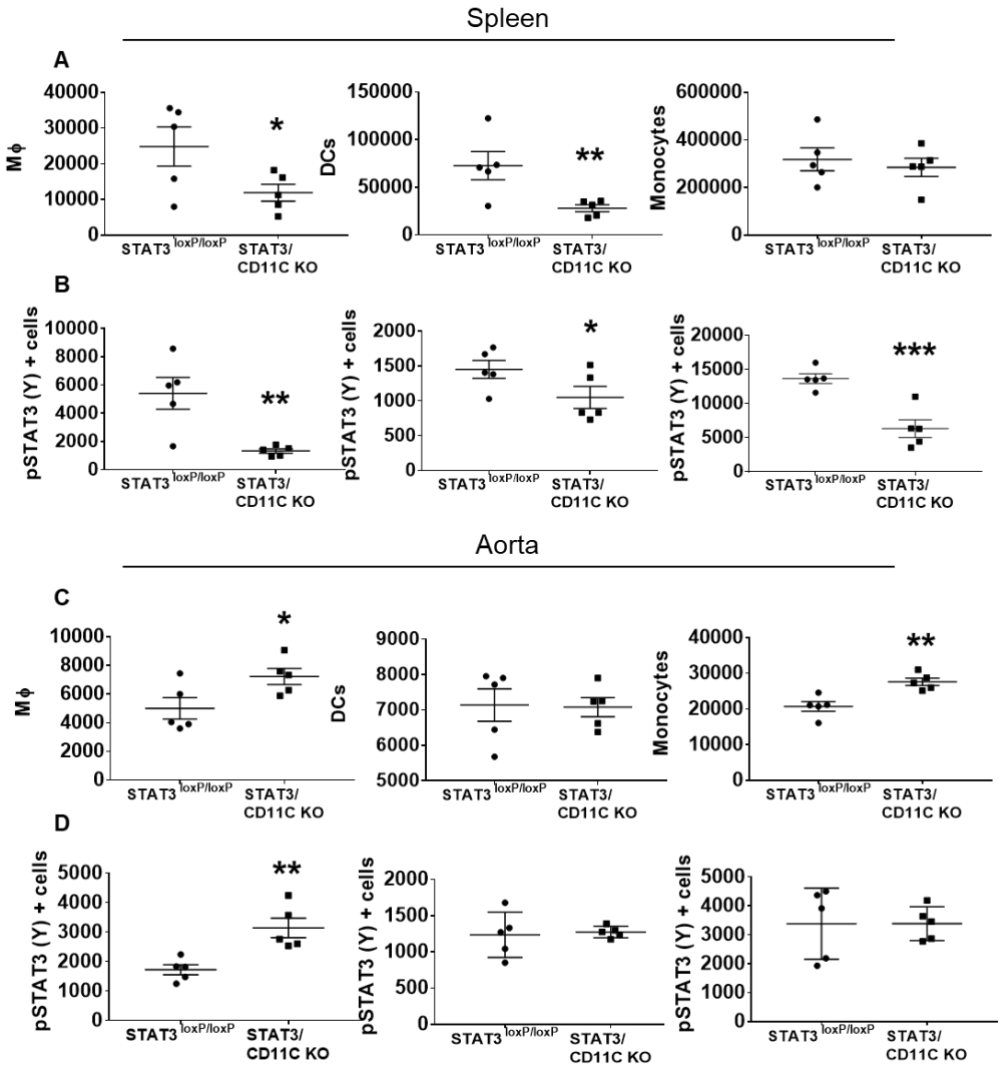

Figure 3-7: Characterization of immune cells and their expression of STAT3 within spleen and aorta of STAT3/CD11c KO mice at baseline. STAT3/CD11c KO and STAT3$^{loxp/loxp}$ mice were sacrificed for their immune cell characterization by flow cytometry. **A.** Mean values of absolute numbers of indicated cell types per spleen. **B**. Mean values of p-STAT3 (Y) expression within the Mφ, DC and monocyte populations per spleen. **C.** Mean values of absolute numbers of indicated cell types per thoracic aorta. **D.** Mean values of p-STAT3 (Y) expression within the macrophage, DC and monocyte populations per thoracic aortas. Statistical differences were determined using one-tailed unpaired *t*-tests (**p*<0.05, ***p*<0.01, ****p*<0.001).

In Chapter II, we found that the presence of NO is crucial for the inhibition of monocyte differentiation and activation during hypertensive levels of stretch on vessels. To further characterize these KO mice and determine whether NO is altered in their vessels, we proceeded to measure NO by ESR in mesenteric arterioles. We found no difference in NO production in

STAT3/CD11c KO mice exposed to Ang II hypertension (Figure 3-8A) compared to STAT3 floxed controls. To determine the effect of DC STAT3 inhibition on renal function, a sodium challenge study was performed as previously described [127]. We assessed whether there could be a potential shift in the pressure-natriuresis curve by injecting mice intraperitoneally with a saline load equal to 10% of their body weight. Mice were then placed in a metabolic chamber for 4 hours and urine volume and sodium content was measured. STAT3 floxed control mice excreted 50% and the STAT3/CD11c KO mice excreted 45% of the initial volume input. There were no differences in percent of sodium output in both experimental groups (Figure 3-8B). These data indicate that there is no apparent protection from renal damage in the STAT3/CD11c KO mice or the controls in response to Ang II hypertension.

We proceeded to measure the immune cells present in the aorta and kidney of STAT3/CD11c KO mice and floxed controls after two weeks of Ang II treatment. We found a trend ($P = 0.06$) of a reduction in the presence of $CD11c^{high}$ cells within the aorta (Figure 3-8C) and kidney (Figure 3-8E) of STAT3/CD11c KO mice compared to controls and no differences in macrophages, monocytes and $Ly6C^{high}$ cells in both tissues. In contrast to this decrease in DCs, there appeared to be a compensatory increase in macrophages within the kidney (Figure 3-8E). Further, we found a trend of a decrease in STAT3 phosphorylation in Y705 in the $CD11c^{high}$ cells from the aorta ($P = 0.1$) (Figure 3-8D) and kidney ($P = 0.08$) (Figure 3-8F). There were no differences in STAT3 phosphorylation in the other cell populations of the aorta and kidney. These data indicate that even after STAT3 deletion in the DCs, the few cells that remain to be positive for STAT3 can activate in response to Ang II and mobilize to secondary lymphoid organs.

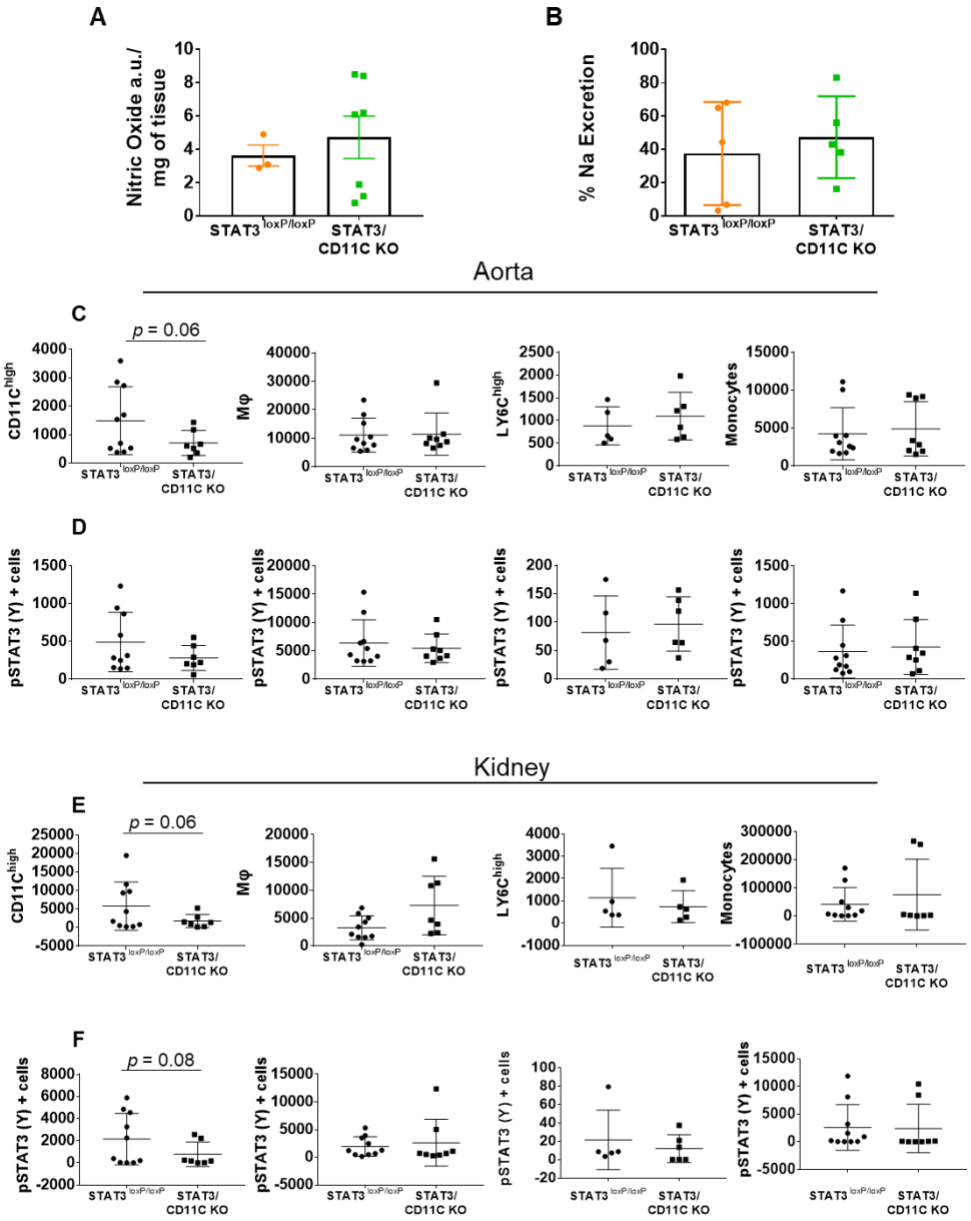

Figure 3-8: Characterization of alteration in vascular NO, renal function and immune cells in the kidney and aorta of STAT3/CD11c KO mice after Ang II induced-hypertension. A. Mesenteric vessels were isolated from guts of STAT3/CD11c KO and STAT3$^{loxp/loxp}$ mice after 14 days of Ang II infusion. NO levels in vessels were quantified by ESR and colloid Fe $(DETC)_2$ and normalized per mg of tissue (control, n = 3; KO, n = 7). **B**. Renal function was assessed by injecting mice intraperitoneally with a saline load equal to 10% body weight and determining urine volume and sodium excretion over the enduing 4 hours using a metabolic chamber (n = 5), this equals the ratio of % sodium excretion. **C**. Flow cytometry was performed to characterize immune cells. Mean values of absolute numbers of CD11c^{high} DCs, Mφs, LY6C^{high} cells and monocytes per thoracic aorta are shown. **D**. Mean values of p-STAT3 (Y) expression within these populations is shown. **E**. Mean values of absolute numbers of CD11c^{high} DCs, Mφs, LY6C^{high} cells and monocytes per kidney. **F**. Mean values of p-STAT3 (Y) expression within these populations is shown (control, n = 10; KO, n = 8). Statistical comparisons were made using unpaired *t*-tests.

NOX2 in hematopoietic cells is important for the hypertensive response and STAT3 activation in DCs: Components of the NADPH oxidase system are upregulated by hypertensive stimuli and inhibition of these components protect mice from both Ang II and DOCA-salt hypertension [56]. Hypertension is associated with increased ROS production by multiple organs and elevated vascular ROS promotes the development of hypertension in various animal models, including Ang II-induced, DOCA-salt hypertension [56-58], Dahl salt-sensitive hypertension and SHR rats [59-61]. NOX2, a component of the NADPH oxidase also known as $gp91^{phox}$, was originally discovered in phagocytes, but now it has been identified in multiple cells including endothelial cells, the tubular cells of the kidney and monocytic cells [34]. Dikalov et al. showed that depletion of NOX2, but not NOX1, NOX4, or NOX5 inhibits Ang II-induced superoxide production [250]. Dikalov et al. and our group has shown that NOX2 knockout mice ($NOX2^{-/-}$) display blunted Ang II-induced hypertension and the superoxide production associated with it.

We sought to determine whether deletion of NOX2 in hematopoietic cells of mice would reduce blood pressure and the transformation of monocytes to DCs and macrophages in addition to activation of STAT3 in response to Ang II hypertension. We performed BMT experiments to determine the source of NOX2 that is relevant to hypertension and measured their BP by radiotelemeter implants. WT mice given WT bone marrow developed severe hypertension after 2 weeks of Ang II infusion (Figure 3-9A). NOX2 deficient mice that received WT bone marrow had intermediate systolic blood pressure. In contrast, WT mice that received NOX2-deficient bone marrow were markedly protected against the effects of Ang II hypertension. These data are compatible with the concept that NOX2 in hematopoietic cells plays a very important role in

hypertension. There was a similar trend in the diastolic blood pressure, but it did not reach significance (Figure 3-9B).

We proceeded to characterize immune cells of BMT recipient mice in the aorta, kidney and spleen after two weeks of Ang II infusion. We found that mice lacking NOX2 in the somatic cells had a striking decrease in monocytes and macrophages in the aorta (Figure 3-9C-D). This is compatible with the scenario that chemokines and vascular adhesion molecules released by the vessels are redox sensitive. In contrast, these cells still accumulated in the vessels when NOX2 was deleted in the hematopoietic cells (Figure 3-9C-D). The kidney did not exhibit this pattern of altered immune cell infiltration suggesting that different mechanisms might guide renal and vascular inflammation (Figure 3-9E-F). We also found that NOX2 deficient DCs in the spleen exhibited a reduction in the presence of DCs as well as a lower STAT3 activation and IsoLG adduct formation (Figure 3-9G) compared to DCs with a functional NOX2. This scenario is compatible with the concept that hydrogen peroxide can modulate STAT3 activation (see Chapter II) and that ROS promote formation of IsoLG adducts [139].

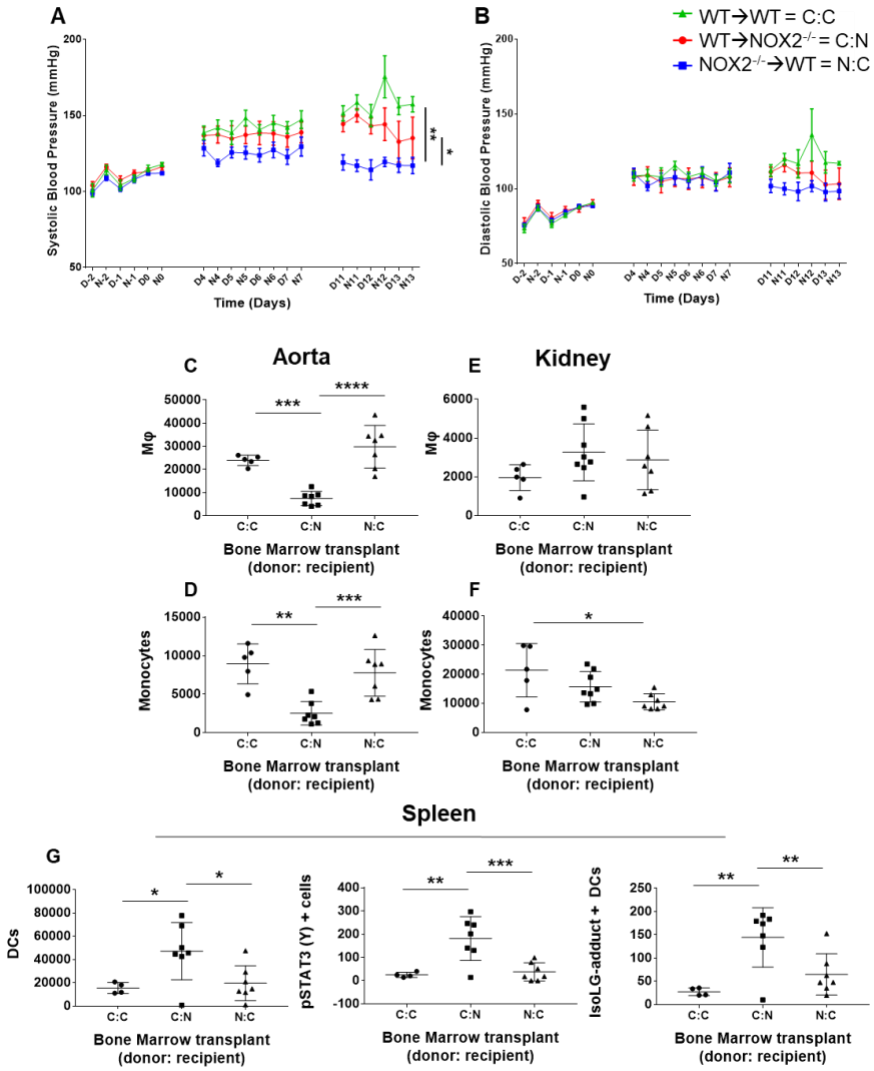

Figure 3-9: Bone marrow transplant studies to determine the relative role of hematopoietic versus somatic NOX2 in Ang II induced hypertension. BMT was performed using NOX2$^{-/-}$ (CD45.2) and WT SJL (CD45.1) mice as either donors or recipients as indicated. Three groups were designated (donor: recipient): C:C (WT to WT, control group) and C:N (WT to NOX2$^{-/-}$) and N:C (NOX2$^{-/-}$ to WT) as chimeric groups. **A**. Telemetry recordings of systolic blood pressure and (**B**) diastolic blood pressure at baseline and during 14 days of Ang II infusion (490 ng/kg/min) (C:N, n = 6; N:C, n = 5; C:C, n = 4). **C**. Quantification of flow cytometry for total of macrophages and (**D**) monocytes per thoracic aorta (C:N, n = 7; N:C, n = 7; C:C, n = 4). **E**. Mean values of absolute numbers of macrophages and (**F**) monocytes per kidneys (C:N, n = 8; N:C, n = 7; C:C, n = 4). **G**. Mean values of absolute numbers of DCs and expression of p-STAT3 (Y) and IsoLG-adducts within the DCs per spleen (C:N, n = 7; N:C, n = 7; C:C, n = 4). Statistical comparisons were made using a two-way ANOVA followed by the Newman-Keuls multiple comparisons test for the telemetry data and one-way ANOVA followed by the Newman-Keuls multiple comparisons test for the flow cytometry analysis (*p<0.05, **p<0.01, ***p<0.001).

Discussion

In this study, we demonstrate that tissue infiltrating monocytes, macrophages and DCs exhibited an increase in phosphorylated STAT3 at day 6 and day 14 after Ang II infusion, specifically in aorta and kidney. We created a CRE-lox mouse that had STAT3 deleted in their $CD11c^{+}$ DCs. These STAT3/CD11c KO mice showed a trend of a reduction in systolic BP compared to STAT3 floxed controls. Finally, we found that bone marrow transplantation from $NOX2^{-/-}$ mice into WT mice lowered systolic BP compared to $NOX2^{-/-}$ mice that received WT bone marrow. WT mice with $NOX2^{-/-}$ bone marrow also had a reduction in STAT3 phosphorylation and IsoLG-adducts in DCs from the spleen. These data suggest that NOX2 in hematopoietic cells promotes hypertension in part by activating STAT3 and these data are compatible with studies I performed in Chapter II showing that hydrogen peroxide likely plays a role in the development of hypertension.

In initial experiments to examine the role of STAT3 *in vivo*, we treated WT mice with Ang II for 6 and 14 days. At this time, we found a striking increase in infiltrating monocytes, macrophages and DCs in the aorta and kidneys compared to sham-infused animals. These cells consistently showed activation of STAT3. Further, STAT3 activation in these immune cells persisted following two weeks of Ang II infusion in aorta, thus, STAT3 activation appears early in hypertension. The site of this immune infiltration was located in the periovascular fat and adventitia. This is compatible with findings from our laboratory that the media is largely spared from these inflammatory cytokines [7] .

In an effort to demonstrate the role of STAT3 *in vivo* in hypertension, I used two approaches. In the first, I administered the small molecule, Stattic, to mice during Ang II infusion. This dose and mode of administration of Stattic was based on a prior study, which the drug was used to treat

head and neck cancer [254]. In our study, Stattic was not effective in reducing the hypertension caused by Ang II, improving vascular function, or surprisingly preventing STAT3 activation. Moreover, treatment with Stattic was not effective in preventing immune activation *in vivo*. The reason for this lack of effect of Stattic might be due to either inadequate dosing, mode of administration, or off-target effects that lead to toxicity. With regard to the last point, we found that approximately 30% of mice treated with Stattic did not survive two weeks of administration. It is therefore unlikely that increasing the dose of Stattic would have been beneficial. These results differ from those of Johnson et al. who used another small molecule inhibitor of STAT3, S31-201, which prevented Ang II-induced hypertension [210]. Future studies using S31-201 might prove informative in probing the role of STAT3 in hypertension and related disorders.

The second approach I used to address STAT3 *in vivo* was to delete STAT3 in DCs using CRE-lox technology. I found that this led to a slight reduction of blood pressure, which did not reach statistical significance. Moreover, deletion of STAT3 in DCs markedly reduced the number of DCs in the spleen. Disappointingly, I found that the STAT3 positive DCs were not significantly reduced in either the aorta or the kidney after Ang II infusion. Further, there was no reduction of infiltration of other immune cells including monocytes and macrophages in these organs. These data are compatible with the concept that STAT3 in necessary for DC formation [229], but the few cells remaining after STAT3 deletion can be mobilized to secondary lymphoid organs such as aorta and kidney upon exposure to Ang II. Importantly, the STAT3/CD11c KO mice displayed poor weight gain and exhibited rectal prolapse similar to that previously reported [255]. During attempts to perform telemetry implantation and Ang II infusion, approximately 50% of STAT3/CD11c KO mice died. Given the high mortality and morbidity of STAT3 deletion in DCs, it is difficult to make conclusions regarding the roles of STAT3 in hypertension using this model.

In Chapter II, I showed that hydrogen peroxide plays a role in the activation of STAT3. A major source of ROS is the NADPH oxidase. Moreover, mice lacking various components of the NADPH oxidase are protected against hypertension. However, the relative role of hematopoietic vs somatic cell NADPH oxidase roles have not been previously defined. In the current studies, I preformed additional experiments to dissect the relative contribution of NADPH oxidase in hematopoietic cells vs somatic cells in STAT3 activation, immune infiltration and hypertension. To accomplish this, I transplanted NOX2 deficient bone marrow into WT mice and vice versa. I also preformed WT to WT bone marrow transplantation as a control. We found that NOX2 in hematopoietic cells seems to have a major role in hypertension. WT mice receiving NOX2 deficient bone marrow were protected from elevation of blood pressure during Ang II infusion. In contrast, NOX2 deficient mice that received WT bone marrow had an intermediate phenotype of hypertension. In the spleen, WT mice that received NOX2 deficient hematopoietic cells had a reduction in the presence of DCs similar to that observed in the STAT3/CD11c KO mice accompanied by a reduction in STAT3 activation and IsoLG-adduct formation confirming the role of NOX2 in this process as previously described [139]. A striking finding in these mice was that there was a marked reduction of macrophage and monocytes infiltration in the vessel wall suggesting a role of tissue NOX2 in promoting recruitment of monocytes and macrophages. This is compatible with the concept that the transcription of adhesion molecules and chemokines involved in monocyte trafficking is redox sensitive [256, 257]. In contrast to the aorta, there was no reduction in monocyte/macrophage recruitment to the kidney suggesting that there are different modulators on vascular and renal infiltration.

In this chapter, we sought to determine the role of STAT3 in hypertension using an *in vivo* approach. We found that immune cells infiltrating secondary lymphoid organs after Ang II

hypertension have activation of STAT3. Further, we found that NOX2 in hematopoietic cells plays a role in the activation of STAT3 and formation of IsoLG adducts, which contribute to the immune activation that occurs in hypertension. These findings give insight into the potential role of ROS, in particular, hydrogen peroxide and the activation of STAT3 in immune cells, which could lead to monocyte activation and transformation similar to our findings in Chapter II.

Chapter IV

Generation of human induced pluripotent stem cells for their differentiation into endothelial cells

Introduction

In Chapter II, I established a novel method to study human monocytes and identified a new mechanism on how they can become activated in hypertension. Monocytes are pleotropic subset of leukocytes that are capable of giving rise to a variety of cells relative to the cardiovascular system including DCs, macrophages and even collagen-forming cells referred to as fibrocytes. Previously, it was thought that monocytes had to transform into DCs or macrophages in order to present antigen. However, recent studies have shown that monocytes can enter tissues and reemerge with minimal differentiation. While in tissues, these monocytes can take up “non-self” antigens and can transport and present these to T cells within secondary lymphoid organs such as lymph nodes and spleen [94]. These could be foreign antigens from bacteria, viruses or could be modified self-proteins sometimes referred to as neo-antigens. Thus, in studying the ability of monocytes to activate T cells, it would be ideal if all the cells present in a model such as mine i.e. monocytes, endothelial cells and T cells were from the same donors.

Thus, in experiments described in this chapter, I sought to establish an experimental model in which I can derive endothelial cells from PBMCs of our monocyte donors using the method of induced pluripotent stem cells (iPSCs). The ultimate goal of this experimental endeavor was to determine the propensity of endothelial cells and monocytes from the same subject to interact and produce an immune response. Ultimately this could be used to characterize the propensity of an individual to develop immune activation in hypertension.

Materials and Methods

Human subjects

We performed studies in which we included male and female normotensive participants who had blood pressures less than 135/80 mmHg. Normal volunteers were included between ages 18-55.

Exclusion criteria included the following: 1) Autoimmune disease or history of inflammatory diseases; 2) Recent vaccinations, within the last 3 months; 3) Confirmed or suspected causes of secondary hypertension; 4) Severe psychiatric disorder; 5) HIV/AIDS; 6) Current treatment with steroids or antihistamines; 7) Liver or renal disease and 8) History of cancer. This was approved by the Vanderbilt Institutional Review Board and conformed to standards of the US Federal Policy for the Protection of Human Subjects.

Human aortic endothelial cells

HAECs (Lonza, Walkersville, MD, USA) were plated on T-75 plates with an initial passage of 4 and fed every other day with EBM-2 medium (Lonza) containing EGM-2 growth factors and supplements (Lonza) and 2% fetal bovine serum (FBS) or Vascular Cell Basal Medium (ATCC®) with Endothelial Cell Growth Kit-VEGF (ATCC® PCS-100-041) and 5% anti-anti (100X, Gibco). Once cells reached 100% confluency, they were split with 0.25% Trypsin-EDTA (1X) (Gibco) and cultures were kept in 37°C incubators with 5% CO_2.

Monocyte isolation and monocyte-human aortic endothelial cells cultures

HAECs (Lonza, Walkersville, MD, USA) were grown to confluency on flexible 6-well culture plates that permit uniaxial stretch (Flexcell® International Corporation, Burlington, NC, USA). These were coated with collagen I and 1% gelatin cross-linked with 0.05% of glutaraldehyde.

Peripheral blood mononuclear cells were isolated from blood by Ficoll-density gradient centrifugation. $CD14^+$ monocytes were further isolated from PBMCs using negative selection with the monocyte isolation kit (Miltenyi Biotec 130-096-537; Miltenyi Biotec, Auburn, CA, USA) as previously described [149]. Monocyte purity was confirmed by flow cytometry using an anti-CD14 conjugated antibody and an 80% or higher purity was considered viable for experimental purposes. Monocytes from each volunteer were added to the endothelial cells previously grown on Uniflex® 6-well culture plates so that we could simultaneous examine the response of one million monocytes to endothelial cells undergoing 5% and 10% uniaxial stretch.

Fluorescence-activated cell sorting and T cell proliferation assay in human cells

Monocyte populations were collected from the endothelial cells co-culture by including the cells in suspension and those that adhered to the endothelium. Adhered monocytes and endothelial cells were released in suspension by digesting the collagen I and 1% gelatin coating with Collagenase A (1 mg/ml, Roche), Collagenase B (1 mg/mL, Roche) and DNase I (0.1 mg/mL, Sigma) in RPMI 1640 medium with 10% FBS for 30 minutes at 37°C. Single cell suspensions were stained for PerCPCy5.5-conjugated anti-CD31 and DAPI (Biolegend) and fluorescence-activated cell sorting (FACS) was used to sort out the $CD31^+$ ECs and select for the remaining monocyte populations using BD FACSAria III instrument (Flow Cytometry Shared Resources, Vanderbilt University). Two days later, the same patients were recruited to draw blood for pan T cell isolation (Miltenyi) from the PBMCs by magnetic labeling and sorting. These T cells were pre-labeled with carboxyfluorescein succinimidyl ester (CFSE) cell proliferation kit (Invitrogen) and cultured with the FACS sorted CD31- cell populations at a 1:10 ratio (monocyte: T cell) for 7 days. Proliferation was measured by the CFSE dilution using flow cytometry

Human-induced pluripotent stem cell generation

PBMCs were isolated by Ficoll-density gradient centrifugation from blood of healthy normotensive volunteers as described in Chapter II. We used the CytoTune® -iPS 2.0 Sendai Reprogramming Kit under feeder-free conditions (Gibco by Life Technologies) to create our human iPSC colonies as previously described [258]. Four days before transduction of virus, isolated PBMCs were seeded in complete PBMC medium (complete StemPro®-34 serum-free medium), in which we added fresh cytokines every day including SCF (100 ng/mL), FLT-3 (100 ng/mL), IL-3 (20 ng/mL) and IL-6 (20 ng/mL). Again, we changed the media daily carefully without disturbing the cells. At the day of virus transduction, we counted the cells and performed transductions in live cells at approximately 300,000 cells per sample. We proceeded to add the Klf4, Oct4, and Sox2 (KOS) virus and the c-Myc virus at a multiplicity of infection (MOI) of 5 (KOS MOI = 5, c-Myc MOI = 5) and the Klf4 virus at an MOI of 3 (hKlf4 MOI = 3) in a total volume of 1 mL. By placing a Parafilm® sealing film, we proceeded to centrifuge the samples at 2250 rpm for 30 minutes at room temperature. Following this step, we resuspended the pellet medium containing the virus and an additional 1 mL of complete PBMC media. The following day we harvested the cells containing the virus and removed the virus by centrifuging the cells at 200 g for 10 minutes and aspirating supernatant. We cultured the live cells in complete PBMC media for 2 days. Next, we seeded the live cells in previously coated Geltrex® matrix (ThermoFisher) and cultured these in complete StemPro®-34 medium without the cytokines. On day 3 to 6 after viral transduction, we replaced media every other day with the same media they were seeded in without disturbing the cells. On day 7 after transduction, we began to transition to the Essential 8® medium (ThermoFisher) by removing half of the StemPro®-34 medium and adding the removed volume of this new media. Twenty-four hours later, we replaced the entire media to the

Essential 8® medium and continued to replace media every day for the next 21 days. We also observed the cells and looked for the emergence of cell clumps, which indicate transformation. Day 15 to 21 after transduction, colonies grew to an appropriate size for transferring. Fully grown colonies were manually picked and transferred to a Geltrex® matrix coated 12-well plates according to manufacturer's instructions. These experiments were performed in a specialized facility for iPSC culture and differentiation.

Differentiation of human iPSCs from PBMCs into endothelial cells

For differentiation, human iPSCs were dissociated using StemPro Accutase (ThermoFisher) and plated on growth factor-reduced Matrigel (BD Biosciences) at a density of 37,00 to 47,000 cells cm^{-2} in mTeSR1 media (STEMCELL Technologies) with 10 µM ROCK inhibitor Y-27632 (Calbiochem). Twenty-four hours later, the medium was replaced with Priming Medium, which consists of N2B27 medium [1:1 mixture of DMEM:F12 (1:1) with Glutamax and Neurobasal media supplemented with N2 and B27 (all from Life Technologies)] with 1 µM CP21R7 (Roche), a GSK3 inhibitor, and 25 ng/Ml of BMP4 (R&D Systems). Three days later, this priming medium was replaced with endothelial cell Induction Medium consisting of StemPro-34® SFM medium (Life Technologies) supplemented with 200 ng/mL VEGF (Miltenyi Biotech) and 2 µM forskolin (Sigma-Aldrich) to induce differentiation of iPSCs into endothelial cells. The following day the Induction Medium was renewed. On day six of differentiation, the endothelial cells were dissociated with StemPro Accutase (ThermoFisher) and selected by magnetic sorting using the CD31 microbeads kit (Miltenyi Biotech).

Flow cytometry

T cell proliferation study: Monocyte/T cell co-cultures were harvested and single cell suspensions were stained for flow cytometry analyses using the following directly conjugated

antibodies including: PerCPCy5.5-conjugated 7-AAD viability staining solution (eBioscience), Pacific Blue-conjugated anti-CD3 (BioLegend), PECy7-conjugated anti-CD8 (BioLegend), and APC Cy7-conjugated anti-CD4 (BioLegend). BD FACSCanto II system was used to run the samples and number of proliferated T cells were calculated and averaged using the FlowJo® software. Gates were set using FMO controls.

Characterization of human-iPSCs-derived endothelial cells: Single cell suspensions were stained for flow cytometry analyses using the following directly conjugated antibodies including: Pacific LIVE/DEAD™ Fixable Violet Dead Cell Stain (Life Technologies), PE-conjugated anti-VE-Cadherin (BioLegend) and PerCPCY5.5-conjugated anti-CD31 (BioLegend). BD FACSCanto II system was used to run the samples and FlowJo® was used for data analysis. Gates were set using FMO controls.

Statistics

All data are expressed as mean ± SEM. One tailed- paired Student's *t*-tests were used to compare the number of proliferated T cells cultured with monocytes exposed to endothelial cells undergoing 5% vs 10% stretch. *P* values are reported in the figures and were considered significant when less than 0.05.

Results

Monocytes exposed to endothelial hypertensive stretch are capable of promoting T cell proliferation: In Chapter II, we described a mechanism in which monocytes can become activated and transform to different subset of cells when cultured with endothelial cells undergoing hypertensive stretch. Further, it has been reported that monocytes can enter tissues and re-emerge into the circulation without differentiation into macrophages or dendritic cells [94]. These cells can transport antigen to lymph nodes and have enhanced ability to drive T cell proliferation. To determine if endothelial stretch conveys this property to monocytes, we obtained T cells from the same monocyte donors after their monocytes had been exposed to endothelial cell stretch for 48 hours. These autologous T cells were labeled with CFSE and co-cultured with monocytes for 7 days and their proliferation was examined by CFSE dilution. These methods are illustrated by Figure 4-1A. Following the gating strategy shown in Figure 4-1B, we measured proliferation within the $CD4^+$ and $CD8^+$ T cells. As shown in Figure 4-1C, monocytes previously exposed to 10% stretched endothelial cells for 48 hours exhibited an enhanced ability to drive $CD4^+$ and $CD8^+$ T cell proliferation as compared to the cells from the 5% stretched endothelial cell cultures. After quantification of these cells, both $CD4^+$ and $CD8^+$ T cells significantly proliferated when cultured with monocytes exposed to endothelial cells undergoing 10% stretch (Figure 4-1D).

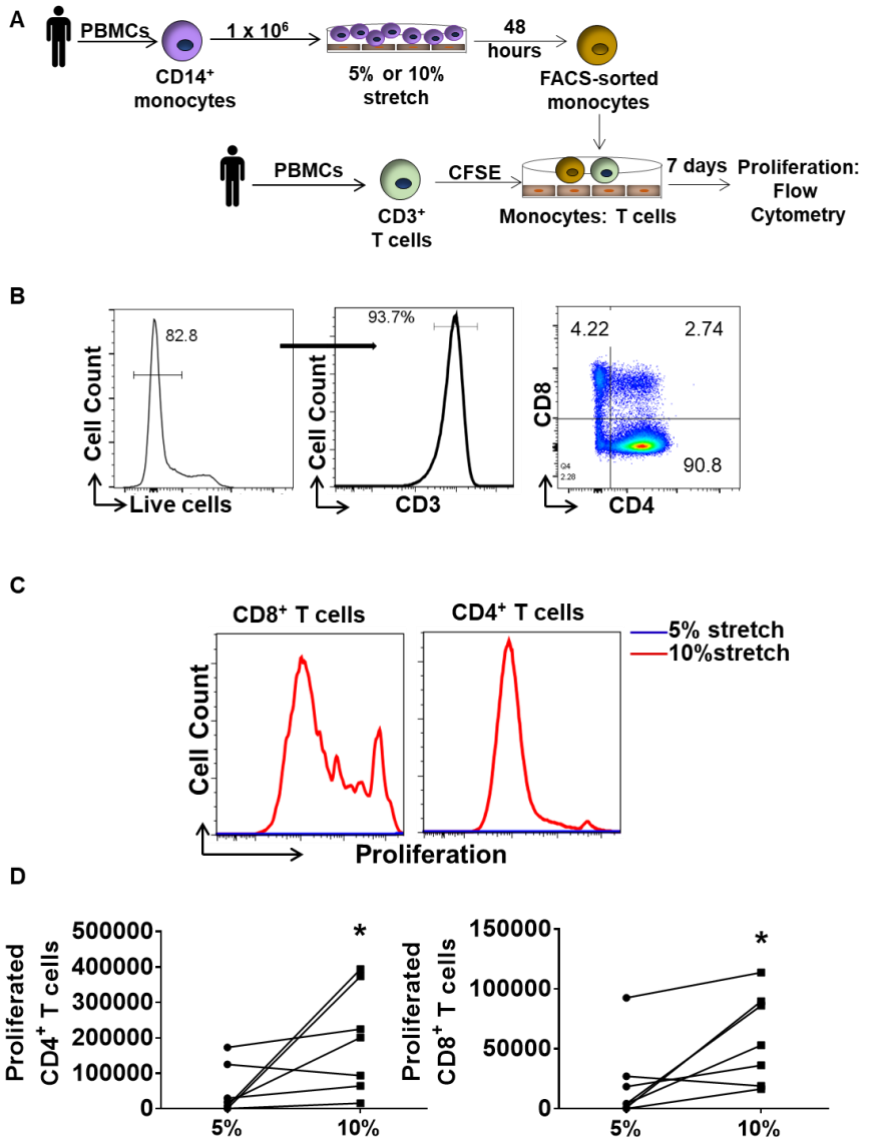

Figure 4-1: Increased endothelial stretch primes human monocytes to induce T cell proliferation. **A.** Monocyte-HAECs cultures were stretched to either 5% or 10% for 48 hours followed by sorting monocytes from HAECs using CD31$^+$ isolation kit and FACS. Monocyte populations were cultured with CFSE-labeled T cells isolated from PBMCs of the same participants. Seven days later, we measured proliferation in the CD4$^+$ and CD8$^+$ T cell populations by flow cytometry. **B**. Flow cytometry gating representatives showing live cells, CD3$^+$ T cells and CD4$^+$ and CD8$^+$ T cells. **C**. Histogram representatives for number of proliferated CD4$^+$ and CD8$^+$ T cells. **D**. Changes in number of proliferated CD4$^+$ and CD8$^+$ T cells after 7 days in culture for each subject are depicted by connected lines (n = 7). Comparisons were made using one-tail paired *t*-tests (*p<0.05).

Generation of human induced-pluripotent stem cells and differentiation to endothelial cells: In Chapter II and the T cell proliferation experiment mentioned above, we used commercially purchased HAECs derived from individuals different from our monocyte donors. To create an environment in which autologous cells were used, we attempted to differentiate human iPSCs into endothelial cells from our PBMC donors. We proceeded to create iPSC colonies by dedifferentiating freshly isolated PBMCs from blood of our human volunteers. Using the CytoTune®-iPS 2.0 Sendai Reprogramming kit, described in more detail in the methods, we introduced Sox2, Oct4, Klf4 and c-Myc to the somatic cells. We were able to grow full-sized iPSC colonies. We manually picked these colonies and cultured these in Geltrex® matrix-coated plates until we acquired more colonies and performed up to 6 passages from the original colony. We were able to confirm the iPSCs by immunofluorescence and the presence of Tra160, an iPSC specific protein as illustrated in Figure 4-2.

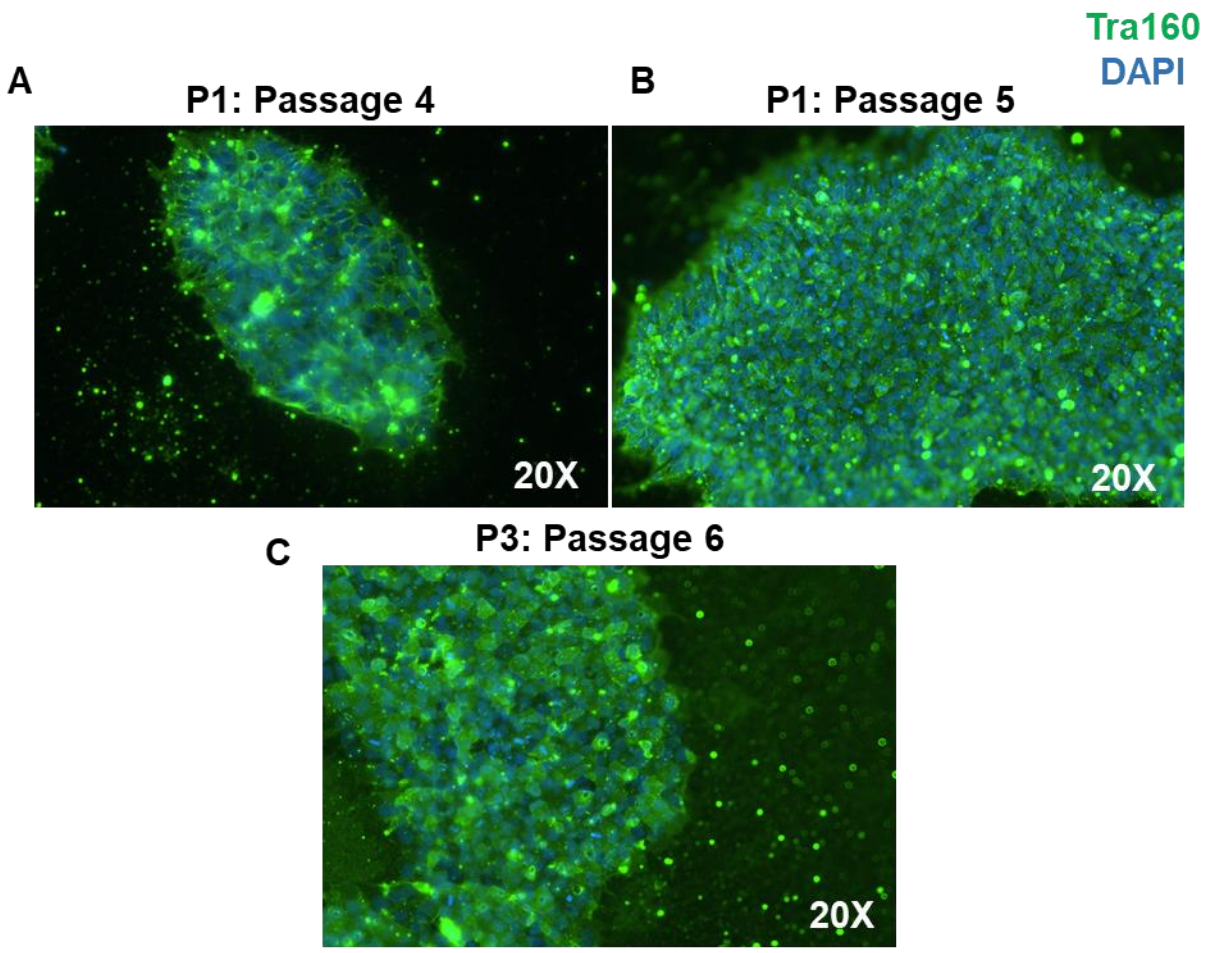

Figure 4-2: Characterization of human induced-pluripotent stem cell colonies. PBMCs were isolated from normal human volunteers and subjected to de-differentiation and transformation into iPSC colonies by introducing Sox2, Oct4, Klf4 and c-Myc genes. **A**. Immunofluorescence for the iPSC specific protein Tra160 was performed in participant 1 passage 4, (**B**) participant 1 passage 5, and (**C**) participant 3 passage 6. DAPI was used to counterstain the nucleus.

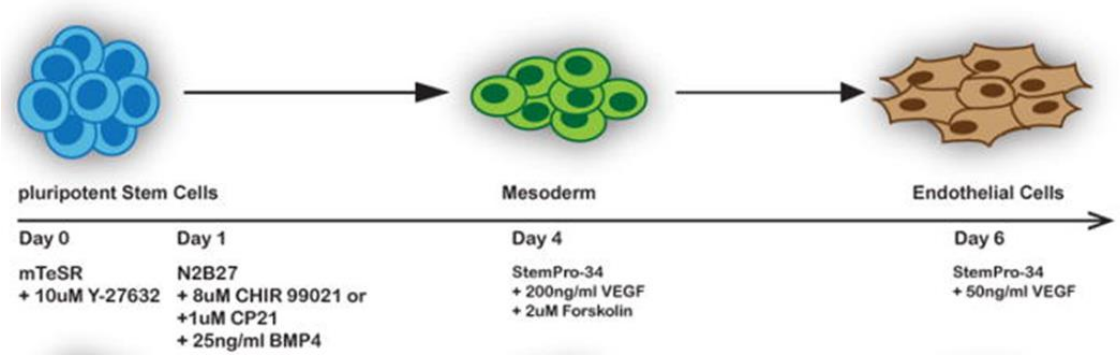

Figure 4-3: Methodology for differentiating human iPSCs into endothelial cells. Adapted from Patsch et al. [259].

To differentiate human iPSCs from PBMCs into endothelial cells we attempted several strategies. In one, we used the previously published method by Patsch et al. illustrated in Figure 4-3 [259]. On day 0, human iPSCs were seeded on Matrigel and cultured in mTeSR1 medium. One day later, the media was changed to the Priming Medium described in more detail in the Methods. After three days of priming, iPS cells were induced for their differentiation into endothelial cells by the addition of VEGF and forskolin. Six days after priming and their differentiation, the endothelial cells were sorted using magnetic beads for CD31 and plated in 0.05% gelatin coated plates to promote their growth and confluency. Visually, these iPSC-derived cells failed to acquire the typical cobblestone appearance of endothelial cells. Thus, to examine the differentiation of human iPSCs into endothelial cells we used flow cytometry to measure the expression of CD31 and VE-Cadherin in these cells and in human aortic endothelial cells as positive controls. Using the gating strategy shown in Figure 4-4A, we found that in this colony of human iPSCs the differentiated cells expressed 0.4% of CD31 and 8.8% of VE-Cadherin compared to the HAECs which expressed 99.6% and 58.6% of these markers respectively (Figure 4-4B-C). Given the lack of the characteristic cell morphology and the lack of CD31 and VE-Cadherin, which are typical markers of endothelial cells, we concluded that this protocol was not successful.

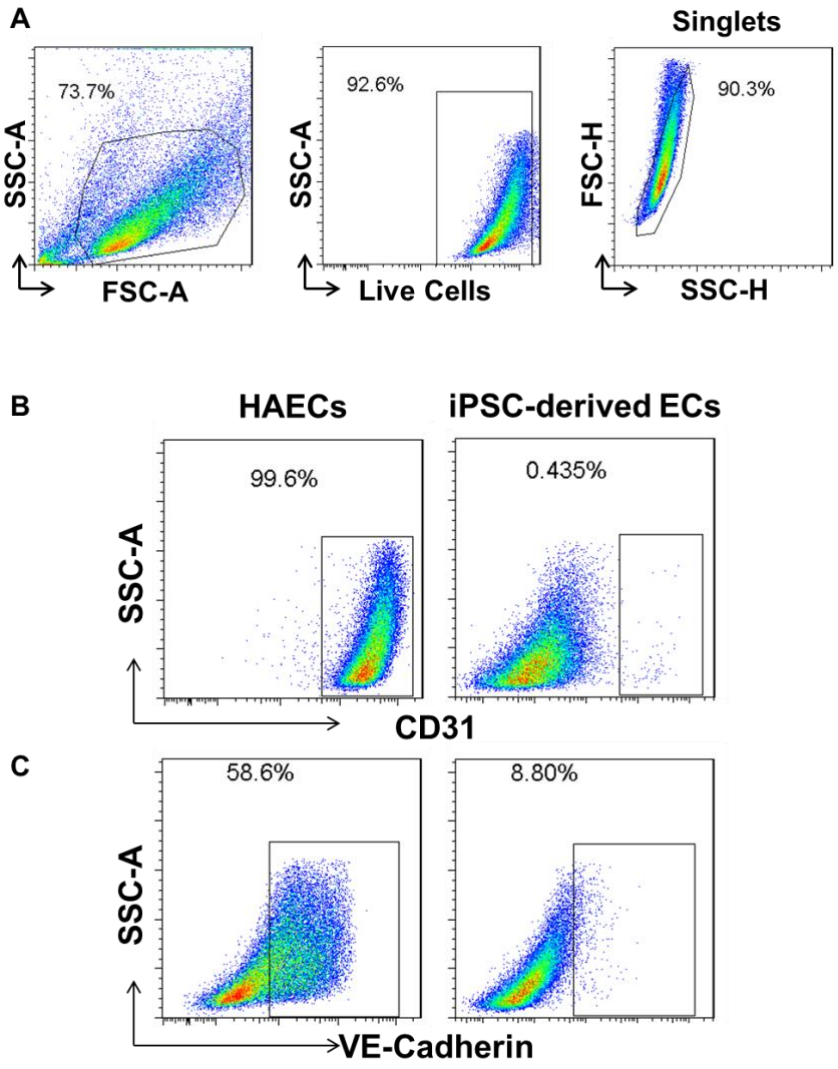

Figure 4-4: Characterization of human iPSCs subjected to differentiation into endothelial cells. Human iPSCs were subjected to differentiation into endothelial cells by BMP4 and GSK3 inhibition to commit these to a mesodermal fate and subsequently exposed these to VEGF and forskolin for their differentiation. Flow cytometry was used to characterized the differentiated cells. **A**. Flow cytometry dot plots are shown for live cells and single cells. **B**. Dot plots showing the expression of CD31 and (**C**) VE-Cadherin on human aortic endothelial cells and our iPSC-derived cells.

Discussion

The major findings in the experiments described in this chapter is that monocytes cultured with endothelial cells undergoing 10% stretch can promote T cell proliferation to a much greater extent than T cells cultured with monocytes exposed to endothelial cells undergoing 5% stretch. A conclusion to be drawn from these experiments is that increased endothelial stretch can convey to monocytes an ability to elicit an autoimmune-like response via T cell activation. In my prior experiments, I showed that monocyte activation involved STAT3 phosphorylation and the production of hydrogen peroxide and IL-6. It is interesting to speculate that these factors released by endothelial cells undergoing stretch arm monocytes to have this immunogenic property.

A caveat of my initial experiments is that the endothelial cells were derived from different humans than were the monocytes and T cells. It is therefore possible that endothelial antigens released in response to 10% stretch from the different host could be presented by the monocytes from the other host to T cells and drive the proliferation observed in Figure 4-1. To avoid this, I sought to develop a system in which autologous T cells, endothelial cells and monocytes were used. In order to do this, we attempted to create iPSCs from freshly isolated PMBCs of our monocyte donors. A second goal was to successfully differentiate these into endothelial cells. Thus, we had two major hurdles to overcome in this effort. In initial experiments, I employed electroporation of AMAXA nucleofactor II® to introduce the transcription factor Klf4, Oct4, Sox2 and c-Myc. This approach proved toxic to our PMBCs and did not yield iPSCs. As our second approach, I employed the Sendai virus approach to introduce these transcription factors as described by Tancos et al. [258]. This successfully yielded colonies of iPSCs as characterized by their appearance and their expression of Tra160 in the formed colonies (Figure 4-2).

Following the development of iPSCs, a second goal was to successfully induce these to become endothelial cells. To accomplish this, I used an approach described by Patsch et al. [259] in which iPSCs were exposed initially to BMP4 and GSK3 inhibition to commit these to a mesodermal fate and subsequently exposed these to VEGF and forskolin for their differentiation. This yielded a transformation of the iPSCs; however, they did not assume the cobblestone appearance of endothelial cells or express CD31 and VE-Cadherin, despite multiple attempts.

It is uncertain why I was not able to successfully differentiate iPSCs into endothelial cells. Even Patsch et al. found that only 62 to 89% of iPSCs became endothelial cells [259]. These investigators also noted the presence of smooth muscle contaminating cells after their endothelial differentiation. It is possible that another source of iPSCs such as fibroblast or B cells would have yielded a higher population of endothelial cells. Others have used endothelial cells differentiated from PBMC-derived iPSCs, however, these are notoriously contaminated by fibroblast and do not yield enough numbers to perform experiments such as mine. After several approaches to produce iPSCs to successfully produce endothelial cells failed, we decided that this was not a valid experimental approach and decided to abandon it.

Chapter V

Conclusions and Future Directions

Synopsis

Hypertension and main observations in thesis

In the past several years, hypertension has been ranked as the leading risk factor for global burden of disease in both developed and underdeveloped countries [213]. According to the new guidelines, approximately 46% of the population in United States has hypertension and the occurrence of this disease increases with age. Hypertension is a major source of morbidity and mortality and promotes atherosclerosis, renal disease, stroke and heart failure [125]. In the past 10 years, emerging evidence has supported a role of immune activation in hypertension. For several decades, the infiltration of T cells, B cells, monocytes and DCs into organs such as the kidney and the vasculature has been observed in both experimental models and humans with hypertension. Data in the last few years have supported the idea that these immune cells enhance blood pressure elevation and contribute to the end-organ damage associated with hypertension [137]. Until now, it has been unclear what factors present in the hypertensive milieu activate immune cells. Research from our laboratory and others have helped to uncover some of the factors involved in the immune activation during hypertension. DCs become activated in hypertension and we found that IsoLG-adducted proteins formed in these cells act as neo-antigens and can promote T cell proliferation and activation [139]. More recently, we found that excess sodium, which accumulates in the interstitium and tissues, activates DCs to produce IL-1β and promote T cell production of IL-17A [149]. In this dissertation, I found a new mechanism in which immune cells can become activated and some of the factors that promote this process. I made the following key observations:

1. Endothelial mechanical stretch, which is increased in hypertension, activates and transforms adjacent human monocytes into the intermediate and CD209 cell phenotypes.
2. This mechanism involves the activation of STAT3 within monocytes. STAT3 is essential for FLT-3-dependent DC development and acts as a transcription factor, inducing expression of cytokines that produce a pro-inflammatory response and can skew T cells toward an inflammatory phenotype.
3. Other factors released from the endothelium undergoing stretch that could cross talk with monocytes and promote this process include ROS, in particular hydrogen peroxide, and IL-6. Further, we found that NO has an inhibitory effect on monocyte transformation in keeping with the concept that there is loss of NO bioavailability in hypertension.

My studies not only used a unique cell culture system, but also extended findings from this system to the *in vivo* situation. One model involved the use of experimental mice exposed to Ang II-induced hypertension and we found that immune cells such as macrophages, DCs and monocytes infiltrate tissues such as kidney and aorta and that these have high levels of STAT3 phosphorylation. In addition, we studied the transformation of the monocyte phenotype in a relatively large population of humans with hypertension and found there is a higher proportion of circulating pro-inflammatory intermediate monocytes as hypertension severity increases and that this population has the highest activation of STAT3. Therefore, the findings I initially observed in the monocyte-endothelial cell culture likely are relevant to experimental and human hypertension.

Future directions

The factors promoting monocyte activation and transformation in response to vascular stretch likely occur in concert with other factors encountered in hypertension including increased

sodium, catecholamines, and prostaglandins. These might all be part of the microenvironment in vessels undergoing stretch during hypertension. Future studies could address how these might work together in promoting monocyte activation and transformation during altered endothelial stretch. For example, one might increase sodium concentrations or add catetcholamines in the monocytes/T cell co-culture system I employed. Adding these factors together could mimic the *in vivo* setting and give insight into potential future therapeutic approaches. Further, future studies should focus on characterizing the three cell phenotypes that were the most strikingly altered by endothelial stretch and hypertension including the intermediate and non-classical monocytes as well as the CD209 population. For example, it would be important to determine if these cells have differences in their ability to produce inflammatory cytokines, or their ability to drive T cell activation and proliferation. It would be important to identify which of these cell populations have the highest accumulation of the IsoLG-adducts, which we have shown can induce T cell proliferation.

To further characterize the intermediate monocytes and the CD209 cells that transform in response to endothelial stretch, it would be valuable to perform RNA sequencing on these to identify new genes associated with hypertension and vascular stretch. Another method we could use to characterize these would be to use Mass cytometry or CyTOF where we would label antibodies with heavy metal ion tags and perform analysis of multiple antibodies (approximately 23) in order to detect the upregulation or downregulation of different proteins. With regard to RNA sequencing, recent studies from Villani et al. describe a new DC ($AXL^{+}SIGLEC6^{+}$) and monocyte population (Mon4) in humans [260]. The origin of these new DC and monocyte cell types and their role in hypertension is not known. In preliminary studies, I have shown that there is an increase in the DCs $AXL^{+}SIGLEC6^{+}$ in response to 10% endothelial stretch. Future studies

should consider further characterizing these populations and determining if they altered by increased endothelial stretch or in hypertension.

Another mechanical force that the endothelium is exposed to is shear stress, which is the tangential drag of blood over the surface of the endothelium. In the clinical setting, atherosclerotic plaques develop preferentially at the arterial branches and curvature, which are regions of disturbed flow and shear stress. Similar to mechanical stretch, shear stress is important for promoting endothelial cell survival, leukocyte transmigration and the homeostasis of the vessel. There are various blood flow patterns that depart from the unidirectional laminar shear stress and these include flow reversal and turbulence [261]. Moderate unidirectional laminar flow is atheroprotective and maintains endothelial cell functionality (15 to 20 dynes/cm^2). Low levels of laminar flow and oscillatory shear stress promote endothelial activation, ROS formation and inflammation. Endothelial cells treated with physiological levels of unidirectional flow have reduced VCAM-1 and E-selectin [262] as well as suppressed expression of IL-1β and TNF [263]. Further, laminar flow stimulates eNOS expression via Akt through the phosphorylation of Ser1177 [264]. Low shear stress and oscillatory shear stress lead to loss of these beneficial effects and thus could interact with the increased mechanical stretch in the vessels that occurs in response to hypertension. In our studies, we did not address the potential effects of shear stress on the stretched endothelium. Future studies could address both mechanical forces on the endothelium and characterize the effects on the activation of the monocytes making this a more physiologically relevant model. Our *in vivo* studies likely encompass alterations of shear flow and stretch associated with hypertension.

In Chapter II, we sought to determine if monocytes are mechanosensitive and can respond to stretch alone without the presence of endothelial cells. However, we did not observe monocyte

transformation or activation in response to stretch alone and this resulted in a vast cell death. We tested monocyte adhesion and transformation when seeded on RGD- or collagen I-coated plates, but we were not able to replicate the findings of when endothelial cells were present. Endothelial cells could be releasing specific factors that promote monocyte survival, but we cannot completely exclude the possibility that these monocytes have mechanoreceptors that respond to endothelial cell adhesion. Monocytes adhered to the endothelial surface might be transduced differently than monocytes adhered to artificial surfaces. As an example, I found that endothelial cells exposed to 10% stretch had high levels of ICAM-1. In future studies, one could examine if ICAM-1-coated plates might be able to transduce monocytes for their transformation and activation.

We found two cell populations that were consistently increased in response to 10% endothelial stretch including the intermediate monocytes and the CD209 cells. Both of these were inhibited by STAT3 inhibition, but scavenging of hydrogen peroxide and IL-6 only prevented intermediate monocyte transformation and not the CD209 population. However, addition of NO donor prevented the transformation of both the intermediate monocytes and the CD209 population. It is interesting to speculate that these subsets might respond differently to NO, IL-6 and hydrogen peroxide. The CD209 cells had high accumulation of IsoLG-adducts and this could be mediated specifically by hydrogen peroxide. Formation of IsoLG-adducts within these cells might be promoting the transformation into the CD209 phenotype. *In vivo*, monocytes undergoing transmigration are in intimate contact with the endothelium-derived NO. This direct interaction with NO likely will have effects on the monocyte biology.

Nitric oxide signals through multiple mechanisms, but the predominant pathway involves the formation of cyclic guanosine monophosphate (cGMP) via the enzyme guanylyl cyclase. This

leads to activation of cGMP-dependent protein kinase (PKG) [265]. PKG phosphorylates multiple downstream targets including RhoA, the myosin-binding subunit, thrombin receptor, and others [266, 267]. A readout for PKG function is the actin binding protein, vasodilator-stimulated phosphoprotein (VASP). In preliminary studies, we have shown phosphorylated VASP in monocytes exposed to endothelial cells undergoing stretch. This indicates that NO in our system might be signaling through cGMP. NO can signal through other mechanisms than cGMP. For example NO, via formation of peroxynitrite via reaction with superoxide, can form nitrotyrosines, which can reduce the ability of tyrosine to be phosphorylated and this can dramatically alter cell signaling [268]. Nitric oxide can also bind to other heme proteins including those in the mitochondria and modulate mitochondrial respiration [269]. NO can also modulate s-glutathionylation by forming peroxynitrite [270]. Thus, future studies can focus on which of these pathways are most important in modulating monocyte phenotype. For example, it would be interesting to determine if cGMP is important in modulating monocyte phenotype. However, further studies characterizing this need to be performed in order to determine how NO talks to monocytes. In addition to nitric oxide, it would be important to further characterize the signals released by the endothelium in response to hydrogen peroxide on monocytes. Hydrogen peroxide is a relatively stable ROS that can promote the activation of principle signaling cascades including ERK, JNK, p38, MAPK and PI3K/Akt [271]. Thus, future studies on determining which of these signaling cascades is involved would deem a valuable addition to this mechanism.

We found that IL-6 plays an important role in the transformation of monocytes into the intermediate phenotype. IL-6 has been shown to both stimulate STAT3 activation and to be produced in response to STAT3 in a feed-forward fashion [231]. STAT activation occurs by

phosphorylation of the SH2 domain and C-terminal transactivation domain [STAT1 (Y701), STAT2 (Y690) and STAT3 (Y705)]. Upon cytokine stimulation, JAKs are recruited to the receptor and becomes phosphorylated and STATs are recruited to the receptor via their SH2 domain and are phosphorylated by JAKs on the respective residues [190]. This phosphorylation enables STATs to either homodimerize or heterodimerize via their SH2 domains and translocate to the nucleus and interact with DNA motifs to promote gene transcription [191]. However, STAT3 is also activated via other mechanisms that are JAK-independent. Other intracellular activators of STAT3 include epidermal growth factor receptor (EGFR), Src and ERK [272]. STAT3 is also activated through serine 727 phosphorylation. This phosphorylation occurs in response to protein kinase C, CDK5 and mitogen-activated protein kinases. Another mechanism of STAT3 activation is reversible acetylation of STAT3 by histone acetyltransferase on a single lysine residue (Lys 685) [273]. This acetylated STAT3 enhances the stability of STAT3 dimers, which is required for DNA-binding and transcriptional activity. In addition, our laboratory has defined a new mechanism by which STAT3 can be activated in the nucleus by PKM2 [228]. In preliminary studies, we found that inhibition of JAK using tofacitinib drug on the monocyte-endothelial cell culture undergoing stretch did not prevent transformation and activation of STAT3. Further studies could be performed to confirm if activation of STAT3 is JAK-independent and to define other mechanism of STAT3 activation in monocytes exposed to endothelial cells undergoing stretch.

Conclusion

Taken together, the studies performed in this thesis have defined a new mechanism by which monocytes and other immune cells become activated in hypertension. The mechanical stretch of vessels that occurs in response to increased blood pressure releases factors including IL-6,

hydrogen peroxide and nitric oxide that modulate the phenotype of nearby monocytes. We have shown that this process of monocyte activation occurs in part via STAT3 and secondary signaling events mentioned above. Our current study provides a previously unrecognized link between mechanical forces affecting the endothelium and activation of monocytes. This allows new insight into how the immune system can be activated in hypertension and for the first time implicates intermediate monocytes as potentially important in this disease. Thus, altered endothelial mechanical forces could have important effects on immune cell function, leading to end organ damage and worsening hypertension.

REFERENCES

1. Bromfield, S. and P. Muntner, *High blood pressure: the leading global burden of disease risk factor and the need for worldwide prevention programs.* Curr Hypertens Rep, 2013. **15**(3): p. 134-6.
2. Lionakis, N., et al., *Hypertension in the elderly.* World J Cardiol, 2012. **4**(5): p. 135-47.
3. Lim, S.S., et al., *A comparative risk assessment of burden of disease and injury attributable to 67 risk factors and risk factor clusters in 21 regions, 1990-2010: a systematic analysis for the Global Burden of Disease Study 2010.* Lancet, 2012. **380**(9859): p. 2224-60.
4. Carretero, O.A. and S. Oparil, *Essential hypertension. Part I: definition and etiology.* Circulation, 2000. **101**(3): p. 329-35.
5. Guyton, A.C., *Renal function curve--a key to understanding the pathogenesis of hypertension.* Hypertension, 1987. **10**(1): p. 1-6.
6. Bobik, A., *The structural basis of hypertension: vascular remodelling, rarefaction and angiogenesis/arteriogenesis.* J Hypertens, 2005. **23**(8): p. 1473-5.
7. Wu, J., et al., *Inflammation and mechanical stretch promote aortic stiffening in hypertension through activation of p38 mitogen-activated protein kinase.* Circ Res, 2014. **114**(4): p. 616-25.
8. Sutton-Tyrrell, K., et al., *Elevated aortic pulse wave velocity, a marker of arterial stiffness, predicts cardiovascular events in well-functioning older adults.* Circulation, 2005. **111**(25): p. 3384-90.
9. Mancia, G., et al., *Sympathetic activation in the pathogenesis of hypertension and progression of organ damage.* Hypertension, 1999. **34**(4 Pt 2): p. 724-8.
10. Norlander, A.E., M.S. Madhur, and D.G. Harrison, *The immunology of hypertension.* J Exp Med, 2018. **215**(1): p. 21-33.
11. Marvar, P.J., et al., *The central nervous system and inflammation in hypertension.* Curr Opin Pharmacol, 2011. **11**(2): p. 156-61.
12. Lob, H.E., et al., *Role of vascular extracellular superoxide dismutase in hypertension.* Hypertension, 2011. **58**(2): p. 232-9.
13. Norlander, A.E., et al., *A salt-sensing kinase in T lymphocytes, SGK1, drives hypertension and hypertensive end-organ damage.* JCI Insight, 2017. **2**(13).
14. Amador, C.A., et al., *Spironolactone decreases DOCA-salt-induced organ damage by blocking the activation of T helper 17 and the downregulation of regulatory T lymphocytes.* Hypertension, 2014. **63**(4): p. 797-803.
15. Sullivan, J.M., *Salt sensitivity. Definition, conception, methodology, and long-term issues.* Hypertension, 1991. **17**(1 Suppl): p. I61-8.
16. Arnal, J.F., L. Warin, and J.B. Michel, *Determinants of aortic cyclic guanosine monophosphate in hypertension induced by chronic inhibition of nitric oxide synthase.* J Clin Invest, 1992. **90**(2): p. 647-52.
17. Itani, H.A., et al., *CD70 Exacerbates Blood Pressure Elevation and Renal Damage in Response to Repeated Hypertensive Stimuli.* Circ Res, 2016. **118**(8): p. 1233-43.
18. Rapp, J.P., *Dahl salt-susceptible and salt-resistant rats. A review.* Hypertension, 1982. **4**(6): p. 753-63.

19. Mattson, D.L., et al., *Chromosome substitution reveals the genetic basis of Dahl salt-sensitive hypertension and renal disease.* Am J Physiol Renal Physiol, 2008. **295**(3): p. F837-42.
20. Mattson, D.L., et al., *Genetic mutation of recombination activating gene 1 in Dahl salt-sensitive rats attenuates hypertension and renal damage.* Am J Physiol Regul Integr Comp Physiol, 2013. **304**(6): p. R407-14.
21. Richer, C., et al., *Antihypertensive drugs in the stroke-prone spontaneously hypertensive rat.* Clin Exp Hypertens, 1997. **19**(5-6): p. 925-36.
22. Luft, F.C., et al., *Hypertension-induced end-organ damage : A new transgenic approach to an old problem.* Hypertension, 1999. **33**(1 Pt 2): p. 212-8.
23. Carrive, P., *Orexin, Stress and Central Cardiovascular Control. A Link with Hypertension?* Neurosci Biobehav Rev, 2017. **74**(Pt B): p. 376-392.
24. Griendling, K.K., et al., *Measurement of Reactive Oxygen Species, Reactive Nitrogen Species, and Redox-Dependent Signaling in the Cardiovascular System: A Scientific Statement From the American Heart Association.* Circ Res, 2016. **119**(5): p. e39-75.
25. Ludin, A., et al., *Reactive oxygen species regulate hematopoietic stem cell self-renewal, migration and development, as well as their bone marrow microenvironment.* Antioxid Redox Signal, 2014. **21**(11): p. 1605-19.
26. Liochev, S.I., *Reactive oxygen species and the free radical theory of aging.* Free radical biology & medicine, 2013. **60**: p. 1-4.
27. Shin, M.H., et al., *Reactive oxygen species produced by NADPH oxidase, xanthine oxidase, and mitochondrial electron transport system mediate heat shock-induced MMP-1 and MMP-9 expression.* Free radical biology & medicine, 2008. **44**(4): p. 635-45.
28. Sies, H., *Oxidative stress: from basic research to clinical application.* Am J Med, 1991. **91**(3C): p. 31S-38S.
29. Buettner, G.R., *The pecking order of free radicals and antioxidants: lipid peroxidation, alpha-tocopherol, and ascorbate.* Arch Biochem Biophys, 1993. **300**(2): p. 535-43.
30. Dikalov, S.I. and D.G. Harrison, *Methods for detection of mitochondrial and cellular reactive oxygen species.* Antioxid Redox Signal, 2014. **20**(2): p. 372-82.
31. Sies, H., *Hydrogen peroxide as a central redox signaling molecule in physiological oxidative stress: Oxidative eustress.* Redox Biol, 2017. **11**: p. 613-619.
32. Loperena, R. and D.G. Harrison, *Oxidative Stress and Hypertensive Diseases.* Med Clin North Am, 2017. **101**(1): p. 169-193.
33. Dikalova, A., et al., *Nox1 overexpression potentiates angiotensin II-induced hypertension and vascular smooth muscle hypertrophy in transgenic mice.* Circulation, 2005. **112**(17): p. 2668-76.
34. Nazarewicz, R.R., et al., *Nox2 as a potential target of mitochondrial superoxide and its role in endothelial oxidative stress.* Am J Physiol Heart Circ Physiol, 2013. **305**(8): p. H1131-40.
35. Guzik, T.J., et al., *Calcium-dependent NOX5 nicotinamide adenine dinucleotide phosphate oxidase contributes to vascular oxidative stress in human coronary artery disease.* J Am Coll Cardiol, 2008. **52**(22): p. 1803-9.
36. van der Vliet, A., *NADPH oxidases in lung biology and pathology: host defense enzymes, and more.* Free Radic Biol Med, 2008. **44**(6): p. 938-55.

37. Ago, T., et al., *Phosphorylation of p47phox directs phox homology domain from SH3 domain toward phosphoinositides, leading to phagocyte NADPH oxidase activation.* Proc Natl Acad Sci U S A, 2003. **100**(8): p. 4474-9.
38. Tamura, M., et al., *p40phox as an alternative organizer to p47phox in Nox2 activation: a new mechanism involving an interaction with p22phox.* FEBS Lett, 2007. **581**(23): p. 4533-8.
39. Babior, B.M., *NADPH oxidase: an update.* Blood, 1999. **93**(5): p. 1464-76.
40. Dikalova, A.E., et al., *Therapeutic targeting of mitochondrial superoxide in hypertension.* Circ Res, 2010. **107**(1): p. 106-16.
41. Zafari, A.M., et al., *Role of NADH/NADPH oxidase-derived H2O2 in angiotensin II-induced vascular hypertrophy.* Hypertension, 1998. **32**(3): p. 488-95.
42. Fukui, T., et al., *p22phox mRNA expression and NADPH oxidase activity are increased in aortas from hypertensive rats.* Circ Res, 1997. **80**(1): p. 45-51.
43. Weber, D.S., et al., *Angiotensin II-induced hypertrophy is potentiated in mice overexpressing p22phox in vascular smooth muscle.* Am J Physiol Heart Circ Physiol, 2005. **288**(1): p. H37-42.
44. Wu, J., et al., *Immune activation caused by vascular oxidation promotes fibrosis and hypertension.* J Clin Invest, 2016. **126**(4): p. 1607.
45. Roxo-Junior, P. and H.M. Simao, *Chronic granulomatous disease: why an inflammatory disease?* Braz J Med Biol Res, 2014. **47**(11): p. 924-8.
46. Fukai, T., et al., *Regulation of the vascular extracellular superoxide dismutase by nitric oxide and exercise training.* J Clin Invest, 2000. **105**(11): p. 1631-9.
47. Harrison, D.G., et al., *Regulation of endothelial cell tetrahydrobiopterin pathophysiological and therapeutic implications.* Advances in pharmacology, 2010. **60**: p. 107-32.
48. Chen, W., et al., *Role of increased guanosine triphosphate cyclohydrolase-1 expression and tetrahydrobiopterin levels upon T cell activation.* The Journal of biological chemistry, 2011. **286**(16): p. 13846-51.
49. Porkert, M., et al., *Tetrahydrobiopterin: a novel antihypertensive therapy.* J Hum Hypertens, 2008. **22**(6): p. 401-7.
50. Laursen, J.B., et al., *Endothelial regulation of vasomotion in apoE-deficient mice: implications for interactions between peroxynitrite and tetrahydrobiopterin.* Circulation, 2001. **103**(9): p. 1282-8.
51. Landmesser, U., et al., *Oxidation of tetrahydrobiopterin leads to uncoupling of endothelial cell nitric oxide synthase in hypertension.* J Clin Invest, 2003. **111**(8): p. 1201-9.
52. Nakazono, K., et al., *Does superoxide underlie the pathogenesis of hypertension?* Proc Natl Acad Sci U S A, 1991. **88**(22): p. 10045-8.
53. Fukui, T., et al., *p22phox mRNA expression and NADPH oxidase activity are increased in aortas from hypertensive rats.* Circulation research, 1997. **80**(1): p. 45-51.
54. Schnackenberg, C.G., W.J. Welch, and C.S. Wilcox, *Normalization of blood pressure and renal vascular resistance in SHR with a membrane-permeable superoxide dismutase mimetic: role of nitric oxide.* Hypertension, 1998. **32**(1): p. 59-64.
55. Adeagbo, A.S., et al., *Cyclo-oxygenase-2, endothelium and aortic reactivity during deoxycorticosterone acetate salt-induced hypertension.* Journal of hypertension, 2005. **23**(5): p. 1025-36.

56. Landmesser, U., et al., *Role of p47(phox) in vascular oxidative stress and hypertension caused by angiotensin II.* Hypertension, 2002. **40**(4): p. 511-5.
57. Cai, H., et al., *NAD(P)H oxidase-derived hydrogen peroxide mediates endothelial nitric oxide production in response to angiotensin II.* The Journal of biological chemistry, 2002. **277**(50): p. 48311-7.
58. Beswick, R.A., et al., *NADH/NADPH oxidase and enhanced superoxide production in the mineralocorticoid hypertensive rat.* Hypertension, 2001. **38**(5): p. 1107-11.
59. Suzuki, H., et al., *In vivo evidence for microvascular oxidative stress in spontaneously hypertensive rats. Hydroethidine microfluorography.* Hypertension, 1995. **25**(5): p. 1083-9.
60. Zhou, X., et al., *NAD(P)H oxidase-derived peroxide mediates elevated basal and impaired flow-induced NO production in SHR mesenteric arteries in vivo.* American journal of physiology. Heart and circulatory physiology, 2008. **295**(3): p. H1008-H1016.
61. Swei, A., et al., *Oxidative stress in the Dahl hypertensive rat.* Hypertension, 1997. **30**(6): p. 1628-33.
62. Li, L., et al., *Tetrahydrobiopterin deficiency and nitric oxide synthase uncoupling contribute to atherosclerosis induced by disturbed flow.* Arteriosclerosis, thrombosis, and vascular biology, 2011. **31**(7): p. 1547-54.
63. Zhang, C., et al., *Upregulation of vascular arginase in hypertension decreases nitric oxide-mediated dilation of coronary arterioles.* Hypertension, 2004. **44**(6): p. 935-43.
64. Chandra, S., et al., *Oxidative species increase arginase activity in endothelial cells through the RhoA/Rho kinase pathway.* British journal of pharmacology, 2012. **165**(2): p. 506-19.
65. Landmesser, U. and D.G. Harrison, *Oxidative stress and vascular damage in hypertension.* Coronary artery disease, 2001. **12**(6): p. 455-61.
66. Theuer, J., et al., *Angiotensin II induced inflammation in the kidney and in the heart of double transgenic rats.* BMC cardiovascular disorders, 2002. **2**: p. 3.
67. Basset, C., et al., *Innate immunity and pathogen-host interaction.* Vaccine, 2003. **21 Suppl 2**: p. S12-23.
68. Kumar, H., T. Kawai, and S. Akira, *Pathogen recognition by the innate immune system.* Int Rev Immunol, 2011. **30**(1): p. 16-34.
69. Janeway, C.A., Jr., *Approaching the asymptote? Evolution and revolution in immunology.* Cold Spring Harb Symp Quant Biol, 1989. **54 Pt 1**: p. 1-13.
70. Parkin, J. and B. Cohen, *An overview of the immune system.* Lancet, 2001. **357**(9270): p. 1777-89.
71. Khocht, A., et al., *Oxidative burst intensity of peripheral phagocytic cells and periodontitis in Down syndrome.* J Periodontal Res, 2014. **49**(1): p. 29-35.
72. Jang, J.H., et al., *An Overview of Pathogen Recognition Receptors for Innate Immunity in Dental Pulp.* Mediators Inflamm, 2015. **2015**: p. 794143.
73. Brubaker, S.W., et al., *Innate immune pattern recognition: a cell biological perspective.* Annu Rev Immunol, 2015. **33**: p. 257-90.
74. Mogensen, T.H., *Pathogen recognition and inflammatory signaling in innate immune defenses.* Clin Microbiol Rev, 2009. **22**(2): p. 240-73, Table of Contents.
75. Palm, N.W. and R. Medzhitov, *Pattern recognition receptors and control of adaptive immunity.* Immunol Rev, 2009. **227**(1): p. 221-33.

76. Deretic, V., T. Saitoh, and S. Akira, *Autophagy in infection, inflammation and immunity.* Nat Rev Immunol, 2013. **13**(10): p. 722-37.
77. Kobe, B. and A.V. Kajava, *The leucine-rich repeat as a protein recognition motif.* Curr Opin Struct Biol, 2001. **11**(6): p. 725-32.
78. Medzhitov, R., P. Preston-Hurlburt, and C.A. Janeway, Jr., *A human homologue of the Drosophila Toll protein signals activation of adaptive immunity.* Nature, 1997. **388**(6640): p. 394-7.
79. Poltorak, A., et al., *Defective LPS signaling in C3H/HeJ and C57BL/10ScCr mice: mutations in Tlr4 gene.* Science, 1998. **282**(5396): p. 2085-8.
80. da Silva Correia, J., et al., *Lipopolysaccharide is in close proximity to each of the proteins in its membrane receptor complex. transfer from CD14 to TLR4 and MD-2.* J Biol Chem, 2001. **276**(24): p. 21129-35.
81. Kim, J.I., et al., *Crystal structure of CD14 and its implications for lipopolysaccharide signaling.* J Biol Chem, 2005. **280**(12): p. 11347-51.
82. Pugin, J., et al., *Cell activation mediated by glycosylphosphatidylinositol-anchored or transmembrane forms of CD14.* Infect Immun, 1998. **66**(3): p. 1174-80.
83. Zanoni, I., et al., *CD14 regulates the dendritic cell life cycle after LPS exposure through NFAT activation.* Nature, 2009. **460**(7252): p. 264-8.
84. Kawai, T. and S. Akira, *Signaling to NF-kappaB by Toll-like receptors.* Trends Mol Med, 2007. **13**(11): p. 460-9.
85. Ghosh, S., M.J. May, and E.B. Kopp, *NF-kappa B and Rel proteins: evolutionarily conserved mediators of immune responses.* Annu Rev Immunol, 1998. **16**: p. 225-60.
86. Prinyakupt, J. and C. Pluempitiwiriyawej, *Segmentation of white blood cells and comparison of cell morphology by linear and naive Bayes classifiers.* Biomed Eng Online, 2015. **14**: p. 63.
87. Hettinger, J., et al., *Origin of monocytes and macrophages in a committed progenitor.* Nat Immunol, 2013. **14**(8): p. 821-30.
88. Goud, T.J., C. Schotte, and R. van Furth, *Identification and characterization of the monoblast in mononuclear phagocyte colonies grown in vitro.* J Exp Med, 1975. **142**(5): p. 1180-99.
89. Ziegler-Heitbrock, L., *Blood Monocytes and Their Subsets: Established Features and Open Questions.* Front Immunol, 2015. **6**: p. 423.
90. Auffray, C., M.H. Sieweke, and F. Geissmann, *Blood monocytes: development, heterogeneity, and relationship with dendritic cells.* Annu Rev Immunol, 2009. **27**: p. 669-92.
91. Swirski, F.K., et al., *Identification of splenic reservoir monocytes and their deployment to inflammatory sites.* Science, 2009. **325**(5940): p. 612-6.
92. Yang, J., et al., *Monocyte and macrophage differentiation: circulation inflammatory monocyte as biomarker for inflammatory diseases.* Biomark Res, 2014. **2**(1): p. 1.
93. Boyette, L.B., et al., *Phenotype, function, and differentiation potential of human monocyte subsets.* PLoS One, 2017. **12**(4): p. e0176460.
94. Jakubzick, C., et al., *Minimal differentiation of classical monocytes as they survey steady-state tissues and transport antigen to lymph nodes.* Immunity, 2013. **39**(3): p. 599-610.
95. Gabrilovich, D.I. and S. Nagaraj, *Myeloid-derived suppressor cells as regulators of the immune system.* Nat Rev Immunol, 2009. **9**(3): p. 162-74.

96. Urbanski, K., et al., *CD14+CD16++ "nonclassical" monocytes are associated with endothelial dysfunction in patients with coronary artery disease.* Thromb Haemost, 2017. **117**(05): p. 971-980.
97. Zawada, A.M., et al., *SuperSAGE evidence for CD14++CD16+ monocytes as a third monocyte subset.* Blood, 2011. **118**(12): p. e50-61.
98. Aiello, R.J., et al., *Monocyte chemoattractant protein-1 accelerates atherosclerosis in apolipoprotein E-deficient mice.* Arterioscler Thromb Vasc Biol, 1999. **19**(6): p. 1518-25.
99. Wenzel, P., et al., *Lysozyme M-positive monocytes mediate angiotensin II-induced arterial hypertension and vascular dysfunction.* Circulation, 2011. **124**(12): p. 1370-81.
100. Patel, A.A., et al., *The fate and lifespan of human monocyte subsets in steady state and systemic inflammation.* J Exp Med, 2017. **214**(7): p. 1913-1923.
101. Passlick, B., D. Flieger, and H.W. Ziegler-Heitbrock, *Identification and characterization of a novel monocyte subpopulation in human peripheral blood.* Blood, 1989. **74**(7): p. 2527-34.
102. Imhof, B.A. and M. Aurrand-Lions, *Adhesion mechanisms regulating the migration of monocytes.* Nat Rev Immunol, 2004. **4**(6): p. 432-44.
103. Rogacev, K.S., et al., *Monocyte heterogeneity in obesity and subclinical atherosclerosis.* Eur Heart J, 2010. **31**(3): p. 369-76.
104. Mikolajczyk, T.P., et al., *Heterogeneity of peripheral blood monocytes, endothelial dysfunction and subclinical atherosclerosis in patients with systemic lupus erythematosus.* Lupus, 2016. **25**(1): p. 18-27.
105. Cros, J., et al., *Human CD14dim monocytes patrol and sense nucleic acids and viruses via TLR7 and TLR8 receptors.* Immunity, 2010. **33**(3): p. 375-86.
106. Katayama, K., et al., *CD14+CD16+ monocyte subpopulation in Kawasaki disease.* Clin Exp Immunol, 2000. **121**(3): p. 566-70.
107. Brunner, P.M., et al., *Infliximab induces downregulation of the IL-12/IL-23 axis in 6-sulfo-LacNac (slan)+ dendritic cells and macrophages.* J Allergy Clin Immunol, 2013. **132**(5): p. 1184-1193 e8.
108. Kawanaka, N., et al., *CD14+,CD16+ blood monocytes and joint inflammation in rheumatoid arthritis.* Arthritis Rheum, 2002. **46**(10): p. 2578-86.
109. Qiu, G., et al., *Adipose-derived mesenchymal stem cells modulate CD14(++)CD16(+) expression on monocytes from sepsis patients in vitro via prostaglandin E2.* Stem Cell Res Ther, 2017. **8**(1): p. 97.
110. Nockher, W.A., L. Bergmann, and J.E. Scherberich, *Increased soluble CD14 serum levels and altered CD14 expression of peripheral blood monocytes in HIV-infected patients.* Clin Exp Immunol, 1994. **98**(3): p. 369-74.
111. Wrigley, B.J., et al., *CD14++CD16+ monocytes in patients with acute ischaemic heart failure.* Eur J Clin Invest, 2013. **43**(2): p. 121-30.
112. Nockher, W.A. and J.E. Scherberich, *Expanded CD14+ CD16+ monocyte subpopulation in patients with acute and chronic infections undergoing hemodialysis.* Infect Immun, 1998. **66**(6): p. 2782-90.
113. Belge, K.U., et al., *The proinflammatory CD14+CD16+DR++ monocytes are a major source of TNF.* J Immunol, 2002. **168**(7): p. 3536-42.
114. Rossol, M., et al., *The CD14(bright) CD16+ monocyte subset is expanded in rheumatoid arthritis and promotes expansion of the Th17 cell population.* Arthritis Rheum, 2012. **64**(3): p. 671-7.

115. Ziegler-Heitbrock, H.W., et al., *The novel subset of CD14+/CD16+ blood monocytes exhibits features of tissue macrophages.* Eur J Immunol, 1993. **23**(9): p. 2053-8.
116. Turner, J.D., et al., *Circulating CD14brightCD16+ 'intermediate' monocytes exhibit enhanced parasite pattern recognition in human helminth infection.* PLoS Negl Trop Dis, 2014. **8**(4): p. e2817.
117. Rogacev, K.S., et al., *Lower Apo A-I and lower HDL-C levels are associated with higher intermediate CD14++CD16+ monocyte counts that predict cardiovascular events in chronic kidney disease.* Arterioscler Thromb Vasc Biol, 2014. **34**(9): p. 2120-7.
118. Soehnlein, O., et al., *Distinct functions of chemokine receptor axes in the atherogenic mobilization and recruitment of classical monocytes.* EMBO Mol Med, 2013. **5**(3): p. 471-81.
119. Ulrich, C., et al., *Increased expression of monocytic angiotensin-converting enzyme in dialysis patients with cardiovascular disease.* Nephrol Dial Transplant, 2006. **21**(6): p. 1596-602.
120. Rogacev, K.S., et al., *CD14++CD16+ monocytes independently predict cardiovascular events: a cohort study of 951 patients referred for elective coronary angiography.* J Am Coll Cardiol, 2012. **60**(16): p. 1512-20.
121. Ziegler-Heitbrock, L., et al., *Nomenclature of monocytes and dendritic cells in blood.* Blood, 2010. **116**(16): p. e74-80.
122. Calzada-Wack, J.C., M. Frankenberger, and H.W. Ziegler-Heitbrock, *Interleukin-10 drives human monocytes to CD16 positive macrophages.* J Inflamm, 1996. **46**(2): p. 78-85.
123. Eligini, S., et al., *Human monocyte-derived macrophages spontaneously differentiated in vitro show distinct phenotypes.* J Cell Physiol, 2013. **228**(7): p. 1464-72.
124. Heptinstall, R.H., *Renal biopsies in hypertension.* Br Heart J, 1954. **16**(2): p. 133-41.
125. Guzik, T.J., et al., *Role of the T cell in the genesis of angiotensin II induced hypertension and vascular dysfunction.* J Exp Med, 2007. **204**(10): p. 2449-60.
126. Crowley, S.D., et al., *Lymphocyte responses exacerbate angiotensin II-dependent hypertension.* Am J Physiol Regul Integr Comp Physiol, 2010. **298**(4): p. R1089-97.
127. Trott, D.W., et al., *Oligoclonal CD8+ T cells play a critical role in the development of hypertension.* Hypertension, 2014. **64**(5): p. 1108-15.
128. Youn, J.C., et al., *Immunosenescent CD8+ T cells and C-X-C chemokine receptor type 3 chemokines are increased in human hypertension.* Hypertension, 2013. **62**(1): p. 126-33.
129. Madhur, M.S., et al., *Interleukin 17 promotes angiotensin II-induced hypertension and vascular dysfunction.* Hypertension, 2010. **55**(2): p. 500-7.
130. Cornelius, D.C., et al., *Administration of Interleukin-17 Soluble Receptor C Suppresses TH17 Cells, Oxidative Stress, and Hypertension in Response to Placental Ischemia During Pregnancy.* Hypertension, 2013.
131. Nguyen, H., et al., *Interleukin-17 causes Rho-kinase-mediated endothelial dysfunction and hypertension.* Cardiovasc Res, 2013. **97**(4): p. 696-704.
132. Itani, H.A., et al., *Activation of Human T Cells in Hypertension: Studies of Humanized Mice and Hypertensive Humans.* Hypertension, 2016. **68**(1): p. 123-32.
133. Mian, M.O., et al., *Deficiency of T-regulatory cells exaggerates angiotensin II-induced microvascular injury by enhancing immune responses.* J Hypertens, 2016. **34**(1): p. 97-108.

134. Wallukat, G., et al., *Patients with preeclampsia develop agonistic autoantibodies against the angiotensin AT1 receptor.* J Clin Invest, 1999. **103**(7): p. 945-52.
135. Chan, C.T., et al., *Obligatory Role for B Cells in the Development of Angiotensin II-Dependent Hypertension.* Hypertension, 2015. **66**(5): p. 1023-33.
136. De Ciuceis, C., et al., *Reduced vascular remodeling, endothelial dysfunction, and oxidative stress in resistance arteries of angiotensin II-infused macrophage colony-stimulating factor-deficient mice: evidence for a role in inflammation in angiotensin-induced vascular injury.* Arterioscler Thromb Vasc Biol, 2005. **25**(10): p. 2106-13.
137. McMaster, W.G., et al., *Inflammation, immunity, and hypertensive end-organ damage.* Circ Res, 2015. **116**(6): p. 1022-33.
138. Vinh, A., et al., *Inhibition and genetic ablation of the B7/CD28 T-cell costimulation axis prevents experimental hypertension.* Circulation, 2010. **122**(24): p. 2529-37.
139. Kirabo, A., et al., *DC isoketal-modified proteins activate T cells and promote hypertension.* J Clin Invest, 2014. **124**(10): p. 4642-56.
140. Xiao, L., et al., *Renal Denervation Prevents Immune Cell Activation and Renal Inflammation in Angiotensin II-Induced Hypertension.* Circ Res, 2015. **117**(6): p. 547-57.
141. Lori, A., et al., *The Spleen: A Hub Connecting Nervous and Immune Systems in Cardiovascular and Metabolic Diseases.* Int J Mol Sci, 2017. **18**(6).
142. Bellinger, D.L., et al., *Innervation of lymphoid organs and implications in development, aging, and autoimmunity.* Int J Immunopharmacol, 1992. **14**(3): p. 329-44.
143. Lob, H.E., et al., *Role of the NADPH oxidases in the subfornical organ in angiotensin II-induced hypertension.* Hypertension, 2013. **61**(2): p. 382-7.
144. Marvar, P.J., et al., *Central and peripheral mechanisms of T-lymphocyte activation and vascular inflammation produced by angiotensin II-induced hypertension.* Circ Res, 2010. **107**(2): p. 263-70.
145. Lob, H.E., et al., *Induction of hypertension and peripheral inflammation by reduction of extracellular superoxide dismutase in the central nervous system.* Hypertension, 2010. **55**(2): p. 277-83, 6p following 283.
146. Carnevale, D., et al., *The angiogenic factor PlGF mediates a neuroimmune interaction in the spleen to allow the onset of hypertension.* Immunity, 2014. **41**(5): p. 737-52.
147. Kopp, C., et al., *(23)Na magnetic resonance imaging of tissue sodium.* Hypertension, 2012. **59**(1): p. 167-72.
148. Wu, C., et al., *Induction of pathogenic TH17 cells by inducible salt-sensing kinase SGK1.* Nature, 2013. **496**(7446): p. 513-7.
149. Barbaro, N.R., et al., *Dendritic Cell Amiloride-Sensitive Channels Mediate Sodium-Induced Inflammation and Hypertension.* Cell Rep, 2017. **21**(4): p. 1009-1020.
150. Kamat, N.V., et al., *Renal transporter activation during angiotensin-II hypertension is blunted in interferon-gamma-/- and interleukin-17A-/- mice.* Hypertension, 2015. **65**(3): p. 569-76.
151. Zhang, J., et al., *Tumor necrosis factor-alpha produced in the kidney contributes to angiotensin II-dependent hypertension.* Hypertension, 2014. **64**(6): p. 1275-81.
152. Satou, R., et al., *Interferon-gamma biphasically regulates angiotensinogen expression via a JAK-STAT pathway and suppressor of cytokine signaling 1 (SOCS1) in renal proximal tubular cells.* FASEB J, 2012. **26**(5): p. 1821-30.
153. Saleh, M.A., et al., *Lymphocyte adaptor protein LNK deficiency exacerbates hypertension and end-organ inflammation.* J Clin Invest, 2015. **125**(3): p. 1189-202.

154. Liu, J., et al., *NAD(P)H oxidase mediates angiotensin II-induced vascular macrophage infiltration and medial hypertrophy.* Arteriosclerosis, thrombosis, and vascular biology, 2003. **23**(5): p. 776-82.
155. Vaziri, N.D. and B. Rodriguez-Iturbe, *Mechanisms of disease: oxidative stress and inflammation in the pathogenesis of hypertension.* Nature clinical practice. Nephrology, 2006. **2**(10): p. 582-93.
156. Liao, T.D., et al., *Role of inflammation in the development of renal damage and dysfunction in angiotensin II-induced hypertension.* Hypertension, 2008. **52**(2): p. 256-63.
157. Karbach, S.H., et al., *Gut Microbiota Promote Angiotensin II-Induced Arterial Hypertension and Vascular Dysfunction.* J Am Heart Assoc, 2016. **5**(9).
158. Wilck, N., et al., *Salt-responsive gut commensal modulates TH17 axis and disease.* Nature, 2017. **551**(7682): p. 585-589.
159. Campbell, J.J., et al., *Chemokines and the arrest of lymphocytes rolling under flow conditions.* Science, 1998. **279**(5349): p. 381-4.
160. Yoshida, M., et al., *Leukocyte adhesion to vascular endothelium induces E-selectin linkage to the actin cytoskeleton.* J Cell Biol, 1996. **133**(2): p. 445-55.
161. Sumagin, R., et al., *LFA-1 and Mac-1 define characteristically different intralumenal crawling and emigration patterns for monocytes and neutrophils in situ.* J Immunol, 2010. **185**(11): p. 7057-66.
162. Ley, K., et al., *Getting to the site of inflammation: the leukocyte adhesion cascade updated.* Nat Rev Immunol, 2007. **7**(9): p. 678-89.
163. Schenkel, A.R., Z. Mamdouh, and W.A. Muller, *Locomotion of monocytes on endothelium is a critical step during extravasation.* Nat Immunol, 2004. **5**(4): p. 393-400.
164. Barreiro, O., et al., *Dynamic interaction of VCAM-1 and ICAM-1 with moesin and ezrin in a novel endothelial docking structure for adherent leukocytes.* J Cell Biol, 2002. **157**(7): p. 1233-45.
165. Muller, W.A., *Leukocyte-endothelial-cell interactions in leukocyte transmigration and the inflammatory response.* Trends Immunol, 2003. **24**(6): p. 327-34.
166. Nieminen, M., et al., *Vimentin function in lymphocyte adhesion and transcellular migration.* Nat Cell Biol, 2006. **8**(2): p. 156-62.
167. Randolph, G.J., et al., *Differentiation of monocytes into dendritic cells in a model of transendothelial trafficking.* Science, 1998. **282**(5388): p. 480-3.
168. Jufri, N.F., et al., *Mechanical stretch: physiological and pathological implications for human vascular endothelial cells.* Vasc Cell, 2015. **7**: p. 8.
169. Anwar, M.A., et al., *The effect of pressure-induced mechanical stretch on vascular wall differential gene expression.* J Vasc Res, 2012. **49**(6): p. 463-78.
170. Adapala, R.K., et al., *TRPV4 channels mediate cardiac fibroblast differentiation by integrating mechanical and soluble signals.* J Mol Cell Cardiol, 2013. **54**: p. 45-52.
171. Naruse, K., T. Yamada, and M. Sokabe, *Involvement of SA channels in orienting response of cultured endothelial cells to cyclic stretch.* Am J Physiol, 1998. **274**(5 Pt 2): p. H1532-8.
172. Suzuki, M., et al., *Up-regulation of integrin beta 3 expression by cyclic stretch in human umbilical endothelial cells.* Biochem Biophys Res Commun, 1997. **239**(2): p. 372-6.

173. Osawa, M., et al., *Evidence for a role of platelet endothelial cell adhesion molecule-1 in endothelial cell mechanosignal transduction: is it a mechanoresponsive molecule?* J Cell Biol, 2002. **158**(4): p. 773-85.
174. Tojkander, S., G. Gateva, and P. Lappalainen, *Actin stress fibers--assembly, dynamics and biological roles.* J Cell Sci, 2012. **125**(Pt 8): p. 1855-64.
175. Loftus, I.M. and M.M. Thompson, *The role of matrix metalloproteinases in vascular disease.* Vasc Med, 2002. **7**(2): p. 117-33.
176. Wang, B.W., et al., *Induction of matrix metalloproteinases-14 and -2 by cyclical mechanical stretch is mediated by tumor necrosis factor-alpha in cultured human umbilical vein endothelial cells.* Cardiovasc Res, 2003. **59**(2): p. 460-9.
177. Liu, X.M., et al., *Physiologic cyclic stretch inhibits apoptosis in vascular endothelium.* FEBS Lett, 2003. **541**(1-3): p. 52-6.
178. Zheng, W., L.P. Christensen, and R.J. Tomanek, *Stretch induces upregulation of key tyrosine kinase receptors in microvascular endothelial cells.* Am J Physiol Heart Circ Physiol, 2004. **287**(6): p. H2739-45.
179. Hurley, N.E., et al., *Modulating the functional contributions of c-Myc to the human endothelial cell cyclic strain response.* J Vasc Res, 2010. **47**(1): p. 80-90.
180. Hishikawa, K. and T.F. Luscher, *Pulsatile stretch stimulates superoxide production in human aortic endothelial cells.* Circulation, 1997. **96**(10): p. 3610-6.
181. Hsieh, N.K., et al., *Nitric oxide inhibition accelerates hypertension and induces perivascular inflammation in rats.* Clin Exp Pharmacol Physiol, 2004. **31**(4): p. 212-8.
182. Goettsch, C., et al., *Long-term cyclic strain downregulates endothelial Nox4.* Antioxid Redox Signal, 2009. **11**(10): p. 2385-97.
183. Ali, M.H., et al., *Mitochondrial requirement for endothelial responses to cyclic strain: implications for mechanotransduction.* Am J Physiol Lung Cell Mol Physiol, 2004. **287**(3): p. L486-96.
184. Ross, R., *Atherosclerosis--an inflammatory disease.* N Engl J Med, 1999. **340**(2): p. 115-26.
185. Spescha, R.D., et al., *Adaptor protein p66(Shc) mediates hypertension-associated, cyclic stretch-dependent, endothelial damage.* Hypertension, 2014. **64**(2): p. 347-53.
186. Wagner, A.H., et al., *Upregulation of glutathione peroxidase offsets stretch-induced proatherogenic gene expression in human endothelial cells.* Arterioscler Thromb Vasc Biol, 2009. **29**(11): p. 1894-901.
187. Saleh, M.A., A.E. Norlander, and M.S. Madhur, *Inhibition of Interleukin 17-A but not Interleukin-17F Signaling Lowers Blood Pressure and Reduces End-organ Inflammation in Angiotensin II-induced Hypertension.* JACC Basic Transl Sci, 2016. **1**(7): p. 606-616.
188. Siveen, K.S., et al., *Targeting the STAT3 signaling pathway in cancer: role of synthetic and natural inhibitors.* Biochim Biophys Acta, 2014. **1845**(2): p. 136-54.
189. Szelag, M., et al., *Targeted inhibition of STATs and IRFs as a potential treatment strategy in cardiovascular disease.* Oncotarget, 2016. **7**(30): p. 48788-48812.
190. Heim, M.H., et al., *Contribution of STAT SH2 groups to specific interferon signaling by the Jak-STAT pathway.* Science, 1995. **267**(5202): p. 1347-9.
191. Paulson, M., et al., *Stat protein transactivation domains recruit p300/CBP through widely divergent sequences.* J Biol Chem, 1999. **274**(36): p. 25343-9.

192. Sengupta, T.K., et al., *Rapid inhibition of interleukin-6 signaling and Stat3 activation mediated by mitogen-activated protein kinases.* Proc Natl Acad Sci U S A, 1998. **95**(19): p. 11107-12.
193. Sadowski, H.B., et al., *A common nuclear signal transduction pathway activated by growth factor and cytokine receptors.* Science, 1993. **261**(5129): p. 1739-44.
194. Wen, Z. and J.E. Darnell, Jr., *Mapping of Stat3 serine phosphorylation to a single residue (727) and evidence that serine phosphorylation has no influence on DNA binding of Stat1 and Stat3.* Nucleic Acids Res, 1997. **25**(11): p. 2062-7.
195. Ng, J. and D. Cantrell, *STAT3 is a serine kinase target in T lymphocytes. Interleukin 2 and T cell antigen receptor signals converge upon serine 727.* J Biol Chem, 1997. **272**(39): p. 24542-9.
196. Grivennikov, S.I. and M. Karin, *Dangerous liaisons: STAT3 and NF-kappaB collaboration and crosstalk in cancer.* Cytokine Growth Factor Rev, 2010. **21**(1): p. 11-9.
197. Chmielewski, S., et al., *STAT1-dependent signal integration between IFNgamma and TLR4 in vascular cells reflect pro-atherogenic responses in human atherosclerosis.* PLoS One, 2014. **9**(12): p. e113318.
198. Agrawal, S., et al., *Signal transducer and activator of transcription 1 is required for optimal foam cell formation and atherosclerotic lesion development.* Circulation, 2007. **115**(23): p. 2939-47.
199. Perwitasari, O., et al., *Inhibitor of kappaB kinase epsilon (IKK(epsilon)), STAT1, and IFIT2 proteins define novel innate immune effector pathway against West Nile virus infection.* J Biol Chem, 2011. **286**(52): p. 44412-23.
200. Pilz, A., et al., *Dendritic cells require STAT-1 phosphorylated at its transactivating domain for the induction of peptide-specific CTL.* J Immunol, 2009. **183**(4): p. 2286-93.
201. Johnson, L.M. and P. Scott, *STAT1 expression in dendritic cells, but not T cells, is required for immunity to Leishmania major.* J Immunol, 2007. **178**(11): p. 7259-66.
202. Lagor, W.R., et al., *Genetic manipulation of the ApoF/Stat2 locus supports an important role for type I interferon signaling in atherosclerosis.* Atherosclerosis, 2014. **233**(1): p. 234-41.
203. Dutzmann, J., et al., *Emerging translational approaches to target STAT3 signalling and its impact on vascular disease.* Cardiovasc Res, 2015. **106**(3): p. 365-74.
204. Wei, L., et al., *IL-21 is produced by Th17 cells and drives IL-17 production in a STAT3-dependent manner.* J Biol Chem, 2007. **282**(48): p. 34605-10.
205. Harris, T.J., et al., *Cutting edge: An in vivo requirement for STAT3 signaling in TH17 development and TH17-dependent autoimmunity.* J Immunol, 2007. **179**(7): p. 4313-7.
206. Gires, O., et al., *Latent membrane protein 1 of Epstein-Barr virus interacts with JAK3 and activates STAT proteins.* EMBO J, 1999. **18**(11): p. 3064-73.
207. Zhou, X., et al., *Pravastatin prevents aortic atherosclerosis via modulation of signal transduction and activation of transcription 3 (STAT3) to attenuate interleukin-6 (IL-6) action in ApoE knockout mice.* Int J Mol Sci, 2008. **9**(11): p. 2253-64.
208. Jarnicki, A., T. Putoczki, and M. Ernst, *Stat3: linking inflammation to epithelial cancer - more than a "gut" feeling?* Cell Div, 2010. **5**: p. 14.
209. Schust, J., et al., *Stattic: a small-molecule inhibitor of STAT3 activation and dimerization.* Chem Biol, 2006. **13**(11): p. 1235-42.

210. Johnson, A.W., et al., *Small-molecule inhibitors of signal transducer and activator of transcription 3 protect against angiotensin II-induced vascular dysfunction and hypertension.* Hypertension, 2013. **61**(2): p. 437-42.
211. Zouein, F.A., et al., *Role of STAT3 in angiotensin II-induced hypertension and cardiac remodeling revealed by mice lacking STAT3 serine 727 phosphorylation.* Hypertens Res, 2013. **36**(6): p. 496-503.
212. Kielbik, M., et al., *Nitric oxide donors: spermine/NO and diethylenetriamine/NO induce ovarian cancer cell death and affect STAT3 and AKT signaling proteins.* Nitric Oxide, 2013. **35**: p. 93-109.
213. Collaborators, G.B.o.D.R.F., *Global, regional, and national comparative risk assessment of 79 behavioural, environmental and occupational, and metabolic risks or clusters of risks, 1990-2015: a systematic analysis for the Global Burden of Disease Study 2015.* Lancet, 2016. **388**(10053): p. 1659-1724.
214. Yang, X.O., et al., *STAT3 regulates cytokine-mediated generation of inflammatory helper T cells.* J Biol Chem, 2007. **282**(13): p. 9358-63.
215. Clarkson, S.B. and P.A. Ory, *CD16. Developmentally regulated IgG Fc receptors on cultured human monocytes.* J Exp Med, 1988. **167**(2): p. 408-20.
216. Wildgruber, M., et al., *The "Intermediate" CD14(++)CD16(+) monocyte subset increases in severe peripheral artery disease in humans.* Sci Rep, 2016. **6**: p. 39483.
217. Layne, K., et al., *Anti-platelet drugs attenuate the expansion of circulating CD14highCD16+ monocytes under pro-inflammatory conditions.* Cardiovasc Res, 2016. **111**(1): p. 26-33.
218. Hwang, H.J., et al., *LECT2 induces atherosclerotic inflammatory reaction via CD209 receptor-mediated JNK phosphorylation in human endothelial cells.* Metabolism, 2015. **64**(9): p. 1175-82.
219. Radej, S., et al., *Immunomodelling Characteristics of Mature Dendritic Cells Stimulated by Colon Cancer Cells Lysates.* Pol Przegl Chir, 2015. **87**(2): p. 71-82.
220. Randolph, G.J., et al., *The CD16(+) (FcgammaRIII(+)) subset of human monocytes preferentially becomes migratory dendritic cells in a model tissue setting.* J Exp Med, 2002. **196**(4): p. 517-27.
221. Du, W., I. Mills, and B.E. Sumpio, *Cyclic strain causes heterogeneous induction of transcription factors, AP-1, CRE binding protein and NF-kB, in endothelial cells: species and vascular bed diversity.* J Biomech, 1995. **28**(12): p. 1485-91.
222. Sokabe, M., et al., *Mechanotransduction and intracellular signaling mechanisms of stretch-induced remodeling in endothelial cells.* Heart Vessels, 1997. **Suppl 12**: p. 191-3.
223. Lehoux, S., et al., *Pulsatile stretch-induced extracellular signal-regulated kinase 1/2 activation in organ culture of rabbit aorta involves reactive oxygen species.* Arterioscler Thromb Vasc Biol, 2000. **20**(11): p. 2366-72.
224. Ikeda, M., H. Kito, and B.E. Sumpio, *Phosphatidylinositol-3 kinase dependent MAP kinase activation via p21ras in endothelial cells exposed to cyclic strain.* Biochem Biophys Res Commun, 1999. **257**(3): p. 668-71.
225. Lehoux, S., *Redox signalling in vascular responses to shear and stretch.* Cardiovasc Res, 2006. **71**(2): p. 269-79.
226. Sayeski, P.P., et al., *Phosphorylation of p130Cas by angiotensin II is dependent on c-Src, intracellular Ca2+, and protein kinase C.* Circ Res, 1998. **82**(12): p. 1279-88.

227. Pinho, M.P., et al., *Dendritic cell membrane CD83 enhances immune responses by boosting intracellular calcium release in T lymphocytes.* J Leukoc Biol, 2014. **95**(5): p. 755-762.
228. Shirai, T., et al., *The glycolytic enzyme PKM2 bridges metabolic and inflammatory dysfunction in coronary artery disease.* J Exp Med, 2016. **213**(3): p. 337-54.
229. Laouar, Y., et al., *STAT3 is required for Flt3L-dependent dendritic cell differentiation.* Immunity, 2003. **19**(6): p. 903-12.
230. Davies, S.S., et al., *Localization of isoketal adducts in vivo using a single-chain antibody.* Free Radic Biol Med, 2004. **36**(9): p. 1163-74.
231. Didion, S.P., *Cellular and Oxidative Mechanisms Associated with Interleukin-6 Signaling in the Vasculature.* Int J Mol Sci, 2017. **18**(12).
232. Lee, Y.W., W.H. Lee, and P.H. Kim, *Oxidative mechanisms of IL-4-induced IL-6 expression in vascular endothelium.* Cytokine, 2010. **49**(1): p. 73-9.
233. Gangoda, S.V.S., et al., *Pulsatile stretch as a novel modulator of amyloid precursor protein processing and associated inflammatory markers in human cerebral endothelial cells.* Sci Rep, 2018. **8**(1): p. 1689.
234. Villavicencio, R.T., et al., *Induced nitric oxide inhibits IL-6-induced stat3 activation and type II acute phase mRNA expression.* Shock, 2000. **13**(6): p. 441-5.
235. Guo, H.F., et al., *High mobility group box 1 induces synoviocyte proliferation in rheumatoid arthritis by activating the signal transducer and activator transcription signal pathway.* Clin Exp Med, 2011. **11**(2): p. 65-74.
236. Urbanski, K., et al., *CD14(+)CD16(++) "nonclassical" monocytes are associated with endothelial dysfunction in patients with coronary artery disease.* Thromb Haemost, 2017. **117**(5): p. 971-980.
237. Choi, B., et al., *The Correlation of CD206, CD209, and Disease Severity in Behcet's Disease with Arthritis.* Mediators Inflamm, 2017. **2017**: p. 7539529.
238. Yang, K., et al., *DC-SIGN and Toll-like receptor 4 mediate oxidized low-density lipoprotein-induced inflammatory responses in macrophages.* Sci Rep, 2017. **7**(1): p. 3296.
239. Zhou, L.J. and T.F. Tedder, *Human blood dendritic cells selectively express CD83, a member of the immunoglobulin superfamily.* J Immunol, 1995. **154**(8): p. 3821-35.
240. Schieffer, B., et al., *Expression of angiotensin II and interleukin 6 in human coronary atherosclerotic plaques: potential implications for inflammation and plaque instability.* Circulation, 2000. **101**(12): p. 1372-8.
241. Mantovani, A., et al., *The chemokine system in diverse forms of macrophage activation and polarization.* Trends Immunol, 2004. **25**(12): p. 677-86.
242. Ben-Shlomo, Y., et al., *Aortic pulse wave velocity improves cardiovascular event prediction: an individual participant meta-analysis of prospective observational data from 17,635 subjects.* J Am Coll Cardiol, 2014. **63**(7): p. 636-46.
243. Sesso, H.D., et al., *Comparison of interleukin-6 and C-reactive protein for the risk of developing hypertension in women.* Hypertension, 2007. **49**(2): p. 304-10.
244. Brands, M.W., et al., *Interleukin 6 Knockout Prevents Angiotensin II Hypertension. Role of Renal Vasoconstriction and Janus Kinase 2/Signal Transducer and Activator of Transcription 3 Activation.* Hypertension, 2010.

245. Wenzel, P., et al., *Heme oxygenase-1 suppresses a pro-inflammatory phenotype in monocytes and determines endothelial function and arterial hypertension in mice and humans.* Eur Heart J, 2015. **36**(48): p. 3437-46.
246. Tanaka, T., M. Narazaki, and T. Kishimoto, *IL-6 in inflammation, immunity, and disease.* Cold Spring Harb Perspect Biol, 2014. **6**(10): p. a016295.
247. Seshiah, P.N., et al., *Angiotensin II stimulation of NAD(P)H oxidase activity: upstream mediators.* Circ Res, 2002. **91**(5): p. 406-13.
248. Guzik, T.J., et al., *The role of infiltrating immune cells in dysfunctional adipose tissue.* Cardiovasc Res, 2017. **113**(9): p. 1009-1023.
249. Julius, S., et al., *The Valsartan Antihypertensive Long-Term Use Evaluation (VALUE) trial: outcomes in patients receiving monotherapy.* Hypertension, 2006. **48**(3): p. 385-91.
250. Dikalov, S.I., et al., *Nox2-induced production of mitochondrial superoxide in angiotensin II-mediated endothelial oxidative stress and hypertension.* Antioxid Redox Signal, 2014. **20**(2): p. 281-94.
251. Wu, J., et al., *Origin of Matrix-Producing Cells That Contribute to Aortic Fibrosis in Hypertension.* Hypertension, 2016. **67**(2): p. 461-8.
252. Dikalov, S. and B. Fink, *ESR techniques for the detection of nitric oxide in vivo and in tissues.* Methods Enzymol, 2005. **396**: p. 597-610.
253. Itani, H.A., et al., *Mitochondrial Cyclophilin D in Vascular Oxidative Stress and Hypertension.* Hypertension, 2016. **67**(6): p. 1218-27.
254. Peyser, N.D., et al., *STAT3 as a Chemoprevention Target in Carcinogen-Induced Head and Neck Squamous Cell Carcinoma.* Cancer Prev Res (Phila), 2016. **9**(8): p. 657-63.
255. Melillo, J.A., et al., *Dendritic cell (DC)-specific targeting reveals Stat3 as a negative regulator of DC function.* J Immunol, 2010. **184**(5): p. 2638-45.
256. Kina, S., et al., *Regulation of chemokine production via oxidative pathway in HeLa cells.* Mediators Inflamm, 2009. **2009**: p. 183760.
257. Khan, B.V., et al., *Nitric oxide regulates vascular cell adhesion molecule 1 gene expression and redox-sensitive transcriptional events in human vascular endothelial cells.* Proc Natl Acad Sci U S A, 1996. **93**(17): p. 9114-9.
258. Tancos, Z., et al., *Establishment of induced pluripotent stem cell (iPSC) line from an 84-year old patient with late onset Alzheimer's disease (LOAD).* Stem Cell Res, 2016. **17**(1): p. 75-77.
259. Patsch, C., et al., *Generation of vascular endothelial and smooth muscle cells from human pluripotent stem cells.* Nat Cell Biol, 2015. **17**(8): p. 994-1003.
260. Villani, A.C., et al., *Single-cell RNA-seq reveals new types of human blood dendritic cells, monocytes, and progenitors.* Science, 2017. **356**(6335).
261. Chistiakov, D.A., A.N. Orekhov, and Y.V. Bobryshev, *Effects of shear stress on endothelial cells: go with the flow.* Acta Physiol (Oxf), 2017. **219**(2): p. 382-408.
262. Gonzales, R.S. and T.M. Wick, *Hemodynamic modulation of monocytic cell adherence to vascular endothelium.* Ann Biomed Eng, 1996. **24**(3): p. 382-93.
263. Matharu, N.M., et al., *Inflammatory responses of endothelial cells experiencing reduction in flow after conditioning by shear stress.* J Cell Physiol, 2008. **216**(3): p. 732-41.
264. Dimmeler, S., et al., *Activation of nitric oxide synthase in endothelial cells by Akt-dependent phosphorylation.* Nature, 1999. **399**(6736): p. 601-5.

265. Jin, R.C. and J. Loscalzo, *Vascular Nitric Oxide: Formation and Function.* J Blood Med, 2010. **2010**(1): p. 147-162.
266. Makhoul, S., et al., *Effects of the NO/soluble guanylate cyclase/cGMP system on the functions of human platelets.* Nitric Oxide, 2018. **76**: p. 71-80.
267. Rainer, P.P. and D.A. Kass, *Old dog, new tricks: novel cardiac targets and stress regulation by protein kinase G.* Cardiovasc Res, 2016. **111**(2): p. 154-62.
268. Rubbo, H. and R. Radi, *Protein and lipid nitration: role in redox signaling and injury.* Biochim Biophys Acta, 2008. **1780**(11): p. 1318-24.
269. Cleeter, M.W., et al., *Reversible inhibition of cytochrome c oxidase, the terminal enzyme of the mitochondrial respiratory chain, by nitric oxide. Implications for neurodegenerative diseases.* FEBS Lett, 1994. **345**(1): p. 50-4.
270. Rychter, M., et al., *S-Nitrosothiols-NO donors regulating cardiovascular cell proliferation: Insight into intracellular pathway alterations.* Int J Biochem Cell Biol, 2016. **78**: p. 156-161.
271. Wittmann, C., et al., *Hydrogen peroxide in inflammation: messenger, guide, and assassin.* Adv Hematol, 2012. **2012**: p. 541471.
272. Rebe, C., et al., *STAT3 activation: A key factor in tumor immunoescape.* JAKSTAT, 2013. **2**(1): p. e23010.
273. Yuan, Z.L., et al., *Stat3 dimerization regulated by reversible acetylation of a single lysine residue.* Science, 2005. **307**(5707): p. 269-73.